

Medical University of South Carolina

MEDICA

MUSC Theses and Dissertations

2001

Cardiac Hypertrophy, Heart Failure, and Regulation of Microtubule Stability

Kristie Lynn Beaton-Blade
Medical University of South Carolina

Follow this and additional works at: <https://medica-musc.researchcommons.org/theses>

Recommended Citation

Beaton-Blade, Kristie Lynn, "Cardiac Hypertrophy, Heart Failure, and Regulation of Microtubule Stability" (2001). *MUSC Theses and Dissertations*. 123.

<https://medica-musc.researchcommons.org/theses/123>

This Dissertation is brought to you for free and open access by MEDICA. It has been accepted for inclusion in MUSC Theses and Dissertations by an authorized administrator of MEDICA. For more information, please contact medica@musc.edu.

CARDIAC HYPERTROPHY, HEART FAILURE,
AND REGULATION OF MICROTUBULE STABILITY

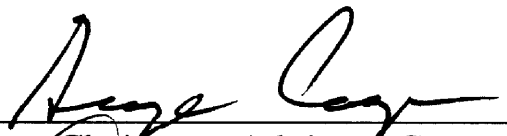
by

Kristie Lynn Beaton Blade

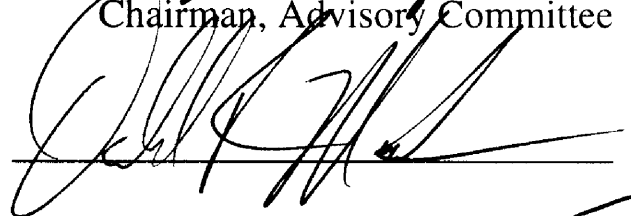
A dissertation submitted to the faculty of the Medical University of South Carolina in
partial fulfillment of the requirements for the degree of Doctor of Philosophy in the
College of Graduate Studies.

Department of Molecular and Cellular Biology and Pathobiology
2001

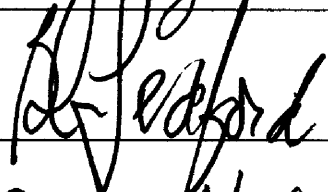
Approved by:



Chairman, Advisory Committee



Paul J. McDermott



Paul V. Helesticka

ACKNOWLEDGEMENTS

I would like to thank my mentors George Cooper and Don Menick for their support and advice, and my committee for their time and advice. I would also like to thank the faculty, students, and workers at the Gazes Cardiac Research Institute, both past and present, for their help and friendship. I would especially like to thank my husband, Bob Blade, and my parents, Paul and Kay Beaton, for their love and patience.

TABLE OF CONTENTS

LIST OF TABLES	iv
LIST OF FIGURES.....	v
ABSTRACT	vii
CHAPTERS	
1: GENERAL INTRODUCTION	1
2: REGULATION OF THE BETA TUBULIN ISOTYPES	14
Introduction	14
Methods	17
Results	25
Discussion	40
3: OVEREXPRESSION OF THE BETA TUBULIN ISOTYPES	46
Introduction	46
Methods	51
Results	60
Discussion	84
4: OVEREXPRESSION OF THE BETA TUBULIN MUTANTS.....	89
Introduction	89
Methods	92
Results	95
Discussion	112
5: GENERAL DISCUSSION	115
LIST OF REFERENCES	124

LIST OF TABLES

Table 3-1. Selection of transfected cells for resistance to G418 and to Taxol	63
Table 3-2. Taxol-resistant cells in a G418 selected population.....	65
Table 4-1. Summary of beta-tubulin mutations in Taxol-resistant CHO cells.....	96
Table 4-2. Cloning efficiencies of HABI _{L215H} transfected cells under various selective conditions	103
Table 4-3. F ₀ offspring of transgenic founders.....	109

LIST OF FIGURES

Figure 1-1. Microtubule structure	9
Figure 2-1. Cloning strategy for the feline tubulin partial cDNAs	18
Figure 2-2. Tissue distribution of beta-tubulin isotypes	27
Figure 2-3. Tubulin isotype mRNA in PAB cats	28
Figure 2-4. Densitometry of isotype mRNA levels in 48 hour PAB cats.....	29
Figure 2-5. Half-life studies of the beta-tubulin RNA	30
Figure 2-6. Treatment of neonatal rat cardiocytes with phenylephrine	33
Figure 2-7. Levels of the beta-tubulin isotypes in skeletal muscle tissue.....	34
Figure 2-8. Beta-tubulin isotype levels in differentiating C2C12 cells	36
Figure 2-9. Autoregulation of tubulin message stability in neonatal and adult cardiocytes.....	38
Figure 3-1. The HAbeta-tubulin proteins are incorporated into the CHO cell microtubular network	62
Figure 3-2. Production of HAbeta-tubulin in transfected cells	66
Figure 3-3. Multiplicity of infection for HAbeta-tubulin adenoviruses.....	68
Figure 3-4. Time course for HAbeta-tubulin adenoviral infection	70
Figure 3-5. The HAbeta-tubulin proteins are incorporated into the microtubules of the adult cardiocyte	72
Figure 3-6. Post-translationally modified alpha-tubulins in HAbeta-tubulin infected cardiocytes	74
Figure 3-7. Cold stability of microtubules in adenovirally infected adult cardiocytes.....	76
Figure 3-8. Overexpression of MAP 4 in adult cardiocytes	79
Figure 3-9. Co-expression of the MAP 4 and HAbetaI proteins in adult cardiocytes.....	81
Figure 4-1. Production of wild-type and mutant HAbetaI-tubulin in transfected cell lines.....	99

Figure 4-2. Cells expressing HAbetaI _{L215H} have reduced alpha-tubulin acetylation	101
Figure 4-3. Taxol selects for transfected cells that express mutant HAbetaI-tubulin.....	105
Figure 4-4. Southern analysis of transgenic mice	108
Figure 4-5. HAbeta-tubulin levels in tissue from a transgenic mouse.....	111
Figure 4-6. Location of mutated residues in the crystal structure of tubulin.....	113

KRISTIE LYNN BEATON BLADE. Cardiac hypertrophy, heart failure, and regulation of microtubule stability. (Under the direction of GEORGE COOPER).

This work focused on the regulation of the different isotypes of beta-tubulin during cardiac hypertrophy, with the specific hypothesis that increased levels of the beta I isotype leads to the increase in microtubule density seen during hypertrophy. Partial cDNAs for the three beta-tubulin isotypes expressed in the heart (I, II, and IV) have been cloned and used to show that there is a differential upregulation of the beta I and beta II isotypes during cardiac hypertrophy. Messenger RNA half-life studies of cells isolated from hypertrophied myocardium have shown that this upregulation is due to increased transcription of the genes encoding those isotypes. This work has also shown the presence in terminally differentiated cells of the co-translational autoregulatory mechanism by which increased free tubulin protein levels leads to decreased mRNA levels.

The beta-tubulin isotypes that are expressed in the heart have been cloned into tetracycline-regulated expression vectors and adenoviral vectors. Overexpression in CHO cells has shown that, contrary to some previous reports, overexpression of beta I, beta II, and beta IV does not affect microtubule stability as measured by taxol resistance. In addition, overexpression of beta I in adult cardiocytes does not affect microtubule stability. However, overexpression of the predominant heart microtubule associated protein, MAP 4, is alone enough to cause increased microtubule stability *in vitro*. Because there is an increase in MAP 4 protein levels during cardiac hypertrophy *in vivo*, we believe that this is the primary mechanism of increased microtubule stability in the hypertrophied myocardium.

This work also focused on development of a mouse model in which to study the effects of microtubule stability on the development of heart failure *in vivo*. Mutation of the beta-tubulin protein in a string of leucine residues destabilized the microtubules in CHO cells. Constructs encoding these mutant tubulin proteins have been inserted into a heart-specific vector and cloned into transgenic mice. Several lines have been initially characterized for levels of expression, and one line has shown heart-specific expression of a mutated beta-tubulin protein. These lines will be used for future studies of the effect of destabilized microtubules on the development of heart failure.

CHAPTER 1: GENERAL INTRODUCTION

Cardiovascular disease is the number one killer of both men and women in this country and a considerable burden, in terms of health care costs, for our economy. Nearly 60 million Americans have one or more types of cardiovascular disease, with about 4.6 million Americans suffering from heart failure (American Heart Association statistics). There are many different common types of cardiovascular disease, including coronary artery disease, hypertension, and valvular diseases; many of them, including those mentioned, cause increased load for the heart muscle. The primary response of the cardiocyte to increased load on a long-term basis is hypertrophy, or growth in mass. Unfortunately, this initially compensatory response to a load increase can eventuate in decompensation and heart failure.

Heart failure is essentially a syndrome characterized by an underlying cardiovascular disease that has resulted in decreased ventricular function causing a combination of systemic symptoms resulting from reduced cardiac output. There are many causes of heart failure including arrhythmias, valve disease, pericardial disease, congenital heart disease, and myocardial disease (1). Most cases of heart failure are caused by myocardial diseases that include coronary artery disease, cardiomyopathy, hypertension, and drug-induced diseases (1). By far the most common causes are coronary artery disease and hypertension. In fact, only about 7% of heart failure cases cannot be attributed to coronary artery disease, hypertension, and valve disease (2). While we know what conditions cause heart failure, and we know the specific signs and

symptoms of heart failure, we do not know at a molecular level what causes the loss in function of the heart muscle during failure.

We do know that heart failure is usually associated with some form of cardiac hypertrophy. Hypertrophy is the compensatory response of the heart to increased load, which is caused by the various diseases mentioned above, as well as by non-disease states such as exercise and pregnancy. Pressure-induced overload, such as is seen during long-term hypertension, often leads to concentric hypertrophy of the left ventricle. The individual heart cells, or cardiomyocytes, enlarge, increasing the ventricular wall thickness in a concentric manner. Because wall stress is proportional to pressure and the chamber radius/ wall thickness ratio, the decreasing chamber radius/ wall thickness ratio from concentric hypertrophy offsets increased afterload, allowing the wall stress to remain normal. During the initial compensatory stages, ejection fraction, which is an indication of systolic function, remains normal, but diastolic filling may be impaired due to reduced compliance of the thickened ventricular wall. Over time, dilatation of the ventricle often occurs, such that the ventricular radius increases and wall stress goes up, causing ejection fraction to decrease. This then increases myocardial oxygen consumption and leads to decreased ability of the heart to pump (for an excellent review of this sequence of events, see (3)).

Little is known about the molecular mechanisms that underlie the shift from compensatory hypertrophy to decompensated heart failure in the presence of continued pathologic increased load. More is known about the sequence of events leading to compensatory hypertrophy, and many studies in this lab as well as others are now focused on the elucidation of the signaling pathways involved in transducing mechanical signals into hypertrophic responses in cardiac muscle. It is well known that a mechanical stimulus is sufficient to cause hypertrophy at the level of the intact heart, isolated cardiac

tissue, and isolated cardiocytes (4). The immediate downstream signals of mechanical stimulation are now being studied, and include several members of growth factor, G-protein, and integrin-coupled signaling pathways (reviewed in (5)). The endpoints of these signaling pathways are fairly well characterized and include increased protein synthesis rates, increased protein content, specific changes in gene regulation programs, and overall growth in size of the cell (for a review of some of these changes, see (6)). One of the more noteworthy changes in gene regulation patterns seen during pressure overload-induced hypertrophy is the recapitulation of an embryonic pattern of gene expression, especially in relation to some of the structural protein isoforms as well as some of the ion channels. Although many of the molecular changes during hypertrophy and heart failure have been elucidated, the exact cause of the decrease in contractile function seen at the whole organ level is not well understood.

A problem with research of cardiac hypertrophy and heart failure that often presents itself is the difficulty of obtaining good models of hypertrophy that mimic what is seen in human disease. While it has a very simple function, the heart is a complex organ, particularly in terms of complex chamber geometry, making it difficult to model as a simple pump. The primary determinant of the heart's structure, in both pathologic and non-pathologic states, is the systolic stress, or afterload, to which each chamber is subjected. For this reason, different models of hypertrophy exhibit different changes at the molecular level, although all display increases in cellular mass and protein content. For this reason, it is important to understand the different ways in which hypertrophy can occur.

Immediately after birth, the heart undergoes rapid changes in mass and morphology based primarily on the changes in afterload that are present. When the lungs are inflated after birth, there is an immediate drop in pressure in the pulmonary arterial

circulation. This, coupled with the sudden demands of the systemic circulation in the newborn, leads to rapid growth of the left ventricle in comparison to the right, as well as closure of the ductus arteriosus. This growth of the left ventricle is due to hypertrophy of existing cardiocytes (7). This physiologic hypertrophy is critical for establishing the structure of the adult heart and is based solely on the presence of changes in afterload for the different chambers. Later in life, the heart continuously adapts to changes in pressure in order to maximize function. Physiologic causes of hypertrophy include exercise and pregnancy-induced hypertrophy. These adaptive forms of hypertrophy are critical for maintaining normal wall stress in the face of increased preload and afterload, and do not lead to decreased cardiac function.

Pathologic causes of hypertrophy, like those mentioned above, often lead to decreased cardiac function. However, not all pathology that leads to hypertrophy is alike. One major distinction that can be made is hypertrophy due to pressure overload, or increased afterload, and hypertrophy due to volume overload, or increased preload. Both stressors can cause the cardiocytes to increase their mass, but each leads to different pathologies at the cellular and whole organ levels. To study hypertrophy, most labs, including this one, choose to use animal models of pressure and volume overload. While there are many models available, I will discuss the models that our lab primarily uses. These include the feline pulmonary artery band and atrial septal defect models, as well as the canine aortic banding model.

The feline models provide a prime example of the difference between pressure and volume overload-induced hypertrophy. The volume overload model is an atrial septal defect (ASD) model in which the interatrial septum is resected during venous inflow occlusion, creating a volume overload of the right ventricle (RV) and leading to right ventricular hypertrophy (8). The pressure overload model is a pulmonary artery band

(PAB) model in which the pulmonary artery is constricted by a band, leading to a sudden and constant increase in the pressure that the right ventricle must pump against and therefore to right ventricular hypertrophy (9). Both models lead to right ventricular hypertrophy with no right heart failure, and both have normal left ventricle (LV) weight/body weight ratios (10). These models are similar in that they each subject the right ventricle to a sudden stress that remains high. The pressure overload model is most analogous to the human condition of primary pulmonary hypertension and the volume overload model to congenital atrial septal defects. While both models lead to cardiac hypertrophy, the ASD model does not cause contractile defects (8), while the PAB model leads to contractile defects at both the organ (9) and the cardiocyte (11) levels.

As discussed above, in humans the bulk of cardiac hypertrophy is LV hypertrophy due to ischemic heart disease following coronary artery disease (CAD) and LV hypertrophy due to long-term hypertension. In these diseases, the hypertrophying stimulus is applied over time, often becoming increasingly worse with time, especially with CAD as more tissue becomes ischemic and necrotic. To more accurately model these common human diseases, this lab uses a canine aortic banding model of LV hypertrophy in which there is a stepwise increase over time in the amount of afterload imposed by a supracoronary ascending aortic band (12). The dogs used in this model randomly segregate into two sets: the first, a “hypertrophy” group, maintains compensated contractile function in the face of a large degree of hypertrophy; the second, a “failure” group, shows abnormalities in contractile function over time in the face of a lesser degree of LV hypertrophy (12). This model most closely resembles the human condition of chronic hypertension, and in fact similar groups are seen clinically in people (12). As to contractile dysfunction at the cellular level, only the failure group exhibits decreases as measured by extent and rate of sarcomere shortening (13). These are the

same dogs in which wall stress, after a certain period, is no longer normalized by hypertrophy (12, 13). These dogs then are similar, in this respect, to the PAB cats, in that individual cardiocytes from these animals display contractile defects (14), while at the same time they probably have uncompensated increased wall stress (G. Cooper, personal communication).

While none of these models closely resembles the most common cause of heart failure, ischemic heart disease secondary to CAD, they offer an excellent opportunity to study the effects of pressure overload-induced hypertrophy with uncompensated increased wall stress, which is present in many patients with CAD. The two pressure overload models present a means to study the question of what, at the molecular or cellular level, leads to a decrease in contractile function of hypertrophied myocardium and hypertrophied cardiocytes during pressure overload-induced hypertrophy. Previous studies in this lab have extensively characterized the defects present in the feline RV pressure overload model. One study showed that, in PAB cats with contractile dysfunction but not ASD cats with no contractile dysfunction, the hypertrophied myocardium showed decreased volume density of cardiocytes and increased connective tissue (15). While these changes could certainly cause the decreased systolic and diastolic function seen in this model, further studies showed that, before the interstitial fibrosis becomes substantial, the individual cardiocytes themselves have decreased contractile function (11). However, there was no obvious difference in morphology between cells isolated from the volume-overloaded and pressure-overloaded RVs (15).

These observations led to the search for a cellular structure that could interfere with contractile function and be responsive to pressure overload, yet not be obvious ultrastructurally (14). One candidate structure turned out to be changed during pressure overload but not volume overload-induced hypertrophy—the microtubular cytoskeleton

(14). In fact, this lab has shown in the feline PAB model that several things concerning microtubules are true. There is an increase in microtubule density (14). There is an increase in microtubule stability, as indicated both by increased microtubule age and increased resistance to destabilizing conditions (10). Finally, the higher density of microtubules leads to an increased viscosity in the cardiocyte that decreases the cell's ability to contract (16). These observations have been extended to the canine aortic banding model. Specifically, it was found that in the failure dogs, which do not normalize wall stress and have contractile dysfunction at the cellular level, there is an increased density of microtubules (13). Importantly, this lab has shown that, in isolated cardiocytes from both the PAB cat RV and the aortic-banded failure dog LV, contractile dysfunction is normalized by dissolution of the microtubules (13, 14). These studies collectively show that a significant cause of decreased contractility at the cardiocyte level in high wall stress states in the cat and dog is densification of the microtubule network.

A primary objective in this lab soon became to discover why high wall stress in the heart could lead to an increased density and stability of microtubules in the cardiocyte. This requires an understanding of the structures and their dynamics. Microtubules are cytoskeletal elements that have a hollow, tubular structure. Most mammalian microtubules are made of 13 protofilaments which are strings of tubulin heterodimers, globular proteins made of an α - and β -tubulin. They function primarily as mechanisms for guiding movement of various components of the cell, including the chromosomes during mitosis, vesicles during membrane transport, and structural proteins in axons of neurons. We speculate that in the mature cardiocyte, which no longer undergoes cell division, the primary function of the microtubules is structural support of the cell, as well as transport of proteins, especially when the cell undergoes growth, or hypertrophy.

The α - and β -tubulin proteins are highly conserved proteins that are present in all eukaryotes and are therefore very ancient on an evolutionary timescale. The proteins are 50% identical at the amino acid level (17), and are therefore structurally very similar. They each bind a GTP molecule, but only the β -tubulin-bound GTP is hydrolyzed during polymerization of the microtubule. For this reason, the site of GTP binding to the β -tubulin molecule is called the exchangeable or E-site, and the site of GTP binding to the α -tubulin molecule is called the non-exchangeable or N-site. The heterodimers form long protofilaments by binding in a linear manner, and the protofilaments aggregate by lateral interaction to form 25 nm diameter hollow tubes. The lateral interactions between protofilaments occur between like monomers (in other words α to α and β to β) except at the seam in a B-type lattice structure (see Figure 1-1). When both ends of a microtubule are free, polymerization and depolymerization can occur at both ends, but there is a net addition at one end, which is termed the “+” end, and a net subtraction at the other end, which is termed the “-“ end. Usually *in vivo*, the “-“ end of the microtubule is fixed to a stabilizing structure that contains a related protein called γ -tubulin.

Although microtubules are polymers, they do not behave as equilibrium polymers, because in steady state they undergo transitions between states of polymerization and depolymerization. Microtubule dynamics are governed principally by the concept of “dynamic instability,” (18) where the polymers alternate between periods of shrinkage, called “catastrophe,” and periods of growth, called “rescue” (reviewed in (19-21)). Therefore, the rate of polymerization, the rate of depolymerization, the frequency of catastrophe, and the frequency of rescue all influence microtubule dynamics. Because microtubule stability is a nonequilibrium behavior, it requires an energy source, and this is supplied by the hydrolysis of the E-site GTP molecule (19). There is evidence,

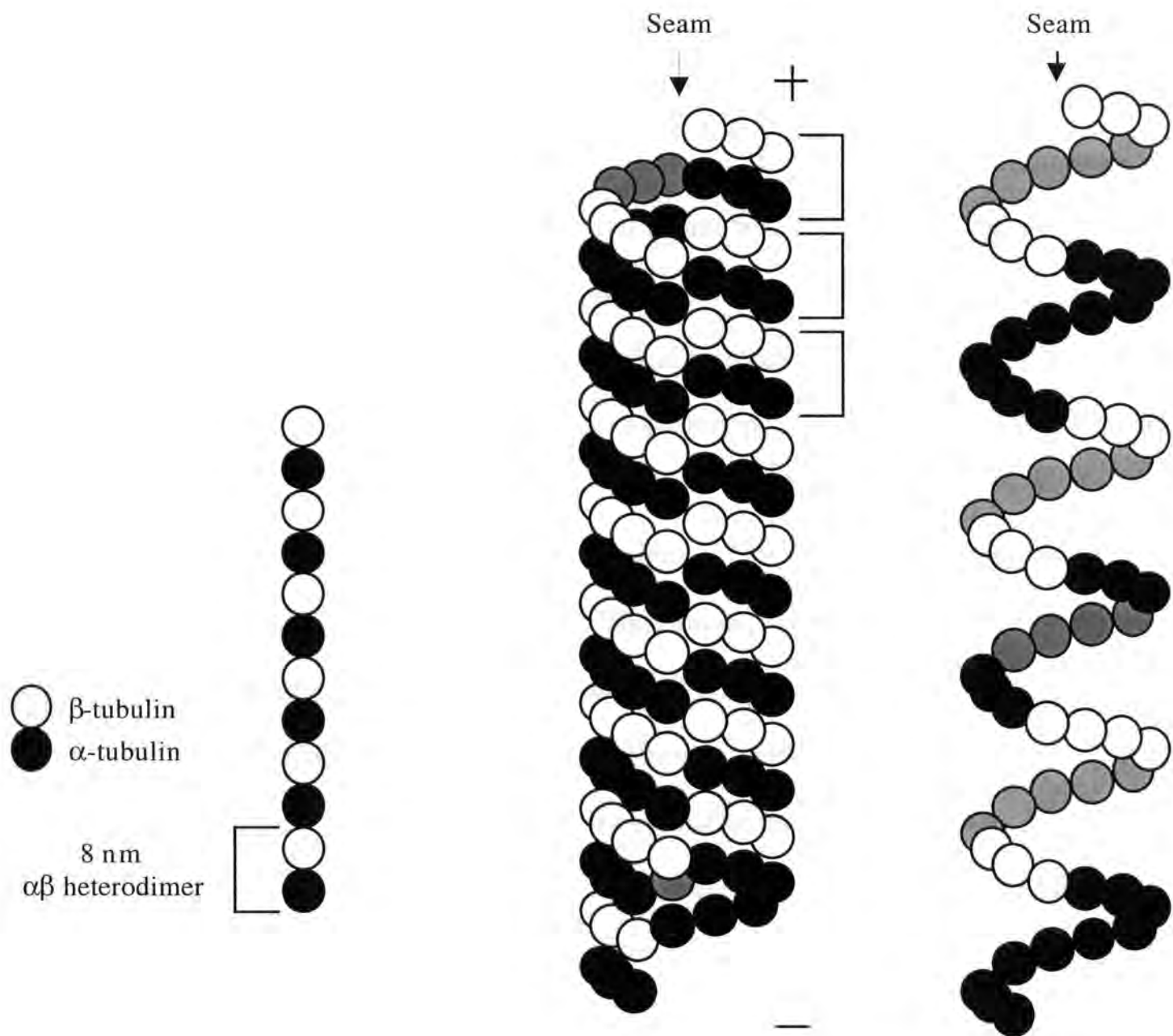


Figure 1-1. Microtubule structure. Head-to-tail interactions of $\alpha\beta$ dimers form linear protofilaments. Thirteen linear protofilaments associate laterally to form 25 nm diameter hollow cylindrical polymers (MTs). The figure shows a 13 protofilament MT with a B-type lattice with seam, the accepted lattice structure for MTs. Lateral interactions between protofilaments are α to α and β to β , except at the seam. A seam is formed because one turn of a 3-start helix results in a rise of 1.5 $\alpha\beta$ tubulin dimers (or 3 tubulin monomers). Plus and minus signs indicate MT polarity and the brackets delineate $\alpha\beta$ dimers within the MT lattice (adapted from (20)).

reviewed in (19), that stabilization of microtubules requires the presence of a GTP cap at the + end, as originally proposed in (18).

Although dynamic instability is active both *in vitro* and *in vivo*, there are differences in microtubule polymerization kinetics (reviewed in (19)). In particular, the polymerization rate of microtubules *in vivo* is much higher and yet the catastrophe frequency is high. Therefore, it is obvious that there are factors at work in the cell environment that influence the various dynamic instability parameters. Work in many labs has focused on finding these factors, and many of them are reviewed in (19) and (20).

The most extensively studied proteins that affect microtubule stability are the microtubule-associated proteins, or MAPs. The fibrous, or non-motor, MAPs are a group of homologous proteins that consist of a basic C-terminal microtubule binding domain and an acidic N-terminal projection domain. These proteins include MAP 1, MAP 2, tau, and MAP 4. Of these, all except MAP 4 are primarily located in the brain. All of these proteins promote the assembly of and stabilize microtubules. The primary MAP present in cardiac tissue is MAP 4, making it a prime candidate for study in relation to microtubule stability in the heart. For this reason, our lab has focused attention on changes in MAP 4 regulation in the hypertrophied heart. Specifically, we have found that there are increased levels of MAP 4 protein as well as mRNA in the PAB cat RV (10).

Other proteins that affect microtubule stability include the *Xenopus* microtubule associated proteins, or XMAPs, which usually promote microtubule stability; factors that increase the incidence of catastrophe, such as Op18/stathmin and XKCM1; factors such as katanin that sever microtubules, making them susceptible to catastrophe; and nucleating factors, such as γ -tubulin (reviewed in (19, 20)). With the exception of γ -tubulin, this lab has not assayed for the presence of these factors in the heart or for

changes in their amount or regulation during pressure overload-induced hypertrophy. The protein γ -tubulin shows no change in the RV during PAB of the feline (10).

While it is clear that all of these proteins may affect microtubule stability, we also searched for other, more subtle, ways that microtubule stability may be changed during pressure overload-induced hypertrophy. In particular, we considered ways that the microtubules themselves might be altered to produce changes in the way they interact with MAP 4, which we believe is an influential factor on microtubule stability in the cardiocyte. Possibilities to be considered include post-translational modifications of the tubulin proteins and/or changes in the types of tubulin proteins expressed. Tubulin proteins are modified in several different ways, including phosphorylation, tyrosination and subsequent detyrosination, polyglutamylation, and polyglycylation (reviewed in (22)). Phosphorylation seems to be the only one of these covalent modifications that might affect binding to MAPs (23), and it occurs only in the β III isotype of β -tubulin, which is not present in cardiac tissue (24).

There are several different mammalian isotypes for the α - and β -tubulin proteins, each of which is encoded by a separate gene. Because these isotypes are regulated in a tissue- and developmentally-specific manner and are highly conserved among species, it has been speculated that they may serve different functions. It has been proposed that the isotypes may show differential binding of MAPs, since they differ significantly at the carboxy-terminal 15 amino acids, which is believed to be the MAP binding region (25, 26). Therefore, we speculate that a differential isotypic make-up of the microtubules themselves might lead to changes in microtubule stability through changes in MAP binding.

The focus of this work was initially on the elucidation of possible mechanisms for increased microtubule stability during pressure overload-induced hypertrophy in the

presence of high wall stress. In particular, the aim was to answer the question of whether or not changes in regulation of the β -tubulin isotypes might directly cause changes in microtubule stability. However, further goals of this work included the elucidation of regulatory mechanisms involved in controlling tubulin production during cardiac development and hypertrophy, observing the possible effects on microtubule stability of overexpression of tubulin isotypes in non-cardiocytes, and exploration of possible effects of mutagenesis of tubulin proteins on microtubule stability in both cardiocytes and non-cardiocytes. The overall goal of the project was to explore the importance of the β -tubulin protein in the determination of microtubule stability in both terminally differentiated cardiocytes and non-terminally differentiated cells.

To achieve these goals, we designed experiments to address several questions and hypotheses. In Chapter 2, we focused our questions on the regulation of the different β -tubulin isotypes in both cardiocytes and non-cardiac cells. Our first hypothesis was that during pressure overload-induced hypertrophy, increased levels of β -tubulin proteins are caused by increased transcription of some of the β -tubulin genes, mimicking the developmental regulation of those genes. Our second hypothesis was that the autoregulatory mechanism elucidated by Don Cleveland and colleagues, whereby increased levels of free tubulin heterodimers lead to instability of the tubulin messages, is not active during pressure overload-induced hypertrophy and, possibly, at all in the terminally-differentiated cardiocyte. In Chapter 3, we wanted to answer the question of whether or not overexpression of different isotypes of β -tubulin could change the stability of the cell's microtubules. Our first hypothesis was that, in non-cardiocytes, overexpression of different isotypes of β -tubulin would not alone cause increased Taxol resistance. Our second hypothesis was that, in the adult cardiocyte, the overexpression of the β I-tubulin isotype would cause increased microtubule stability, mimicking what is

seen during pressure overload-induced hypertrophy in the heart. In Chapter 4, we addressed the question of whether or not certain β -tubulin mutants could confer decreased microtubule stability in non-cardiac cells and adult cardiocytes. Our hypothesis was that overexpression of β -tubulin mutants could confer Taxol resistance on cultured cells due to their ability to decrease microtubule stability.

CHAPTER 2: REGULATION OF THE BETA TUBULIN ISOTYPES

INTRODUCTION

This chapter focuses on the work that was done to elucidate the changes in regulation that occur for the β -tubulin multigene family during cardiac hypertrophy and development. Research in this lab has shown that during pressure overload-induced hypertrophy in the PAB feline model, there is an increase in density (14) of the microtubule network. It was initially hypothesized that increased density of microtubules might be caused by an extending force shifting the equilibrium of the polymer to the polymerized state (14, 27). However, the fact that the levels of both free and polymerized tubulin proteins increased and did so only after hypertrophic growth had begun rather than immediately following the stimulus (28), led us to hypothesize that there were factors during pressure overload-induced hypertrophy that might lead to increased stability of the microtubules themselves (10). Indeed, it was found that during PAB in the feline, there is an increased density of microtubules that occurs along with an increased level of MAP 4 (10).

While increased levels of MAP 4 could account for the change in microtubule stability, some studies in other cell systems indicate that the correlation may not be so simple. In particular, in Chinese hamster ovary (CHO) cells, overexpression of MAP 4 did not affect microtubule morphology or stability (29). However, other studies have shown, for muscle cells, that MAP 4 has a role in differentiation and morphogenesis and in the organization of the microtubule array (30). The concomitant increase in free tubulin protein levels and MAP 4 protein levels during cardiac hypertrophy was

intriguing in light of the fact that MAPs are known to be regulated coordinately with different β -tubulin and α -tubulin isotypes during neuronal development (31). This led us to believe that changes in regulation of specific tubulin isotypes might be occurring during pressure overload-induced hypertrophy.

To test this hypothesis, antibodies specific for the β -tubulin isotypes I, II, III, IVb, and V were made and used for Western blotting of proteins isolated from pressure-overloaded and normal cardiac tissue (24). The predominant β -tubulin species is β IVb, and the β I and β II proteins are expressed at low levels in the normal adult heart (24). Importantly, however, the β IVb protein remains normal during PAB in the RV, and the β I and β II proteins are increased (24). Western blotting with proteins isolated from cardiac tissue from various developmental stages of the rat showed that the hypertrophic regulation of the different β -tubulin isotypes essentially recapitulated their regulation during cardiac development (24). A common theme of hypertrophy, as mentioned before, is the upregulation of normally embryonically expressed proteins by increases in transcription. Therefore, this led to our first hypothesis: changes in the β -tubulin isotypes during pressure overload-induced hypertrophy are due to increases in transcription of the genes that encode them.

Tubulin protein levels are normally regulated by an automatic feedback loop in which increased levels of free heterodimers directly decrease tubulin message stability, leading to decreased levels of tubulin message (reviewed in (32)). The exact mechanism of this autoregulatory action has never been fully explained, but many of the specifics were elucidated by Don Cleveland's lab in the 1980's. Early experiments showed that when cells were treated with microtubule altering drugs then pulse labeled for newly synthesized proteins, if the drug treatment increased unassembled microtubule dimers then α - and β -tubulin protein synthesis decreased. However, if the drug treatment decreased

levels of unassembled dimers, α - and β -tubulin protein production increased (33, 34). Further, Cleveland's lab showed that direct microinjection of free tubulin dimers in an amount equal to 25-50% of the cell's total tubulin levels suppressed new α - and β -tubulin protein synthesis (35). This decrease in α - and β -tubulin protein synthesis corresponded with a decreased level of both α - and β -tubulin mRNA (36). Cleveland's lab further confirmed, in experiments with enucleated cells, that the autoregulation occurs through alteration of mRNA stability (37). More experiments showed that only polysome-bound mRNA's were involved (38); these mRNA's had to contain coding sequence for the first four amino acids and must be translated to at least codon 42 (39). Cleveland then proposed a model of tubulin regulation in which free tubulin heterodimers bind directly or indirectly to the first four amino acids of a tubulin protein that is being actively transcribed from a polysome-bound mRNA, causing degradation of the mRNA by an unknown mechanism (32). In our model, however, we consistently see increased levels of both free tubulin protein as well as tubulin mRNA (28). This observation led to our second hypothesis: the autoregulation of β -tubulin message stability by free tubulin heterodimers does not occur in the terminally differentiated adult cardiocyte.

To explore transcriptional regulation of the β -tubulin isotypes we used isotype-specific probes and Northern analysis to determine the levels of the β -tubulin mRNAs before and after pressure overload-induced hypertrophy. In addition, we explored possible cell culture systems to allow us to investigate directly the transcriptional regulation of the β -tubulin promoters. Finally, to study the autoregulation of tubulin message stability, we used freshly isolated neonatal and adult cardiocytes in combination with depolymerization of the microtubule network and Northern analysis of tubulin mRNA levels.

METHODS

Cloning of 3' UTRs of β I, β II, and β IV tubulin cDNAs. A diagram of the cloning strategy is shown in Figure 2-1. For β I and β IV, the oligos RBTCR1 and T7 were used for first round PCR from a feline heart cDNA library. Specifically, 1 μ l of a 1×10^{10} PFU/ ml feline heart cDNA library (Stratagene, La Jolla, CA) was amplified in the presence of 200 μ M dNTPs, 4mM $MgCl_2$, 1 μ M each primer, 1x Taq polymerase buffer and 5 units Taq DNA polymerase (Gibco BRL, Gaithersburg, MD). The reaction was cycled as follows: 4 minutes at 94° C; 5 cycles of 45 seconds at 94° C, 1 minute at 55° C, and 1 minute at 72° C; 30 cycles of 45 seconds at 94° C, 1 minute at 48° C, and 1 minute at 72° C; and 10 minutes at 72° C, in a Perkin Elmer Cetus DNA Thermal Cycler (Perkin Elmer, Foster City, CA). Eighteen μ l of the reaction was electrophoresed on a 2% agarose TBE gel, denatured, and transferred for southern blot analysis with end-labeled BTCONS oligo. An approximately 500 bp positive band was seen (data not shown). Another gel was run and this band was stabbed with a pipet tip and used for another round of PCR using the same conditions as above with the oligos BTCONS and T7. The product was electrophoresed on a gel and showed a predominant band of around 350 bp (data not shown). Fifty μ l of the PCR product was cleaned using a Promega (Madison, WI) Wizard PCR Prep kit, and the cleaned product was used for ligation into Novagen's (Madison, WI) PT7 Blue T-Vector. The ligations were transformed into DH5 α cells (Gibco BRL), mini-preps were done on several of the clones (Promega Wizard Mini-Prep kit), and the clones were confirmed by sequence analysis (Sequenase, USB, Cleveland, OH).

For β II, RTPCR was performed on total RNA isolated from cat brain using a modified version of the 3' RACE protocol described previously (40). Specifically, 2 μ g of cat brain total RNA was denatured at 70° C with 20 pmol RTPCR1 primer and put on ice for 1 minute. The denatured RNA was then incubated at roomtemperature for 10

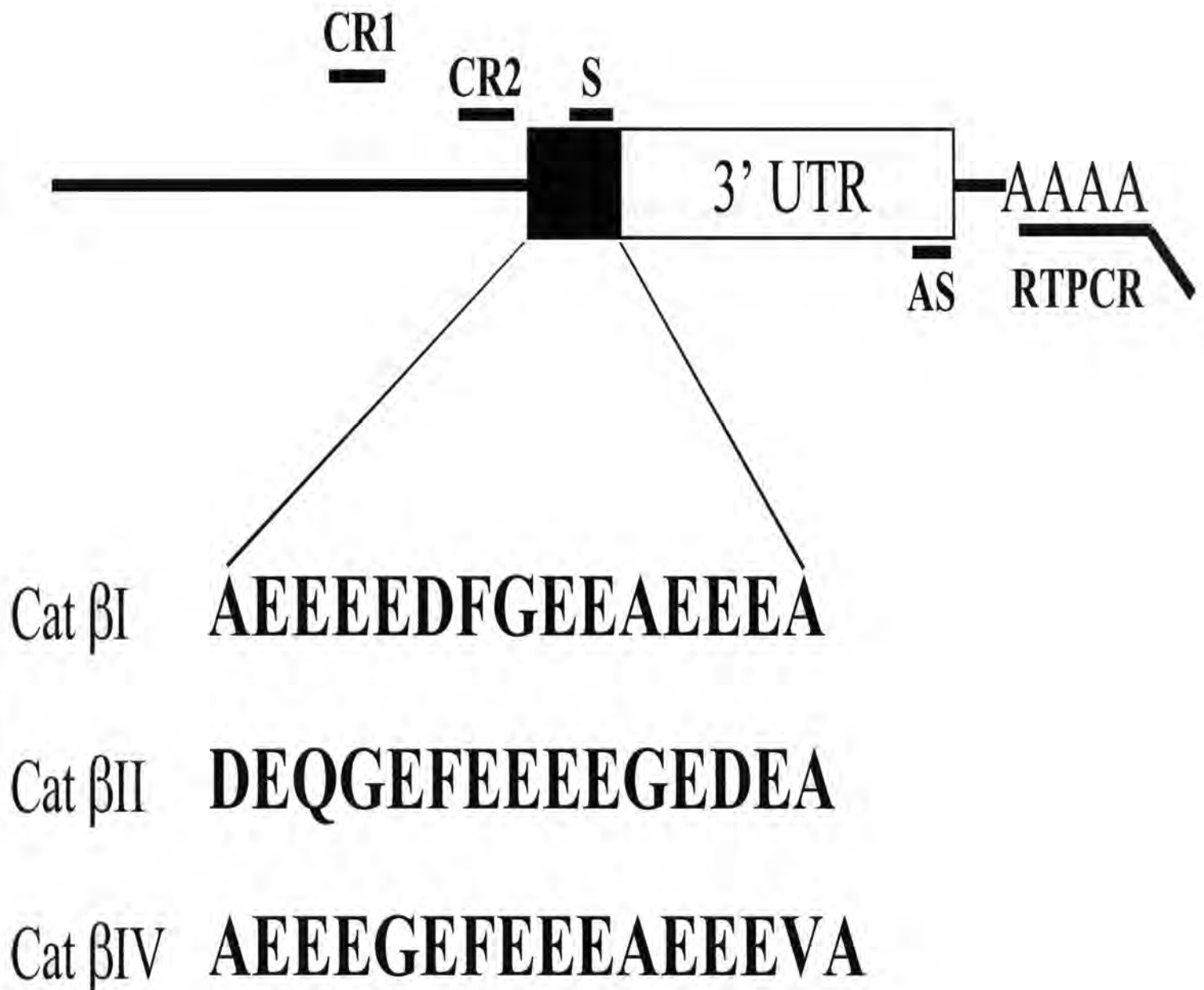


Figure 2-1. Cloning strategy for the feline tubulin partial cDNAs. PCR of a cat heart cDNA library or RTPCR of total RNA from cat brain tissue was used as outlined in the Methods section. The black box corresponds to the C-terminal amino acid isotype-defining region for each clone (the amino acid sequence for each isotype is shown below). The CR1 primer refers to the RBTCR1 primer mentioned in the text and the CR2 refers to the BTCONS. Both are sense primers from the highly conserved region just upstream of the isotype-defining regions. The RTPCR primer refers to the RTPCR1 primer mentioned in the text; another primer called RTPCR2 in the text corresponds to the non-poly A portion of this primer. Both are anti-sense primers and their sequences are given in (24). The S and AS primer sets were all isotype-specific and were used to amplify the cloned cDNAs in the presence of radioactively labelled dCTP to make double-stranded probes for northern analysis. The figure is not drawn to scale.

minutes, 43 °C for 50 minutes, and 70 °C for 15 minutes with 200 units of Superscript II reverse transcriptase (Gibco BRL), 20mM Tris-HCl (pH 8.4), 50mM KCl, 25mM MgCl₂, 2 μg bovine serum albumin, 0.5mM of each dNTP, and 10mM DTT in a 20 μl volume. A similar reaction was run without reverse transcriptase to rule out contamination with genomic DNA. The cDNAs were treated at 37 °C for 20 minutes with 2 units of RNase H (Gibco BRL) and diluted to 50 μl with dH₂O. Ten μl was then amplified in the presence of 200 μM dNTPs, 4mM MgCl₂, 1 μM each of RBTCR1 and RTPCR2, 1x Taq polymerase buffer, and 5 units Taq DNA polymerase (Gibco BRL) as follows: 5 minutes at 94 °C; 30 cycles of 40 seconds at 94 °C, 2 minutes at 52 °C, and 3 minutes at 72 °C; and 15 minutes at 72 °C in a Perkin Elmer Cetus DNA Thermal Cycler (Perkin Elmer). Eighteen μl of each reaction was then run on a 1% TBE gel and transferred overnight for Southern analysis with end-labeled BTCONS. A 450 bp band from the reaction containing reverse transcriptase hybridized to the radioactive probe, confirming the presence of a β-tubulin cDNA. No band lit up in the no reverse transcriptase reaction (data not shown). One μl of each reaction was then used for a second round of amplification using the BTCONS and RTPCR2 primers. Eighteen μl was run on a 1.6% gel, and a prominent 300 bp band was seen (data not shown). Sixty μl of this PCR product was cleaned using the Wizard PCR Prep kit from Promega, and 4 μl of the cleaned product was ligated into the PT7Blue T-vector and transformed into DH5α cells. Several transformants were sequenced, and the presence of a βII clone was confirmed.

Southern blot analysis. Tris-borate-ethylenediamine tetraacetic acid agarose gels were depurinated 15 minutes in 0.25N hydrochloric acid, denatured 15 minutes in 0.5N sodium hydroxide/ 1.5M sodium chloride, and equilibrated 15 minutes in 1M tris pH 7.5/ 1.5M sodium chloride. They were then transferred with capillary transfer using 10x sodium chloride/ sodium citrate buffer onto a Duralon membrane (Stratagene). End-labeled oligo

probes were made by incubating 1 pmol of oligo with 15 units of T4 polynucleotide kinase (Promega) and 25 μCi of α ^{32}P -dATP in 25 μl of 1x T4 PNK buffer.

Ligations. For all ligations, a 10:1 molar ratio of insert to vector was used with 50 ng of vector. Ligations were performed overnight at 12-16°C with 3 units of T4 DNA Ligase (Promega), 1X Ligase buffer, 1mM ATP, and 10mM DTT in a 10 μl volume. One or two μl were then transformed into 50 μl DH5 α Subcloning Efficiency competent cells using the manufacturer's protocol (Gibco BRL).

Right ventricular pressure overloading. Pressure overload hypertrophy of the feline right ventricle (RV) was created by placement of a 2.9 mm inner diameter band around the proximal pulmonary artery (9). Because the RV mass increase stabilizes by 2 weeks after a step increase in load (28), at 2 weeks after surgery intravascular pressures were measured in these and in control cats. Values in the systemic circulation were the same for both groups. At 2 weeks, RV systolic pressure was doubled, and there was a 59% increase in the ratio of RV to body weight; the mass of the normally loaded same animal control left ventricle (LV) was unchanged. At various time points after the start of pressure overload, the hearts were removed, RV mass was determined, and tissue was isolated from both the RV and LV free wall. Alternatively, after the hearts were removed, Ca^{2+} -tolerant quiescent cardiocytes were isolated enzymatically from the RV and LV separately (41). All operative procedures were carried out under full surgical anesthesia; all procedures and the care of the cats were in accordance with institutional guidelines.

Northern blot analysis. Isotype specific oligonucleotides were used to amplify the 3' untranslated regions of each cDNA by PCR in the presence of α - ^{32}P labeled dCTP. These labeled probes were then used for Northern blot analysis of total RNA isolated from the left and right ventricles of normal and pulmonary artery banded cats, as well as RNA from various other tissues isolated from a normal cat. Total RNA was isolated from the

RV and LV of the same hearts and from various tissues (42). The RNA samples were dissolved in 500 μ l of diethylpyrocarbonate-treated water and quantified spectrophotometrically at a 260/280 nm extinction coefficient. To assess RNA quality and to assure equal loading of RV and LV RNA for Northern blots, 3-5 μ g RNA samples were stained with ethidium bromide and run on 1% agarose check gels. We then electrophoresed 5-7 μ g RNA samples on denaturing 2% formaldehyde, 1% agarose gels followed by 1.5 hours of pressure driven blotting or overnight capillary driven blotting to nylon membrane (Duralon, Stratagene). Alternatively, 5 μ g of total RNA was applied by vacuum directly onto a nylon membrane using a slot-blotting apparatus (Schleicher & Schuell, Keene, NH). The RNA was immobilized on the nylon membrane by UV cross-linking (Stratalinker, Stratagene). The membrane was prehybridized for at least 1 hour at 42°C in a solution containing 50% (v/v) deionized formamide, 0.2% (w/v) Ficoll, 0.02% (w/v) polyvinylpyrrolidone, 6x SSC, 5% (w/v) dextran sulphate, 100 μ g denatured salmon sperm DNA, and 0.1% (w/v) SDS. The membrane was then hybridized in the same solution with at least 10 million CPM/ ml of denatured probe for 12-24 hours at 42°C. The blots were then washed two times with 2x SSC/ 0.1% SDS for 20 minutes, and once with 0.2x SSC/ 0.1% SDS at 42°C. Finally, they were washed with 0.2x SSC/ 0.1% SDS at 60°C for 15 minutes and processed for autoradiography. Each RV versus LV blot was probed with BII, BI, and BIV sequentially, and was stripped in between each probing. Finally, each blot was stripped and probed with a glyceraldehyde-3-phosphate dehydrogenase (GAPDH) probe PCR-generated from feline GAPDH cDNA.

mRNA stability. Hearts were removed from control cats and from cats 2 weeks after RV pressure overloading. Cardiocytes isolated enzymatically (41) from the RV and LV separately were incubated at 37°C in 1.8 mM Ca²⁺ mitogen-free M-199 medium at pH 7.4. The cardiocytes were either untreated or exposed to 5 μ g/ml actinomycin D for 0, 4,

8, or 18 hours. To test the effect of an acute increase in the cytosolic concentration of tubulin heterodimers on tubulin mRNA stability, further control and hypertrophied cardiocytes were simultaneously exposed to both 5 μ g/ml actinomycin D and 10 μ M colchicine for 0 or 4 hour. Total RNA was then extracted from the cells for Northern blot analysis using the three isotype-specific β -tubulin probes or a probe that recognizes the isotype-common region of feline β -tubulin mRNA (28).

Phenylephrine treatment of rat neonatal cardiocytes. Primary cardiocytes were obtained from day 2-3 neonatal rats by previously published methods (43, 44). Briefly, ventricular myocardium was isolated from 40-50 neonatal rats. The tissue was finely minced, rinsed, and placed in a suspension culture flask. A mixture of 2.4 units/ml partially purified trypsin, 2.7 units/ml chymotrypsin, and 0.94 units/ml elastase in calcium- and magnesium-free Hanks' salt solution buffered with 30 mM HEPES, pH 7.4, was repeatedly added to the suspension culture flask for six 20-minute incubations at 37 $^{\circ}$ C to dissociate the cardiocytes. After each incubation, dissociated cells were centrifuged at 500xg and resuspended in modified Eagle's medium supplemented with 10% newborn calf serum (Gibco BRL). To enrich for cardiocytes, the cells were pooled and subjected to differential plating for 90 minutes. Cardiocytes were plated at a density of 1 X 10⁶ cardiocytes per 100 mm dish and maintained overnight in modified Eagle's medium supplemented with 10% newborn calf serum, antibiotics (Penicillin 100U/ml, Streptomycin 100 μ g/ml, and Amphotericin B 0.25 μ g/ml), and essential and non-essential amino acids (Gibco BRL). The next day, the cells were switched to serum-free supplemented medium. Cells were treated with 100 μ M phenylephrine or 10 μ M verapamil for 48 hours. Cells were then rinsed 2x with ice-cold PBS, pH 7.4, and RNA was isolated (42).

Western blot analysis of tubulin isotypes. Proteins were transferred from SDS-PAGE gels at 100 V for one hour to a PVDF membrane (Millipore, Bedford, MA). The membranes were then blocked for one hour at room temperature with 10% (w/v) non-fat dry milk in tris-buffered saline/ 0.1% (v/v) Tween-20 (TBST). Next, the membranes were incubated with antibodies to the β -tubulin isotypes (24) in TBST + 1% (w/v) non-fat dry milk overnight at 4°C or 2 hours at room temperature. Additionally, an antibody that detects all β -tubulin isotypes was used (Amersham, Arlington Heights, IL). The antibody concentrations used were 1:10,000 for β IV and β II, 1:5,000 for β I, and 1:3000 for the common β -tubulin antibody. After several washings with TBST, the blots were incubated in 1% (w/v) non-fat dry milk in TBST with horseradish peroxidase-conjugated secondary antibodies (Dupont NEN, Boston, MA). The blots were then detected with ECL reagent (Dupont NEN) and subjected to autoradiography.

Skeletal muscle development of tubulin. To confirm that tubulin isotype expression during skeletal muscle development was similar to expression during cardiac muscle development, Western blotting of total protein from neonatal and adult rat skeletal muscle tissue was used. The hamstring muscles of a 1-day old neonatal and an 8-month old adult rat were isolated and flash frozen in liquid nitrogen. One hundred mg of tissue was homogenized in 2 ml of boiling lysis buffer (1% (w/v) SDS, 1 mM sodium orthovanadate, 10 mM Tris HCl, pH 7.4, and 0.5 mM DTT) for about 1 minute with a tissue homogenizer (Tekmar, Cincinnati, OH). The homogenized samples were then boiled for an additional 5 minutes and spun at 14,000 RPM in an Eppendorf tabletop microfuge for 15 minutes. The supernatant was transferred to clean tubes and protein concentrations were determined using a bicinchoninic acid assay system (Pierce, Rockford, IL) according to manufacturer's protocol. Equal amounts of total protein from

neonatal and adult tissues were electrophoresed on a 10% tris-glycine pre-cast acrylamide gel (Novex, San Diego, CA).

Differentiation of C2C12 myoblasts. C2C12 myoblasts were purchased from ATCC (Rockville, MD) and cultured according to supplier's protocol. Specifically, cells were grown in Dulbecco's modified Eagle's medium (DMEM) with 10% fetal bovine serum and antibiotics (Penicillin 100U/ml, Streptomycin 100 $\mu\text{g}/\text{ml}$, and Amphotericin B 0.25 $\mu\text{g}/\text{ml}$). When cells were at least 80-90% confluent, the serum medium was removed and replaced with DMEM +2% horse serum. After 3-9 days, cells were scraped in lysis buffer (see above) and total protein was isolated. Total protein was also isolated from non-differentiated cells, protein concentrations were determined as above, and equal amounts of protein from myoblasts and myotubes were subjected to SDS-PAGE. Western blotting was performed with the β -tubulin antibodies as described above.

Treatment of cardiocytes with colchicine. Neonatal and adult cardiocytes were isolated as described above. The cells were plated and treated in maintenance medium with 10 μM colchicine or vehicle for 12 hours. The adult cardiocytes were treated in either the presence or absence of 10^{-7} M insulin.

RESULTS

Previously, this lab has shown increased free and polymerized tubulin protein levels during pressure overload-induced cardiac hypertrophy (28, 45). We hypothesized that this was due to increased transcription of the tubulin genes. However, there are at least ten different genes that encode the various α - and β -tubulin isotypes, leaving the possibility that only some of the genes are upregulated. Studies with isotype-specific β -tubulin antibodies generated in this laboratory showed that, indeed, only some of the β -tubulin isotypes are increased during pressure overload-induced hypertrophy. Specifically, the normally embryonically expressed isotypes, β I and β II, are increased in both the free and polymerized microtubule fractions in pressure-overloaded myocardium, whereas the predominant adult isotype, β IV, remains unchanged (24).

To test the hypothesis that increased gene transcription causes increased protein levels for the different tubulin isotypes, we used Northern analysis of PA-banded cat tissue. The largest non-conserved sequences present in the β -tubulin genes are the 3' untranslated regions (UTRs), which differ from isotype to isotype and from species to species. Therefore, it was first necessary to clone the 3' UTRs of each cDNA from the cat in order to generate isotype-specific probes. Figure 2-1 shows the strategy that was used to clone the partial cDNAs (see Methods). For β I and β IV, we used oligonucleotides specific for the 3' end of the conserved region of the genes and 3' vector sequence to amplify β -tubulin 3' UTRs from a feline heart cDNA library. For β II, we used the conserved region oligos and oligo-dT for RTPCR of total cat brain RNA. PCR products were then cloned and sequenced. Isotype-specific probes were generated using PCR to amplify and radioactively label only the 3' UTRs. We ran the templates on a gel and used Southern analysis with each probe to determine the washing conditions that would ensure specificity of each probe (data not shown). Northern analysis of total RNA from various

tissues was used to determine if the probes were indeed isotype-specific. Figure 2-2 shows that the expression of the different isotypes in the cat is consistent with previous tissue studies done in the mouse (46, 47), indicating that the probes are isotype-specific. Additionally, β I, which has an alternate polyadenylation site and therefore two different transcripts (48), was the only probe which hybridized to two bands, further indicating the probes' specificity.

The data from Northern blots performed with RNA from hypertrophied versus normal tissue show that there is some increase in the levels of all heart β -tubulin isotypes during pressure overload-induced hypertrophy (Figure 2-3). The changes in RNA levels peak at 48 hours of pressure overload and have not returned to basal levels even after 2 weeks of pressure overload. However, qualitatively the data show that the changes in β I and β II seem to be much greater than the change seen in β IV. Densitometry performed on slot blots from two different 48 hour cats shows that there is at least a two-fold greater increase in the levels of β I than in the levels of β IV during hypertrophy (Figure 2-4). The data confirm that the greater amounts of β I and β II proteins seen during pressure overload-induced hypertrophy are indeed due to increases in the levels of the messenger RNAs encoding those proteins.

To test the hypothesis that changes in the tubulin mRNA levels are due to transcriptional regulatory mechanisms, we checked whether or not there are any changes in message stability in the normal versus hypertrophied cardiocyte. The isotype-specific probes were used to determine message stability for each of the β -tubulin mRNAs in hypertrophied cardiocytes isolated from the PA-banded adult felines. Figure 2-5 shows that, while the half-life of each β -tubulin isotype's mRNA is different, the half-lives are the same in the normal and pressure-overloaded cardiocytes from the PAB cat (24). This data qualitatively shows no large changes in the half-lives of the β -tubulin isotypes. This

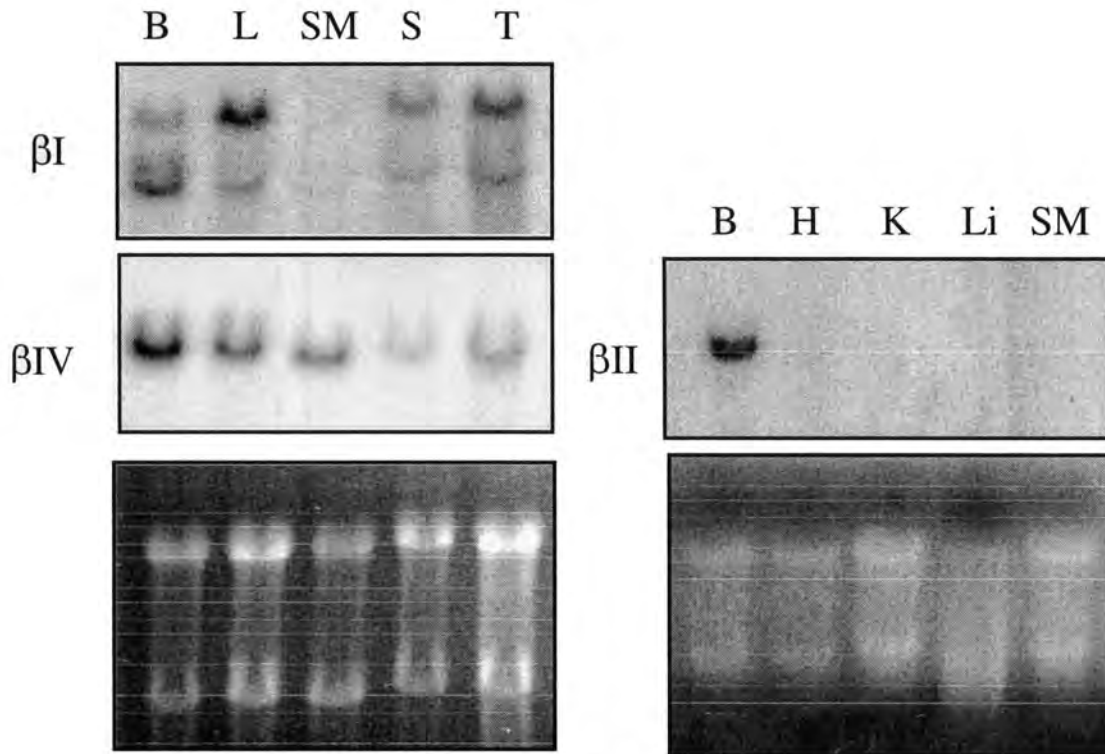


Figure 2-2. Tissue distribution of β -tubulin isotypes. These northern blots show the tissue distribution in the cat of the 3 β -tubulin isotypes which are expressed in the heart. Total RNA was isolated, run on a 1% agarose gel, transferred to nylon membranes, and probed with radioactively labeled probe as discussed in the methods. The pictures underneath show the ethidium bromide-stained gels before transfer of the RNA. B=brain, L=lung, SM=skeletal muscle, S=spleen, T=thymus, H=heart, K=kidney, and Li=liver.

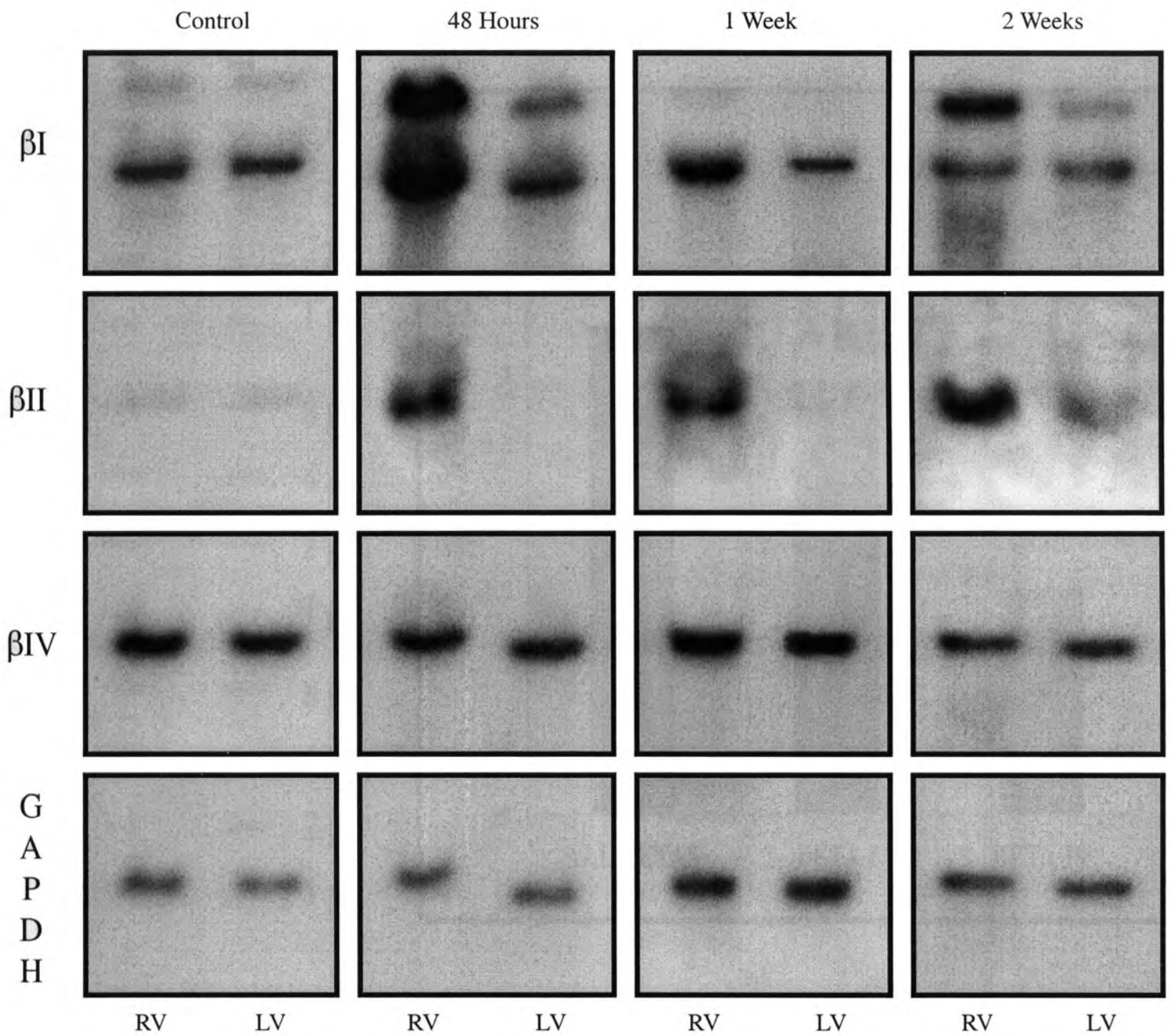


Figure 2-3. Tubulin isotype mRNA in PAB cats. These northern blots were made with total RNA isolated from the left and right ventricles of PA banded cats. The bands were left from 48 hours to 2 weeks before the cats were sacrificed, as indicated above the blots. The blots were stripped and re-probed in the order of β II, β I, β IV, and GAPDH, which was used as a control for RNA loading.

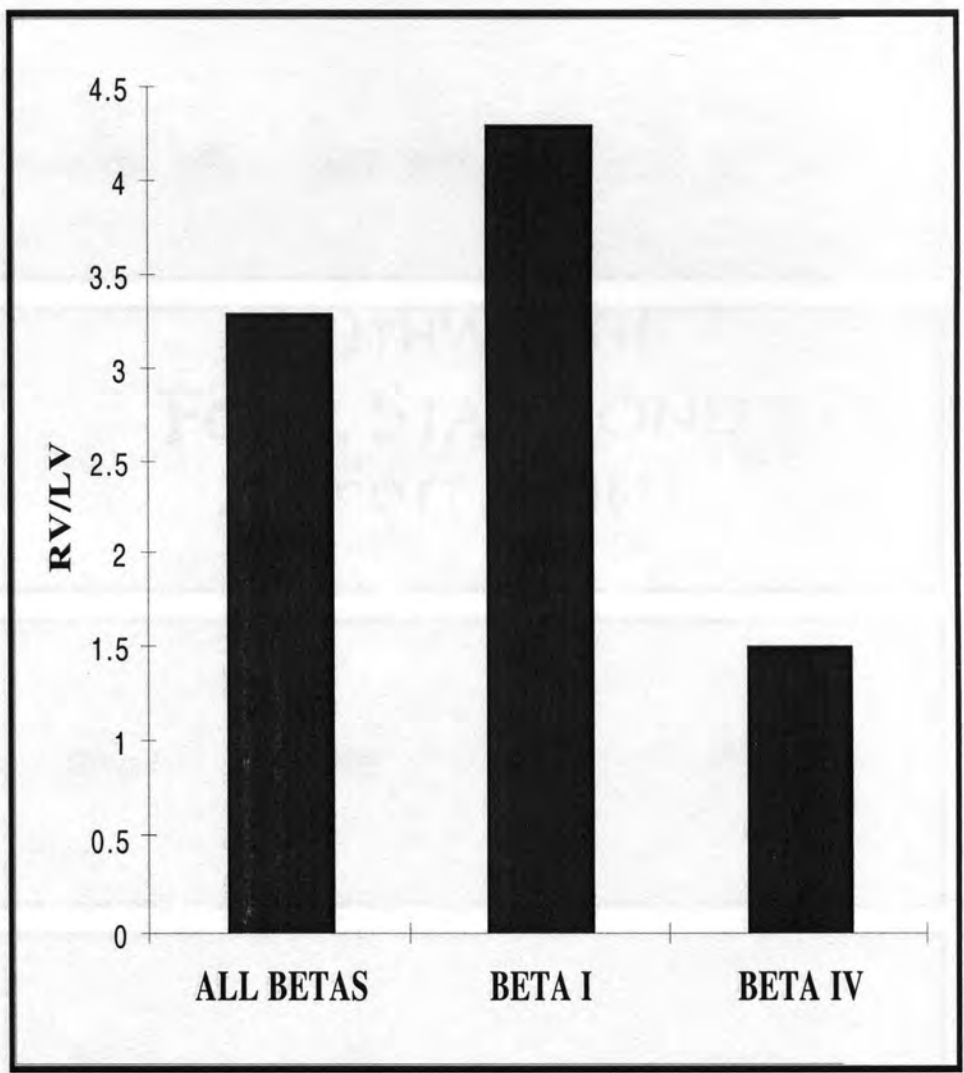
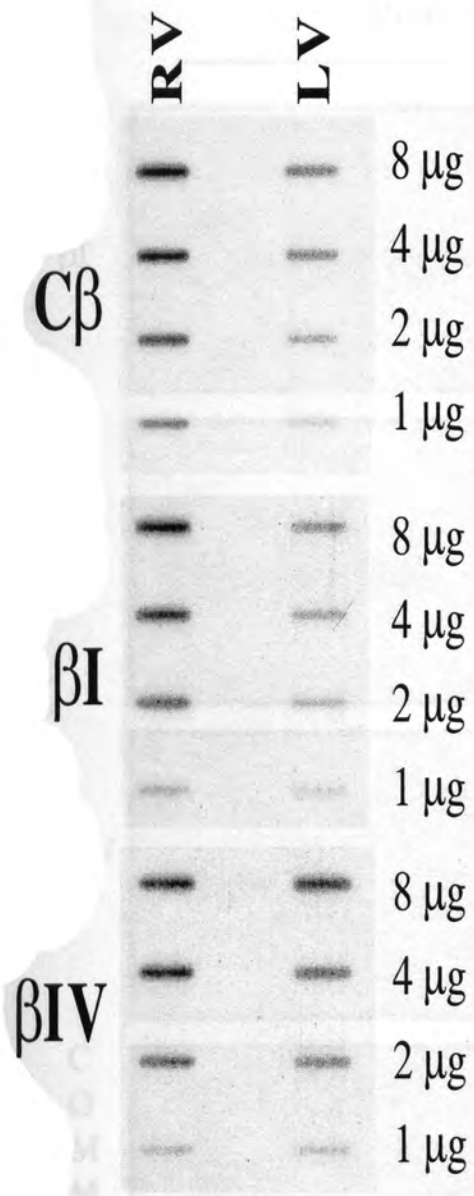


Figure 2-4. Densitometry of isotype mRNA levels in 48 hour PAB cats. Different amounts of total RNA from the LV and RV of 48 hour PAB cats were loaded on a slot blot apparatus and probed with the common β -tubulin, β I, and β IV isotype probes. Sample blots from 1 cat are shown. Densitometry was performed on one cat using the NIH Image program, and values in the linear range of the concentration blot were used to obtain the average values for the RV/ LV ratio as shown in the graph.

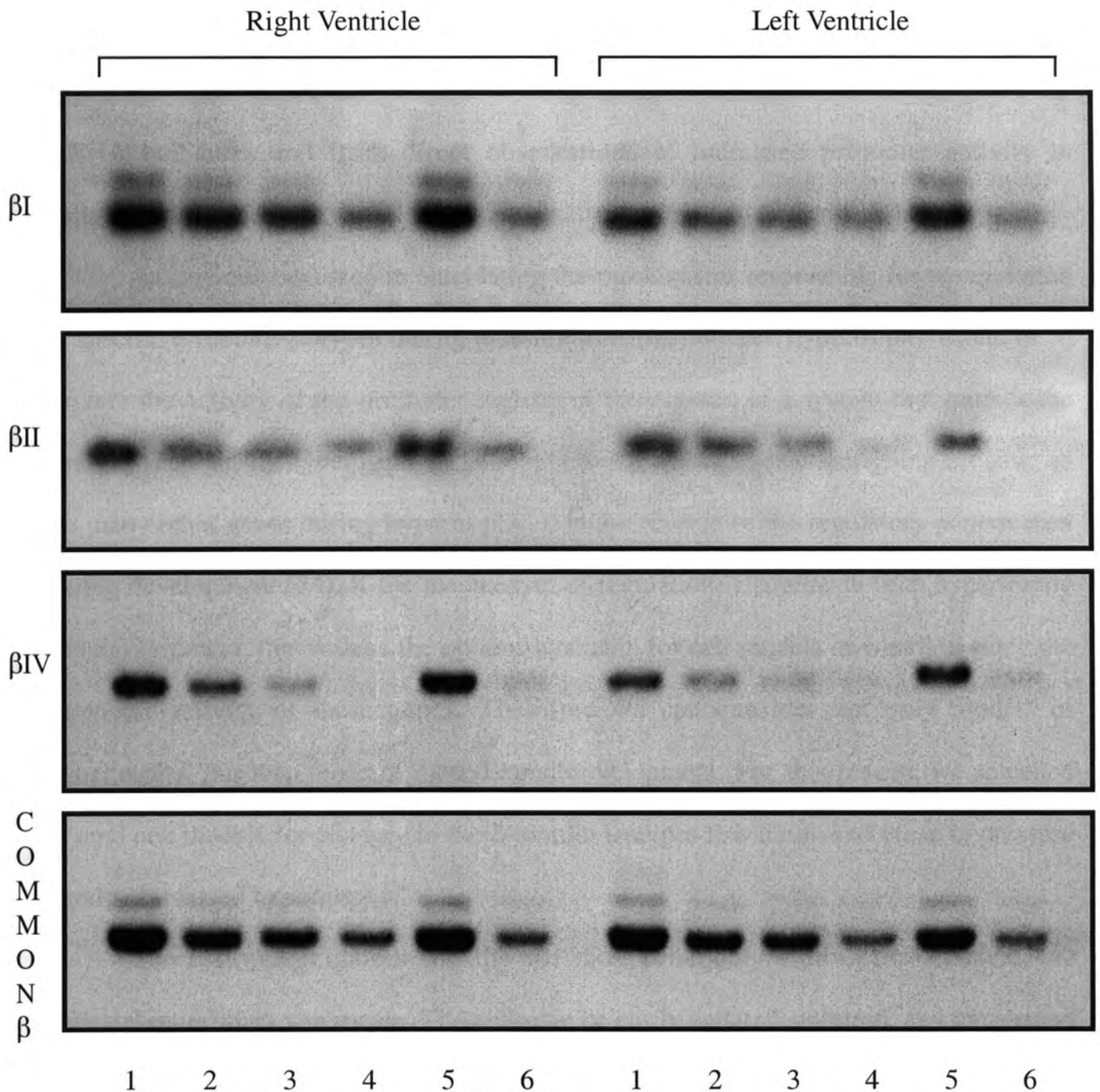


Figure 2-5. Half-life studies of the β -tubulin RNA. These northern blots show the results of half-life experiments done in the adult feline. Right ventricular and left ventricular cardiocytes were isolated from a 2-week PAB cat and treated with actinomycin D in suspension in cell media to arrest mRNA synthesis for 18 hours. Total RNA was isolated after 1=0 hours, 2=4 hours, 3=8 hours, and 4=18 hours of actinomycin D treatment. Lanes 5 and 6 show cardiocytes incubated with both colchicine and actinomycin D for 0 and 4 hours respectively.

indicates that while there may be a contribution from increased RNA stability, the bulk of the mRNA increase comes from increased production. However, definitive proof of this hypothesis must come from quantitative comparisons of the mRNA level changes to the mRNA half-lives and from direct observations of increased promoter activity in transfection experiments.

An obvious next step in elucidating the mechanisms responsible for upregulation of specific β -tubulin isotypes during pressure overload-induced hypertrophy would be to explore the activity of the promoter regions of these genes in a system that mimics the changes seen during hypertrophy. The regulation of these genes is intriguing because, as for many other genes during hypertrophy, it is the reverse of the regulatory pattern seen during development (24). If the mechanism of regulation is similar in both hypertrophy and development, this widens the options available for cell models in which to study the promoter activity of these genes. Therefore we can consider not only models of hypertrophy, but also those of mesodermal development. For this reason, we screened several cell models for changes in the β -tubulin isotypes that mimicked those of pressure overload-induced hypertrophy.

The first model chosen was the one most commonly used in the literature, the neonatal rat primary cardiocyte. The cells can be easily isolated, cultured, and transfected with plasmid DNA. Neonatal rat cardiocytes undergo hypertrophy in several different ways, including stimulation with α -adrenergic agonists, such as phenylephrine, as well as growth factors, such as IGF-1, angiotensin II, endothelin I, and others (6). In addition, hypertrophy can be induced by electrical stimulation (49) and mechanical stretch (5). All of these manipulations increase the size of the cells, lead to a more organized myofibrillar structure, and cause the upregulation of many genes normally stimulated during hypertrophy. We therefore assessed the difference in β -tubulin mRNA levels between

neonatal cardiocytes treated with an α -adrenergic agonist, phenylephrine, and cells whose contraction was arrested by a calcium channel blocker, verapamil. Primary rat neonatal cardiocytes were cultured without serum for 2 days and then treated with phenylephrine or verapamil for 48 hours before being lysed for total RNA isolation. The RNAs were then subjected to Northern analysis with a probe that hybridized to all β -tubulin mRNAs. Figure 2-6 shows a representative slot blot from 1 experiment in which cells were treated for 48 hours and summary data from densitometric analysis of 3 similar experiments. Clearly, there is a consistent increase in the levels of β -tubulin mRNA in phenylephrine- versus verapamil-treated cells. However, this increase is not nearly as much as that seen in pressure-overloaded myocardium. Similar small changes were also seen with angiotensin and endothelin-1, both of which are known to stimulate hypertrophy in cultured neonatal rat cardiocytes (data not shown). Because such small changes in transcriptional activity are difficult to reproducibly study, we decided to explore models of mesodermal differentiation.

There are several skeletal muscle cell lines available that show differentiation from myoblasts to multinucleate myotubes upon withdrawal of serum. To confirm that the changes in β -tubulin gene regulation during skeletal muscle development correlate to those seen in cardiac muscle development, we isolated total proteins from skeletal muscle tissue from neonatal and adult rats and did Western blots with the β I, β II, and β IV antibodies. Figure 2-7 shows that there is a large decrease in the levels of β I and β II, and an increase in the level of β IV from the neonatal to the adult rat. This agrees with previous data we obtained from mouse cardiac tissue (24), making a differentiating and transfectable skeletal muscle cell line a feasible candidate for studies of the β -tubulin genes.

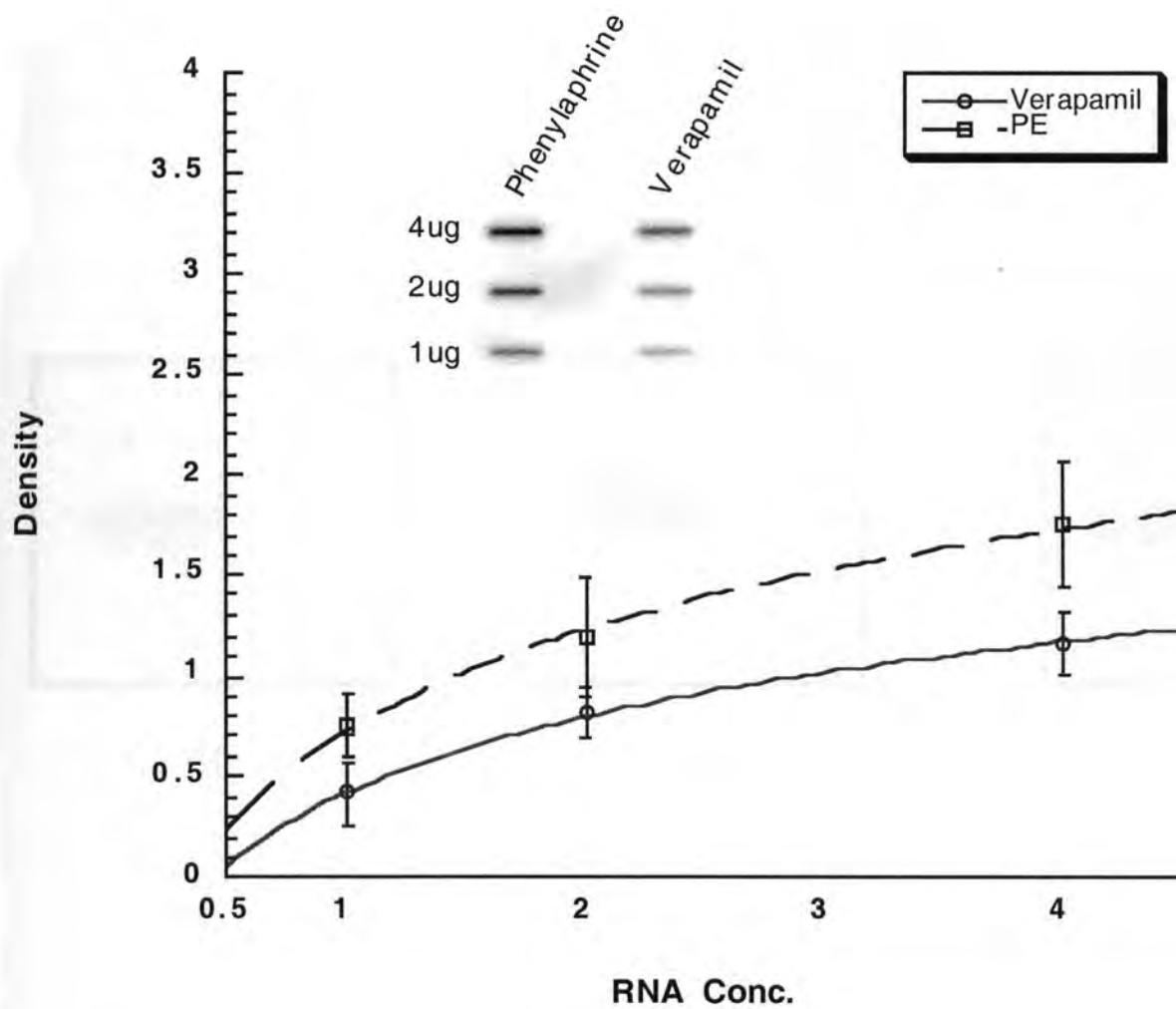


Figure 2-6. Treatment of neonatal rat cardiocytes with phenylephrine. The graph shows summary data from 3 experiments showing a small but consistent increase in the levels of β -tubulin mRNA in cells that were treated with the α -adrenergic agonist phenylephrine versus cells whose spontaneous contraction was arrested by verapamil. The inset shows a slot blot analysis from one experiment where different amounts of RNA were loaded to better quantify the signals in a linear range.

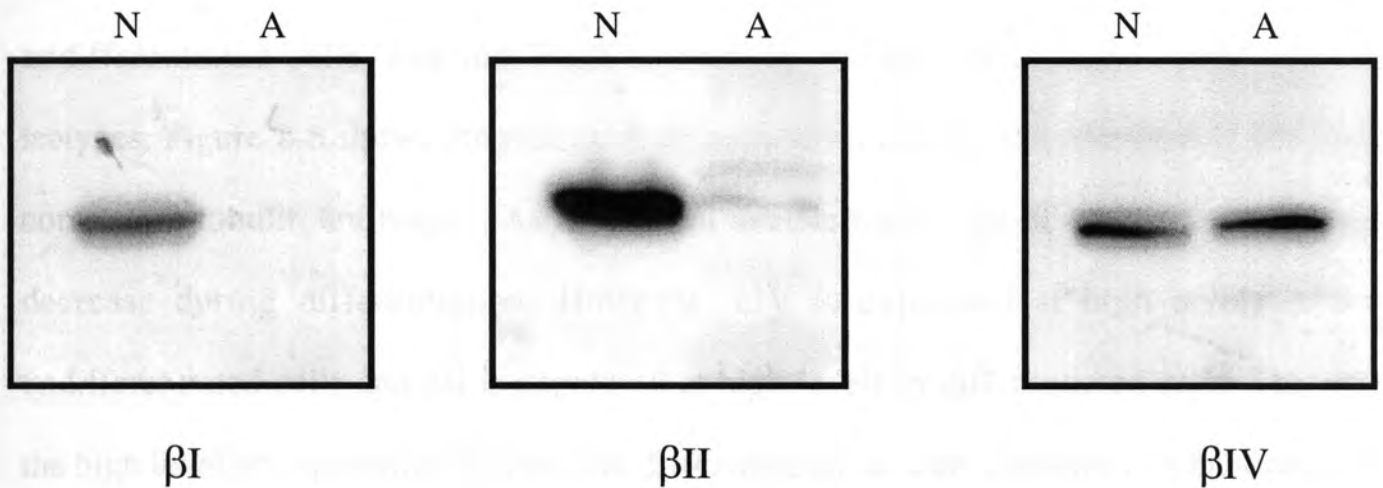


Figure 2-7. Levels of the β -tubulin isotypes in skeletal muscle tissue. Total protein was isolated from skeletal muscle tissue of neonatal (N) and adult (A) rats. Western blots were performed with the β I, β II, and β IV isotype antibodies. The data show that the isotypes have the same distribution in skeletal muscle tissue that they have in cardiac tissue.

To explore this option, we cultured a readily available cell line, the C2C12 mouse skeletal muscle cell line, in serum. Upon serum withdrawal from 100% confluent cells, the cells fused and formed large, multinucleate myotubes. However, about 30-50% of the cells remained as mononucleate myoblasts, and the myotubes that did form did not show extensive sarcomeric organization. We isolated total protein from both serum-starved and undifferentiated cells, and did Western blotting to look for changes in the tubulin isotypes. Figure 2-8 shows the results of Western blots probed with the β I, β II, β IV, and common β -tubulin antibodies. As in skeletal muscle tissue, the β I tubulin isotype does decrease during differentiation. However, β IV is expressed at high levels in the undifferentiated cells and β II is expressed at high levels in differentiated cells. This and the high level of expression for β I in the differentiated cells are contrary to what occurs in both embryonic and adult skeletal muscle and cardiac muscle tissue.

It is our suspicion that the serum-starved C2C12 cells are not homogeneously differentiated to a point where they have the same pattern of β -tubulin isotype expression that is present in adult tissue. We attempted to find conditions that would improve the percentage of fully differentiated cells. We tried addition of certain growth factors, such as insulin and low percentages of serum, removal of thyroxine, and electrical stimulation (50). While many of these manipulations improved the percentage of differentiated cells, none caused a complete switch from the embryonic to the adult pattern of β -tubulin isotype expression that is seen in skeletal and cardiac tissue. We later tried using other skeletal muscle cell lines as well as different C2C12 subclones, but none will differentiate in culture to a point where the β -tubulin isotype expression mimics that of adult tissue. We are exploring other mesodermal cell lines in an attempt to find a suitable cell model for the study of the β -tubulin promoters.

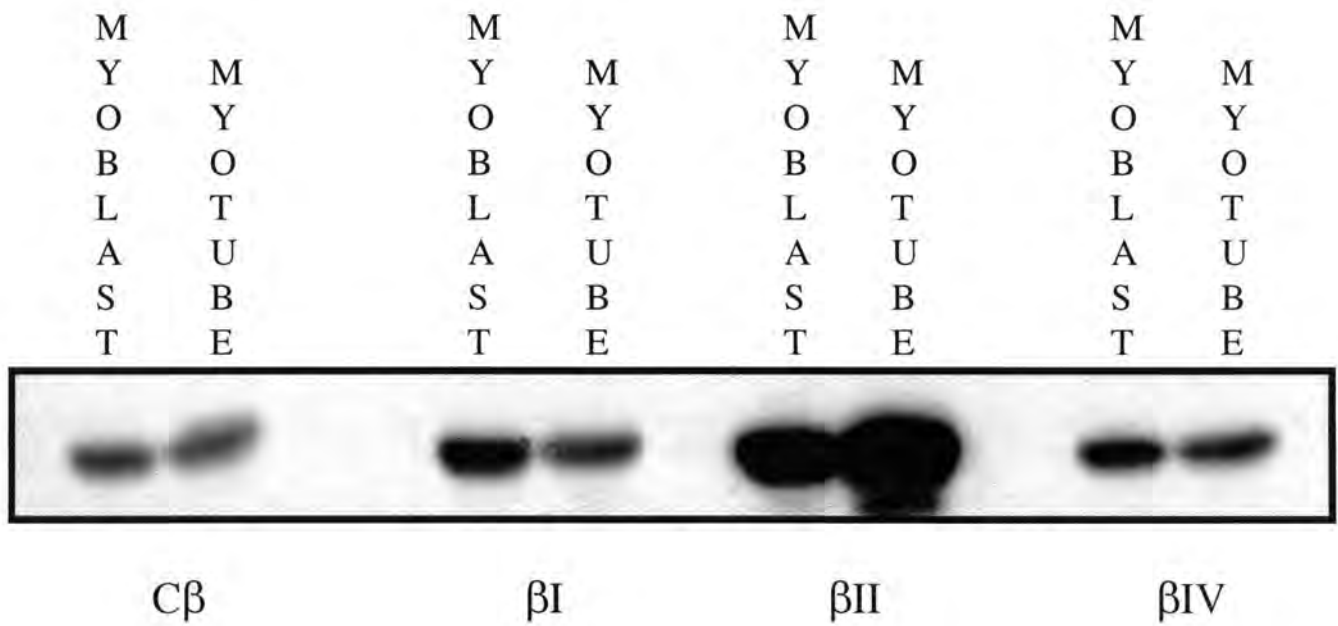


Figure 2-8. β -tubulin isotype levels in differentiating C2C12 cells. Total protein was isolated before and after serum starvation from cultured myoblasts and myotubes, respectively. Western blots were performed with antibodies to all the β -tubulins (common β , $C\beta$) and the different isotypes. The data are different than those that were obtained for skeletal muscle tissue (see Figure 2-7), especially for the βII isotype.

In the pressure overloaded right ventricle of a PAB cat, there is both an increase in the levels of free tubulin protein and the message for that protein (24, 28). This raises an intriguing dilemma about the regulation of the β -tubulin genes. Specifically, the most extensively studied mechanism of tubulin regulation to date has been the autoregulation of message stability by free tubulin protein (reviewed in (32)). According to this model, free tubulin heterodimers either directly or indirectly bind to the amino terminus of the tubulin protein as it is being translated, leading to increased degradation of the ribosome-bound message. In the pressure-overloaded myocardium, we consistently see increases in both free tubulin protein and tubulin message levels, which seems to contradict this regulatory mechanism. As we showed in Figure 2-5, while the free tubulin protein levels are increasing during hypertrophy, the message stability remains constant. This brings forward the possibility that the most well-studied regulatory mechanism for tubulin expression is not a key player in the regulation of tubulin expression in the heart.

To first test the hypothesis that this regulatory mechanism is not used in the normal cardiocyte, we treated both neonatal rat cardiocytes and adult feline cardiocytes with colchicine to rapidly depolymerize the microtubules and, therefore, cause an increase in free tubulin heterodimers. Northern analysis showed there was decreased tubulin mRNA after colchicine treatment in the neonatal cardiocyte, but not the adult cardiocyte (Figure 2-9). This led us to wonder if the autoregulation of message stability was not present in a fully differentiated cell. However, half-life studies in which cardiocytes were treated with colchicine and actinomycin D seemed to contradict this, as we saw a rapid decrease of β -tubulin message (see Figure 2-5). Since the autoregulatory mechanism relies on active protein synthesis, we repeated the colchicine studies in the adult cardiocytes using insulin as a stimulus for protein synthesis. In the presence of insulin, colchicine causes a rapid decrease in tubulin message, also shown in Figure 2-9.

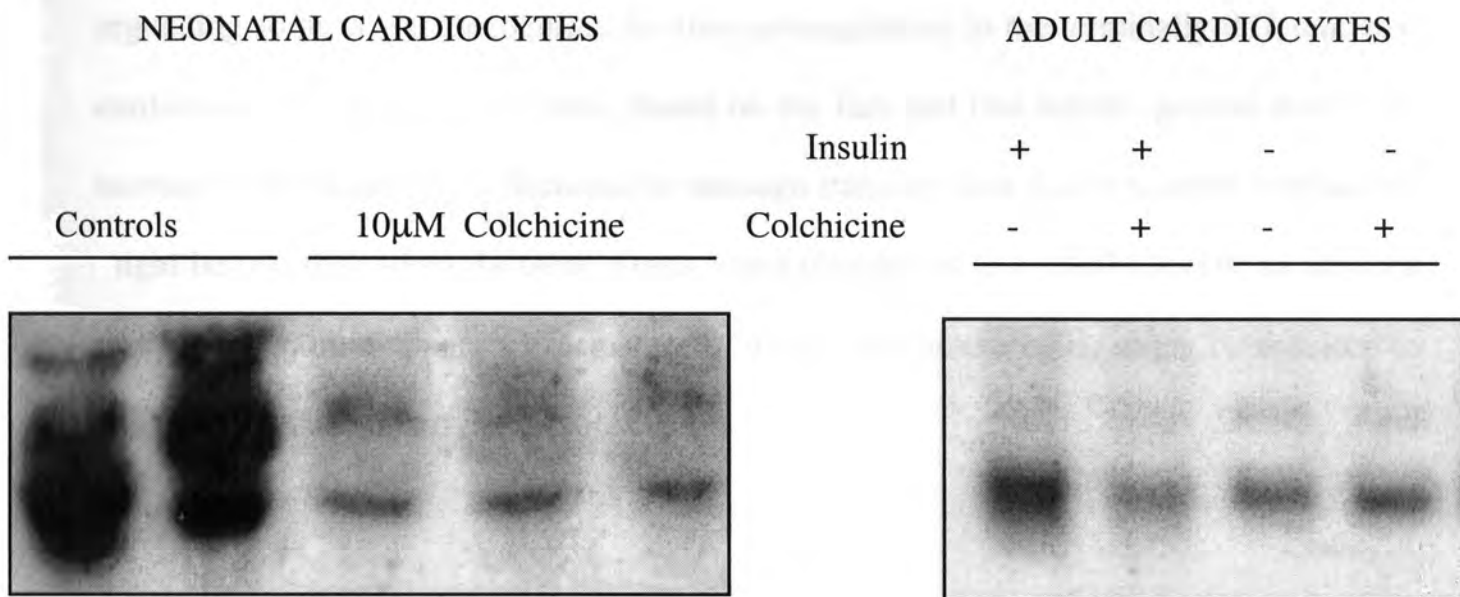


Figure 2-9. Autoregulation of tubulin message stability in neonatal and adult cardiocytes. Total RNA was isolated from cultured cardiocytes that had been treated with or without colchicine or insulin. These northern blots were probed with the common tubulin probe and show that both neonatal and adult cardiocytes display decreased levels of β -tubulin mRNA in the presence of large and rapid increases in the levels of free tubulin heterodimers. Colchicine treatment was for 12 hours.

We believe, therefore, that this regulatory mechanism can be present in terminally differentiated cardiocytes, but that it might require stimulation of protein synthesis to occur simultaneously with a rapid depolymerization of the microtubules. It is also possible, however, that insulin, through its activation of protein kinases, might be regulating some co-factor required for this autoregulation in the terminally-differentiated cardiocyte. We propose, however, based on the fact that free tubulin protein levels can increase without causing a decrease in message stability, that this regulatory mechanism might be rate-dependent. In other words, rapid changes in free tubulin levels, as are seen just before spindle apparatus formation in mitotically active cells, might be required to activate this mechanism.

DISCUSSION

Hypertrophy is the primary response of the adult heart to increased load; it involves an increase in protein synthesis rates and protein levels to promote growth and enlargement of cells that are incapable of mitosis. However, rather than just an overall increase in synthesis rates, hypertrophy involves a very finely orchestrated series of changes in both translational and transcriptional regulation that leads to a phenotype distinct from normal cells. Some changes in gene transcription have well-known functional consequences. For instance, the gene for a ribosomal transcription factor, UBF, that activates transcription of rDNA is upregulated during hypertrophy of cultured neonatal cardiocytes, an important step for the ribosome biogenesis needed for hypertrophy (51, 52). However, most changes in gene transcription during hypertrophy have less characterized effects. Study of transcriptional changes during cardiac hypertrophy are confounded by the fact that they vary from model to model and species to species (for a review of changes in gene transcription during cardiac hypertrophy see (6)).

One pattern that has emerged is the re-expression during cardiac disease of genes that are normally only expressed during development or differentiation. One classic example is the switch in expression of the myosin heavy chain (MHC) isoforms during hypertrophy in the rodent (reviewed in (6)). Normally, the adult rat ventricle expresses mostly the α MHC isoform, an isoform that has a faster ATPase activity than the predominantly expressed fetal β MHC isoform. However, during pressure overload-induced hypertrophy (but not exercise, hyperthyroidism, or volume overload-induced hypertrophy), the rat cardiomyocyte begins to express the β MHC isoform. This has functional significance in that it slows the ATPase activity and allows for a slower, more productive contraction (6). This isoform switch was not believed to occur in humans

largely because the predominant adult MHC in humans is already β MHC. However, more recent data using quantitative RT-PCR has shown that, at an RNA level at least, there is a substantial amount of α -MHC expression in normal human hearts and that this expression drops to almost nothing in failing human heart tissue (53, 54).

In light of past evidence showing a re-expression of fetal isoforms of some proteins during pressure overload hypertrophy, it was not surprising to find this phenomenon for the β -tubulin isotypes. In fact, it was a somewhat welcome finding, because it presented a great opportunity to study non-cardiac specific genes and their developmental regulation. The tubulin isotypes are regulated developmentally in other tissues as well as heart, affording an opportunity to study more basic questions about terminal differentiation. For instance, during brain development the β II tubulin gene has a 3.6-fold greater level of transcription in early development compared to adult levels (55). While posttranscriptional mechanisms seem to play the predominant role in increasing levels of specific β -tubulin isotypes during brain development (55), transcriptional regulation of the genes does occur in a developmentally specific manner. Any regulatory pathways that are found governing the expression of the tubulin genes during cardiac hypertrophy might give clues to more global mechanisms of gene regulation during growth and/or terminal differentiation.

Because the β -tubulin genes are developmentally regulated by transcription, we hypothesized that, like other embryonically expressed genes such as ANF and α -MHC, the tubulin genes are transcriptionally regulated during hypertrophy. We tested this hypothesis by analysis of the levels and stability of the β -tubulin isotype mRNAs during hypertrophy. We found that the genes for β I and β II indeed were likely regulated transcriptionally during cardiac hypertrophy. However, other mechanisms of gene regulation must be occurring, because we consistently saw increases in β IV tubulin

mRNA levels while the protein did not appear to change. Other labs have shown that β -tubulin mRNA can be degraded in an isotype-specific manner (56), so it is possible that a combination of transcriptional and post-transcriptional regulatory mechanisms are being used to control the levels of the specific β -tubulin isotypes during hypertrophy. It is also highly likely that these same regulatory mechanisms are controlling these genes during cardiac, and possibly, skeletal muscle development.

Because of possible parallels between hypertrophic and developmental regulation, we explored cellular models of hypertrophy and development to use for promoter studies of the β -tubulin genes. One model of hypertrophy, phenylephrine-treated neonatal rat cardiocytes, showed small increases in total β -tubulin mRNA levels. However, no change was seen in the protein levels of either β I or β II tubulin in this model (data not shown). Additionally, other labs have shown that, clearly, increased β -tubulin message in this model is caused by increased message stability, not changes in regulation of transcription (57). Cellular models of skeletal muscle development, in particular the serum-starved C2C12 cell line, do not display the same changes in β -tubulin isotype regulation that is seen in skeletal muscle tissue. This is probably due to the lack of homogeneity present in the population of cells on any given plate. Current studies in this lab are focused on finding a cell model that would allow for the study of the β -tubulin promoters in a way that would give insight into their hypertrophic and developmental regulation.

High levels of expression of free β -tubulin protein in the context of increased levels of β -tubulin mRNA was a surprising finding, considering that normally β -tubulin mRNA stability is decreased by increasing levels of free tubulin (reviewed in (58)). This observation afforded an opportunity to study another form of gene regulation in a terminally differentiated cardiocyte, specifically, the co-translational regulation of β -tubulin message stability by the β -tubulin protein itself. Changes in levels of free tubulin

proteins occur most notably right before mitosis, when the interphase microtubules are depolymerized in preparation for the formation of the mitotic spindle. For this reason, it seems logical that a terminally differentiated cell might lose the ability to regulate its tubulin levels in this manner, since it no longer really needs it. When we first observed a difference in the way that dividing neonatal cardiocytes and non-dividing adult cardiocytes handled depolymerization of microtubules, we hypothesized that terminally differentiated cells indeed did lack this autoregulatory mechanism. However, we found that terminally differentiated cardiocytes were able to utilize this autoregulatory mechanism when they were treated with insulin. This finding can be interpreted in several different ways, given the complex signaling pathways that are activated by insulin.

We originally designed the experiments on insulin-treated adult cardiocytes with the idea that the cells might not be down-regulating their β -tubulin mRNA after exposure to colchicine because of low protein synthesis rates. In other words, because the autoregulatory downregulation of β -tubulin mRNA levels requires active protein synthesis, stimulation of protein synthesis might be needed in these cells to engage the autoregulatory mechanism. Insulin is known to stimulate protein synthesis in a number of different ways (reviewed in (59) and (60)). Specifically, insulin acts through the tyrosine kinase insulin receptor and insulin receptor substrate (IRS) proteins to activate several phosphatidylinositol 3-kinase (PI 3-kinase) and Ras-dependent pathways. Through PI 3-kinase, the kinase mTOR (mammalian target of rapamycin) is activated, leading to the parallel phosphorylation of eukaryotic initiation factor-4E binding proteins (eIF-4EBPs or 4E-BPs) and the p70 ribosomal S6 protein kinase (reviewed in (59)). 4E-BPs inhibit protein translation initiation by competitive binding to eIF-4E, whose association with eIF-4G is important for the formation of the eIF-4F initiation complex (61).

Phosphorylation of these proteins leads to dissociation from eIF-4E and relieves this translational inhibition in many different cell types (reviewed in (59)). Insulin also stimulates translation initiation directly through phosphorylation and activation of eIF-4E (reviewed in (59)). Finally, insulin also stimulates translation initiation through activation of eIF-2B, a guanine nucleotide exchange factor for eIF2 (also reviewed in (59)).

A simple interpretation of these experiments would be that stimulation of protein synthesis is indeed required for downregulation of β -tubulin mRNA levels in response to colchicine treatment of adult cardiocytes. However, insulin has a wide array of effects on the cell that are unrelated to protein synthesis. For instance, through the Ras/Raf/MEK signal transduction pathway, insulin stimulates immediate early gene expression (reviewed in (60)). In addition, through PI 3-kinase, insulin activates the FKHR (ForKhead in Human Rhabdomyosarcoma) transcription factor family, which in turn stimulates the transcription of genes involved in apoptosis, glucose production, and entry into the cell cycle (reviewed in (62)). Finally, insulin also regulates cell morphology changes and glucose transport, mostly through PI 3-kinase dependent pathways, and often in ways that alter the actin cytoskeleton in L6 myotubes (reviewed in (60)). The exact mechanism of β -tubulin autoregulation of its own mRNA levels is unknown. Therefore, it is possible that there exists some co-factor required for this mechanism that is normally either not activated or physically unavailable at the site where it is needed in the adult cardiocyte. Insulin signaling might cause the activation or cytoskeletal rearrangements needed to engage this cofactor that hypertrophic signaling does not provide. However, the end result of these experiments shows that the terminally differentiated cardiocyte is capable of utilizing the β -tubulin autoregulation pathway.

So could there be another reason that during pressure overload-induced hypertrophy, there is concomitant increase in both message levels and free protein levels?

In particular, previous microinjection studies have shown that even increases in intracellular tubulin content of as little as 25%-50% normally invoke the autoregulatory mechanism (35). We propose that the most important factor in determining whether autoregulation of tubulin message stability occurs might be the rate at which free tubulin heterodimers appear. In other words, cells are capable of withstanding a large increase in the levels of free tubulin protein as long as the increase is gradual. We can imagine that the cardiocyte, because of the combination of growth and stress stimuli it is receiving following pressure overload, changes its transcription patterns to one of a developing cell, complete with increases in levels of tubulin mRNA. This in turn leads to a gradual increase in the level of β -tubulin proteins, and eventually increased amounts of microtubules. A sudden increase in tubulin protein levels, that occurs, for instance, after depolymerization of microtubules with colchicine, causes a decrease in tubulin mRNA stability, exactly as is seen after sudden depolymerization in mitotically active cells. This theory still allows that the autoregulatory mechanism is in place to affect the amount of tubulin message translated after the rapid depolymerization of interphase microtubules. Determination of the factor or factors that are involved in mediating this effect remains an important task for cell biologists, as it hints at a highly novel mechanism for posttranscriptional regulation of message levels.

CHAPTER 3: OVEREXPRESSION OF THE BETA TUBULIN ISOTYPES

INTRODUCTION

This chapter focuses on the work that was done to explore whether changes in β -tubulin isotype levels could directly cause changes in microtubule stability. Because mammalian α - and β -tubulin isotypes are so highly conserved across species and because they exhibit tissue- and development-specific expression, many have proposed that the isotypes have functional significance. Most of the data in the past, however, have suggested otherwise. For instance, when purified bovine brain tubulin, which includes the brain-specific β II and β III isotypes, is injected into 3T3 fibroblasts, it co-assembles with endogenous tubulin into all the microtubules of the cell (63). More strikingly, when a hybrid chicken-yeast β -tubulin was made that contained the extremely divergent C-terminus of a yeast β -tubulin, it co-assembled in 3T3 fibroblasts without alteration in microtubule function (64). There have been many similar studies in which tubulin isotypes are known to be interchangeable (65-69).

However, there are cases, both *in vitro* and *in vivo*, where tubulin isotypic makeup does have an affect on microtubule function and/or stability (reviewed in (22, 70, 71)). For instance, studies in Elizabeth Raff's lab (72) showed that, in *Drosophila*, expression of different tubulin isotypes does have an effect on microtubule structure and function. If the *Drosophila* β 3 tubulin is expressed in male germ cell lines in place of the testis-specific β 2, axoneme formation and meiotic spindle formation are blocked. If β 2 and β 3 are co-expressed in male germ-line cells, the males become sterile and have an abnormal

morphology of the outer doublet microtubules of the axoneme. This only occurs if the $\beta 3$ levels are at greater than 20% of the total tubulin population.

Studies in the lab of Richard Ludueña have focused on the question of whether or not the β -tubulin isotypes have intrinsic differences in their assembly kinetics. Immunoaffinity chromatography was used to isolate isotypically pure $\alpha\beta$ II, $\alpha\beta$ III, and $\alpha\beta$ IVa tubulin heterodimers from bovine brain (73). The purified dimers all assembled more rapidly *in vitro* than a mixed population of heterodimers (73, 74). More specifically, in the presence of tau or MAP 2, the $\alpha\beta$ II and $\alpha\beta$ III heterodimers assemble more readily than $\alpha\beta$ IV (73). Moreover, microtubules made up of $\alpha\beta$ III heterodimers are more dynamic than microtubules made up of $\alpha\beta$ II, $\alpha\beta$ IV, or mixed populations of heterodimers (75). Remarkably, mixing the $\alpha\beta$ III heterodimers with increasing amounts of $\alpha\beta$ II could modulate this dynamic behavior. At a ratio of 20% β II/ 80% β III, the microtubules behaved as did pure β III microtubules, but at a ratio of 50%/ 50%, the microtubules behaved more like β II microtubules (75).

Obviously, the presence of MAPs and other regulators of microtubule stability *in vivo* might alter any affect of intrinsic differences in β -tubulin isotypes on the kinetics of microtubule assembly. There is, however, evidence that the isotypes might confer differing stabilities on microtubules in the cell. In particular, several studies have shown differences in isotype make-up for populations of stable microtubules. In neuronal P19 cells that are induced to differentiate, there is selective sorting of β II tubulin into colchicine-stable microtubules (76). In this lab, we have data that show that β I tubulin selectively sorts into cold-stable microtubules in the heart during pressure overload-induced hypertrophy (24). Some of the most extensive correlative studies that have been made are the ones that explore changes in β -tubulin isotype expression in drug-resistant cell lines.

Cells can acquire resistance to microtubule poisons in several ways (reviewed in (77)). Studies in Fernando Cabral's laboratory at the University of Texas Medical School, Houston, TX, have reported a way in which CHO cells can acquire resistance to Taxol by altering their β -tubulin to affect microtubule stability (77, 78). Taxol is a drug that acts to disrupt microtubule dynamics by stabilizing microtubules. Therefore, these mutations in the β -tubulin molecule affect microtubule kinetics in such a way as to decrease microtubule stability, thereby counteracting the effects of the drug (79). Studies in other labs have also implicated increased expression of certain isotypes of β -tubulin for causing the resistance found in many tumor cell lines to Taxol and other microtubule poisons. These have included reports of increased β II tubulin in a Taxol-resistant murine cell line (80); reports of increased expression of β I, β II, β III, and β IVa in the drug-resistant A549 human lung cancer cell line and increased expression of β I, β III, and β IVa in Taxol-resistant human ovarian tumors (81); studies in K562 human leukemia cells that have implicated β IVa-tubulin in Taxol resistance (82); and studies in DU-145 human prostate carcinoma cells that have revealed an increase in β III and β IVa-tubulin expression in association with resistance to estramustine, another drug that affects microtubule assembly (83).

While these studies show a correlation of certain β -tubulin isotypes with stable populations of microtubules, they do not directly prove a cause and effect relationship. In light of the fact that previous studies have mostly supported the idea that the different isotypes do not affect microtubules, direct experimentation is needed to prove anything more than a simple correlation. In our studies of pressure overloaded RV tissue, we established that there is an increased stability of microtubules concomitant with an increased level of expression of the β I and β II-tubulin isotypes. Because the β II isotype makes up only 5% of the β -tubulin protein expressed after induction by pressure

overload-induced hypertrophy (24), we did not feel that it could make an appreciable difference in microtubule stability. For this reason, we focused our attention on the β I isotype and its effect on microtubule stability. In collaboration with Fernando Cabral, we have studied the effect of stable transfection and overexpression of the β I-tubulin isotype in Chinese hamster ovary (CHO) cells. By adenoviral infection, we have also studied the effect of overexpression of the β I tubulin isotype in the adult cardiocyte. We felt that it was important to study the effects of β I expression in this system compared to the effects in cardiocytes, because a discrepancy seemed to exist between our data and data generated in other labs as to the possible consequences of β I-tubulin expression. Specifically, we have shown increased expression of β I in the presence of hyperstable microtubules, and even shown sorting of β I into cold-stable microtubules (24). Other labs, however, have shown increased expression of β I in mitotically active cells that are resistant to Taxol, a microtubule-stabilizing drug. In the previously mentioned studies in F. Cabral's lab, it has been well established that cells with resistance to Taxol due to β -tubulin mutations have hypostable microtubules. Presumably, changes in isotype expression, if they were indeed causative of drug resistance, would also lead to decreased stability of the microtubules.

We felt that it was possible that β I-tubulin overexpression would lead to altered stability of microtubules primarily because of increased affinity for MAPs. Therefore, there might be cell-specific modulation of the response to β I-tubulin overexpression based on what factors are present in the cell's milieu. In addition, it seemed likely that cells that are resistant to certain drugs have many changes in their phenotype other than just β -tubulin composition, due to the way they are selected. To further elucidate effects of β I overexpression in different systems, we asked the following questions: does overexpression of β I or other tubulins in CHO cells directly cause increased resistance to

Taxol and does overexpression of β I tubulin in the adult cardiocyte directly cause increased microtubule stability?

METHODS

Construction of β -tubulin isotype-specific overexpression vectors. CHO CBI is a previously described class I β -tubulin cDNA (84, 85). It was modified to express a 9 amino acid hemagglutinin (HA) tag at the C-terminus (86). Mouse class II and IVb β -tubulin cDNAs (47) were originally named M β 2 and M β 3 and were kindly provided by Nicholas Cowan at New York University, NY, NY. To obtain regulated expression, pcDNA3 (Invitrogen, Carlsbad, CA) was modified to incorporate the features of a tetracycline regulated vector system and the new plasmid was named pTOPneo; this vector contains a minimal cytomegalovirus (CMV) promoter downstream from 7 copies of the *tetO* operator sequence for tetracycline regulated expression (87). A 1.5 kb Hind III/Not I fragment from plasmid BlskHABI (86) containing the entire HABI-tubulin coding sequence was cloned into the unique Hind III/ Not I sites of pTOPneo to create pTOPneo-HABI. This vector conveniently contains, upstream of the HA tag, a blunt-end Eco47 III restriction site. The BII and BIVb cDNAs were then cloned into the same vector in place of the BI cDNA in-frame with the HA tag as follows. PCR was used to amplify the cDNAs provided by N. Cowan using primers that inserted a 5' Hind III site and left a blunt 3' end. This was accomplished using *Pfu* polymerase (Stratagene), which does not leave a single A overhang. The PCR products were then gel-purified, cleaned using the Qiaquick Gel Purification kit (Qiagen, Valencia, CA), and ligated into the Hind III/Eco47 III digested pTOPneo-HABI vector. The full length of the coding region for each construct was then sequenced to ensure that no errors were introduced during the PCR amplification. The β -tubulin isotype-specific cDNAs were now under the control of a tet-regulated CMV promoter; in addition, this vector contained a G418 resistance gene to allow for selection of stable transfectants.

Construction of the pTOPpuro-tTA vector. A plasmid carrying the coding sequence of the tetracycline-regulated transactivator (tTA) was made by first replacing the neomycin resistance gene of pTOPneo with the puromycin resistance gene from the vector pPUR (Clontech, Palo Alto, CA), to create pTOPpuro. The sequence for tTA was then added by cloning a 1 kb Eco RI/ Bam HI fragment from the plasmid pUHD 15-1 (87) into pTOPpuro to create pTOPpuro-tTA. This plasmid was transfected into CHO cells to create the CHO cell line tTApuro 6.6.

Transfection, selection, and maintenance of CHO cell lines. The growth medium for all cells was alpha modification of minimum essential medium (α MEM) containing 5% fetal bovine serum, 50 U/ml penicillin, and 50 μ g/ml streptomycin (all from Gibco BRL). Plasmid DNA was prepared using the QIAfilter Plasmid Maxi Kit (Qiagen) according to the manufacturer's instructions, and used to transfect CHO strain tTApuro 6.6a. Transfections were carried out using 1 μ g of plasmid DNA (0.2 μ g in the case of HA β I_{L228F}) and Lipofectamine (Gibco BRL) according to the manufacturer's instructions, except that the growth medium contained 1 μ g/ml tetracycline (Sigma, St. Louis, MO) to prevent expression of the transfected DNA until time of analysis. Stable transfected cell populations were selected and maintained at 37° C, 5% CO₂ in growth medium that contained 1 μ g/ml tetracycline and 2 mg/ml G418 (Gibco BRL).

Selection of Taxol-resistant cells. To determine whether expression of specific β -tubulin isoforms could confer Taxol resistance, CHO strain tTApuro 6.6a was transfected with each of the HA tagged cDNAs in parallel. Cells from each transfection were then trypsinized and reseeded in duplicate into 6-well dishes containing normal growth medium with tetracycline (5-10 X 10² cells), medium with G418 plus tetracycline (5-10 X 10⁴ cells), or medium with 0.2 μ g/ml Taxol and no tetracycline (5-10 X 10⁴ cells). The dishes were incubated at 37° C for 7 days until colonies appeared. Wells that failed to

produce any visible colonies were incubated an additional week and scanned microscopically to be certain we would not miss any slow growing colonies. Cells from one set of duplicate wells were trypsinized and used for propagating the culture for further testing, and cells in the second set of wells were stained with methylene blue as previously described (88) to count the number of resistant colonies.

In addition to their direct selection, selections for Taxol-resistant cells were also carried out on cell populations that had previously been selected in G418 and were therefore enriched for cells expressing the transfected β -tubulin. In this case the cells selected in G418 plus tetracycline were trypsinized and reseeded in duplicate into 6-well dishes at high ($4\text{-}5 \times 10^3$) and low (150-200) cell density in normal medium without tetracycline for 6 hours to allow induction of transgene expression. Prior studies indicate that 3 hours is the earliest time that significant production of the transfected tubulin can be detected (F. Cabral, unpublished data). Following the 6-hour induction, one set of duplicate wells was changed to medium containing $0.2 \mu\text{g/ml}$ Taxol while the other set of wells remained in normal medium without tetracycline.

Western blotting of CHO cell extracts. To measure the relative accumulation of transfected versus endogenous β -tubulin, transfected cell populations that had undergone selection were seeded into 24-well dishes in the continued presence or absence of tetracycline and incubated overnight (~20 hours) at 37°C . The medium was aspirated, the cells were washed 2 times with phosphate buffered saline (PBS, Gibco BRL), and the cells were then lysed by the addition of $100 \mu\text{l}$ of hot (100°C) sodium dodecyl sulfate (SDS) sample buffer (89). Protein and DNA in the lysate were precipitated by the addition of 5 volumes of cold (4°C) acetone/ NH_4OH (20/1), the DNA was fished out with a thin gauge needle, and the protein was centrifuged at 12,000 g for 5 minutes.

The pellet was redissolved in 30 μ l of SDS sample buffer and 5-15 μ l were run on a 7.5% polyacrylamide SDS minigel (Bio-Rad Laboratories, Hercules, CA). Proteins were electrophoretically transferred onto a nitrocellulose membrane and probed with a mixture of mouse monoclonal antibodies to β -tubulin (Tub 2.1, 1:2000 dilution, Sigma) and actin (C4, 1:5000 dilution, ICN Biomedicals, Costa Mesa, CA). This was followed by incubation in peroxidase-conjugated goat antimouse IgG (1:2000 dilution, Cappel Laboratories, Cochranville, PA) and detection by chemiluminescence (Kirkegaard & Perry Laboratories, Gaithersburg, MD) using the manufacturer's instructions.

Immunofluorescence of CHO cells. Cells were grown on glass coverslips to approximately 70% of confluence and fixed in methanol (-20° C) for at least 10 min as previously described (86). The primary antibody used was mouse monoclonal 12CA5 (Boehringer Mannheim Corp., Indianapolis, IN), specific for the HA tag. This was followed by fluorescein-conjugated goat antimouse IgG (Cappel Laboratories). Photographs were taken on TMAX 400 film (Eastman Kodak, Rochester, NY) using an Optiphot microscope equipped with epifluorescence and a 40X fluor objective (Nikon Inc., Melville, NY).

The pAd.CMV-LINK system for construction of recombinant adenovirus. We used the system developed by Chartier *et. al.* (90) to construct adenoviruses for use in the infection of adult feline cardiocytes. This system employs recombination of a vector that contains most of the adenovirus genome with a shuttle vector that has a CMV promoter upstream of the E3 region as well as a multicloning site and SV40 polyadenylation signal in place of the E1 region. The shuttle vector recombines in bacteria through homology in the 0-1 map unit and 9-16 map unit regions. The resulting recombinant adenovirus contains most of the DNA for the Ad 5 serotype adenovirus, minus the E1 region, which is replaced by the cloned gene along with a poly A sequence. Both the parent adenovirus

genomic vector and the shuttle vector contain sequences that allow them to be propagated in bacterial culture supplemented with ampicillin. Therefore both are linearized before recombination to prevent contamination of non-recombined ampicillin-resistant colonies.

Mutagenesis of HA-tagged β IV cDNA to remove an internal Nar I site. Because recombination with adenoviral DNA required linearization of the pAd construct with Nar I and Nhe I, we needed to remove any Nar I or Nhe I sites in the tubulin cDNAs before cloning them into the pAd.CMV-LINK.1 shuttle vector. There was only one such site, a Nar I, at nucleotide number 49 of the β IV cDNA coding sequence. We used PCR primers to mutate the C at nucleotide number 51 to a T in order to remove this sequence without affecting the amino acid sequence. Mutagenesis was carried out using the Quickchange Site Directed Mutagenesis kit from Stratagene.

PCR of cDNA for cloning into pAD.CMV-LINK.1 shuttle vector. HA-tagged β I and β IV tubulin cDNAs were amplified using Pfu polymerase (Stratagene). Briefly, the pTOPneo-HABI and pTOPneo-HABIV vectors were amplified with 500 nM each of PCR primers that inserted an upstream blunt end and a downstream Hind III site. The reactions included 200 μ M of each dNTP, about 200 ng of template DNA, 2.0 units of Pfu Polymerase, and 1x Pfu polymerase buffer. The reactions were cycled 1x 45 seconds at 94°C; 25x 45 seconds at 94°C, 45 seconds at 65°C, and 2.5 minutes at 72°C; and 1x 10 minutes at 72°C. The products, by virtue of the primer sequences, had a 5' blunt end in the 5' UTR of each cDNA and a 3' Hind III site just past the stop codon following the HA tag. The products were ethanol-precipitated, resuspended in a small volume of ddH₂O, and electrophoresed on a 1% agarose gel. The 1.2 kb products were then cut out of the gel with a scalpel, and the DNA was isolated with the Qiaquick Gel Extraction kit from Qiagen. The products were then digested with 5 units of Hind III at 37°C overnight. The digested DNAs were purified using the Qiaquick PCR Purification Kit (Qiagen) and

ligated into an Eco RV/Hind III-digested pAd.CMV-LINK.1 vector. The clones were transformed into *E. coli* DH5 α cells, colonies were picked, and clones were screened for the correct sequence throughout the entire coding region to ensure that no unwanted mutations were introduced during PCR amplification. To verify that the CMV promoter constructs were capable of overexpression in the 293 kidney cell line, 4 μ g of each DNA was transfected into an 80% confluent 60 mm plate of cells using Lipofectamine (Gibco BRL), according to manufacturer's protocol. After 48 hours in 10% fetal bovine serum, the cells were scraped into 1x SDS loading buffer (89) to isolate total protein. Equal amounts were then loaded onto 7% Tris-acetate gels (Novex), along with extract from non-transfected 293 cells, and Western blotting was performed with an anti-HA polyclonal antibody (Zymed, San Francisco, CA, USA), at a 1: 2000 dilution.

Recombination of the shuttle vector with adenoviral DNA. The viral DNA vector pTG3602 was recombined with the pAd shuttle vector constructs in the *E. coli* strain BJ5183. Briefly, 200 μ l of competent cells were transformed with 50 ng of Cla I linearized pTG3602 and 2 μ g of the Nar I/Nhe I fragment from the pAd.CMV/HAB β I and β IV vectors. Colonies were screened for positive recombinants by restriction digestion with Xho I and southern blotting using probes specific for the coding regions of the β -tubulins. Positive clones were then transformed into *E. coli* DH5 α cells, and large-scale DNA isolations were done with each clone (Qiagen). This DNA was then used to manufacture adenovirus by transfection into 293 cells.

Production of adenovirus. Approximately 2 μ g of Pac I digested β -tubulin/adenoviral DNA recombinant was transfected into 50% confluent 293 cell cultures in 60-mm plates using Lipofectamine. The cells were fed every 2 days until plaques started to form (7-10 days post-transfection). When the cells were almost completely lysed (approximately 12 days post-transfection), they were scraped into their media and taken through 3 freeze-

thaw cycles in liquid nitrogen. The cell debris was then centrifuged for 5 min. at 900g and some of the supernatant was added to 100% confluent cultures of 293 cells on 60-mm dishes. Protein was isolated after 1 day to check for expression of HA-tagged β -tubulin by Western blot. The remaining supernatant was used to overlay confluent 293 cells for plaque purification. After a 4-hour incubation with 1-3 ml of viral supernatant, the cells were overlaid with 0.5% agarose/DMEM. After about 7 days, individual plaques were picked and used to infect 60-mm dishes of confluent 293 cells. When the cells were lysed, the overlying media was used to infect a 150-mm dish of confluent 293 cells. Again, after lysis, the media was used to infect 15-20 150-mm dishes for a large-scale adenoviral preparation. The cells were scraped after 1 day (when they began to show cytotoxicity, but had not yet lysed) into 5 ml PBS per dish, and the cells were centrifuged and resuspended in 10 ml total PBS. The cells were then taken through several freeze-thaw cycles. The cell debris was centrifuged at 900 g for 5 min., and the supernatant was put onto a CsCl gradient as follows: 500 μ l of 1.5 g/ml CsCl, 3 ml 1.35 g/ml CsCl, 3 ml 1.25 g/ml CsCl, and 5 ml viral lysate. The tubes were spun in an ultracentrifuge at 35,000 RPM for 2 hours at 4°C with no brake. The white adenoviral band was withdrawn and dialysed overnight against PBS with 10% glycerol. The virus was then aliquotted and stored in liquid nitrogen.

Adenoviral infection of feline adult cardiocytes. Adult feline cardiocytes were isolated as in chapter 2. The cells were plated on laminin-coated coverslips at a density of 3.1×10^4 cells/ cm^2 or on laminin-coated cell culture dishes at a density of 1.9×10^5 cells/ cm^2 in M199 media with antibiotics. After 18-24 hours, the cells were placed in Piper's media (5 mM creatine, 5 mM taurine, 2 mM carnitine, 100 μ M ascorbate, 0.25 mM phenylalanine, 0.2% bovine serum albumin, 10 μ M AraC, 0.1 μ M insulin, and 100 IU/ml Penicillin-Streptomycin in M199 medium) with differing amounts of adenovirus. After 18-24 hours,

the medium was changed to Piper's without adenovirus. The cells were then cultured for different times, depending on the experiment.

Western blotting of protein isolated from infected cells. Protein was isolated from adult feline cardiocytes and 293 cells using 1% SDS lysis buffer as described in chapter 2. Equal amounts of protein were then loaded onto a 7% tris-acetate gel (Novex). After transfer to PVDF membrane the blots were probed either with an antibody to β -tubulin, as described in chapter 2, or a polyclonal rabbit antibody to the HA tag as described above. In one experiment, the proteins from infected adult cardiocytes were probed with the antibodies to the tyr-, glu-, and $\Delta 2$ -tubulin proteins at a concentration of 1:10,000, 1:2000, and 1:10,000, respectively (10).

Immunofluorescence of adult feline cardiocytes. Cells plated on glass coverslips were extracted in 1% Triton X-100 in microtubule stabilization buffer, washed 3 times in the same buffer, and fixed in 3.7% formaldehyde as described in (10). For double-labeling of the HA tag and α -tubulin, the coverslips were blocked in 10% donkey serum in 0.1 M glycine/ PBS, and incubated overnight at 4°C with 1:100 dilution of monoclonal HA antibody (12CA5, Boehringer Mannheim, Indianapolis, IN) and 1:50 dilution of an α -tubulin antibody (YL1/2, Harlan, Indianapolis, IN). The cells were then washed 3X in PBS and incubated 2 hours at room temperature with FITC-conjugated anti-mouse IgG and Cy3-conjugated anti-rat IgG (Jackson ImmunoResearch Laboratories, West Grove, PA). The cells were then washed 3X in PBS and mounted on glass microscope slides in a glycerol mounting solution (Molecular Probes, Eugene, OR). For double-labeling of the HA tag and post-translationally modified α -tubulin molecules, the primary antibodies were the HA antibody (Boehringer Mannheim, 1:100) and a 1:50 dilution of either the tyr-, glu-, or $\Delta 2$ -tubulin antibodies (10); the secondary antibody for the α -tubulin staining was a Cy3-conjugated anti-rabbit IgG (Jackson). For double-labeling of the HA and Myc

tags, a 1:100 dilution of a polyclonal anti-myc antibody (Upstate Biotechnology, Lake Placid, NY) and a Cy3-conjugated anti-rabbit secondary (Jackson) were used. For some of the experiments, double-labeling of the HA tag and unmodified α -tubulin protein was achieved by using the same primary antibodies mentioned above, but using an FITC-conjugated anti-rat IgG and a Cy3-conjugated anti-mouse IgG. Confocal micrographs were then made using an Olympus Fluoview Confocal Microscope (Olympus Optical Co., Ltd., Tokyo, Japan).

Nocodazole treatment of adult cardiocytes. Before fixation and immunofluorescence, the cells were treated for 0, 1, 1.5, or 2 hours in 0.3, 3.0, or 30 μ M nocodazole in M199 medium. The extraction procedure was then carried out in the continual presence of the same concentration of nocodazole.

Cold-stability of microtubules in adult cardiocytes. Before fixation and immunofluorescence, the cells were treated for 0, 0.5, 1, 1.5, or 2.0 hours at 4°C, 6°C, or 8°C in 25mM HEPES buffered M199. The extraction procedure was then carried out with ice-cold buffers, except for the untreated control cells.

RESULTS

Because growth of mitotically active cells is often inhibited by changes in the microtubular cytoskeleton, we wanted to ensure that initial transfections in CHO cells were carried out in the absence of exogenous gene overexpression. For this reason, we cloned the β -tubulin isotypes into a vector whose expression was controlled. We used a tetracycline-regulated vector originally described by Gossen and Bujard (87) that contains a CMV promoter downstream of seven copies of the *tetO* operator from *E. coli*. The constructs then were transfected into a CHO cell line, tTA_{puro6.6a}, that expresses the tetracycline regulated transactivator (tTA) under tetracycline control (91). The tTA transactivator is a fusion protein composed of the wild-type tetracycline repressor protein from *E. coli* (TetR) and the VP16 activation domain (AD) of herpes simplex virus. The fusion protein is regulated by tetracycline so that it only binds to the *tetO* operator when tetracycline is absent, allowing the VP16 AD to activate the CMV promoter. Therefore, in this system, the gene of interest is only expressed in the absence of tetracycline or its derivatives. The vector also contained a G418 resistance gene so that stable transfectants could be selected.

Almost all of the β -tubulin isotypes, including β I, β II, β III, and β IVa, have been reported to be increased in drug-resistant cells. To find out if changes in β -tubulin isotype expression actually can cause drug resistance, or if they are correlative, we expressed the β I, β II, and β IVb isotypes in CHO cells. CHO cells normally express the β I, β IVb, and β V isotypes in a 70:25:5 ratio (92). This afforded an opportunity to explore not only the ability of different isotypes to confer drug resistance, but also the opportunity to examine whether normally non-expressed isotypes are stable when overexpressed. For this, we determined if the exogenous β -tubulin proteins were incorporated into microtubules after transfection of CHO cells. The cDNAs were fused to an HA epitope tag to allow for easy

detection of the exogenously expressed gene. Transient transfections were carried out and the cells were stained with an antibody to the HA tag. Figure 3-1 shows cells that were transiently transfected with the HA β I, HA β II, and HA β IVb, constructs, as well as a construct containing a mutant β I tubulin that has a leucine to phenylalanine substitution at residue 228; this construct is known to cause resistance to Taxol when overexpressed in CHO cells (93). After removal of tetracycline from the media to allow expression of the cDNAs, antibodies to the HA tag detected proteins throughout the microtubule network, indicating that all of the constructs were expressing functional proteins that could assemble into microtubules.

Next, transfections were carried out to determine if overexpression of specific isotypes could confer Taxol resistance. For this, several different selective conditions were used. One group of cells was exposed to medium with tetracycline. These nonselective conditions should allow all cells to grow regardless of whether they do or do not express the transfected cDNA. Tetracycline was included to suppress transfected HA β -tubulin expression and circumvent the possibility that the overexpressed protein might prove toxic to cell survival. This control group was used as the baseline to calculate transfection efficiencies. A second group of cells received medium containing G418 plus tetracycline. The G418 was expected to select cells that were stably transfected and expressed the neomycin resistance gene in the plasmid. Tetracycline was again included to eliminate any possible toxicity from overexpression of HA β -tubulin. These conditions should select the total stably transfected cell population. A final group of cells received medium containing Taxol but no tetracycline. The expectation was that removal of tetracycline would allow expression of the transfected HA β -tubulin, while inclusion of Taxol would determine whether the HA β -tubulin could confer Taxol resistance. The results of this experiment are summarized in Table 3-1. All the transfections produced

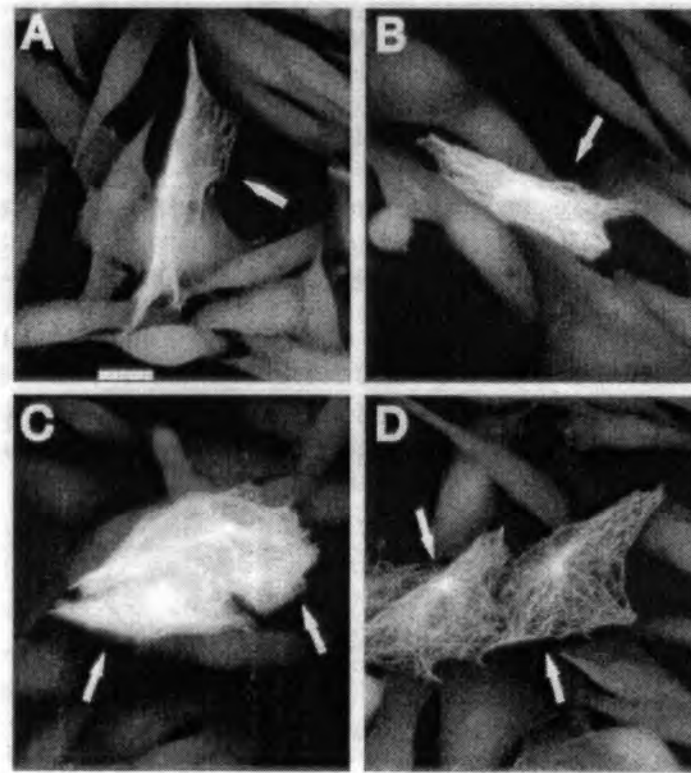


Figure 3-1. The HA β -tubulin proteins are incorporated into the CHO cell microtubular network. Cells from CHO strain tTA_{puro} 6.6a were seeded onto glass coverslips and transfected with HA β _I (A), HA β _{II} (B), HA β _{IVb} (C), or HA β _{I(L228F)} (D) cDNA. At 24 hours posttransfection, the cells were extracted with a microtubule stabilizing buffer, fixed, and stained with an antibody specific to the HA tag. Arrows indicate the positions of cells expressing the transfected HA β -tubulin. Bar, 10 μ m.

Table 3-1. Selection of transfected cells for resistance to G418 and to Taxol

	<i>HAβI</i>	<i>HAβII</i>	<i>HAβIVb</i>	<i>HAβI_{L228F}</i>
αMEM + tet	62400 (1)	70200 (1)	63700 (1)	81400 (1)
G418 + tet	242 (3.9 X 10 ⁻³)	298 (4.2 X 10 ⁻³)	240 (3.8 X 10 ⁻³)	80 (1 X 10 ⁻³)
TX	0 (<1.6 X 10 ⁻⁵)	0 (<1.4 X 10 ⁻⁵)	0 (<1.6 X 10 ⁻⁵)	9 (1 X 10 ⁻⁴)

Cells transfected with various HAβ-tubulin cDNAs were seeded onto tissue culture dishes containing no selective drug (αMEM + 1 μg/ml tetracycline), 2 mg/ml G418 + 1 μg/ml tetracycline, or 0.2 μg/ml Taxol (TX). For each selection, the number of surviving colonies is shown along with the cloning efficiency in parentheses. The cloning efficiency in αMEM + tetracycline was arbitrarily set at 1 for each transfected cell line. Note that the number of colonies in αMEM + tetracycline was multiplied by 100 because 100-fold fewer cells were seeded compared to the other selections.

Table 3-2. Taxol-resistant cells in a G418 selected population

	<i>HAβI</i>	<i>HAβII</i>	<i>HAβIVb</i>	<i>HAβI_{L228F}</i>
α MEM	190	195	197	147
TX	0	0	0	44

Cells transfected with the various HA β -tubulin cDNAs were first selected in G418 + tetracycline and were then replated under non-selective conditions (α MEM) or in 0.2 μ g/ml Taxol (TX). The number of colonies that survived under each set of conditions is shown.

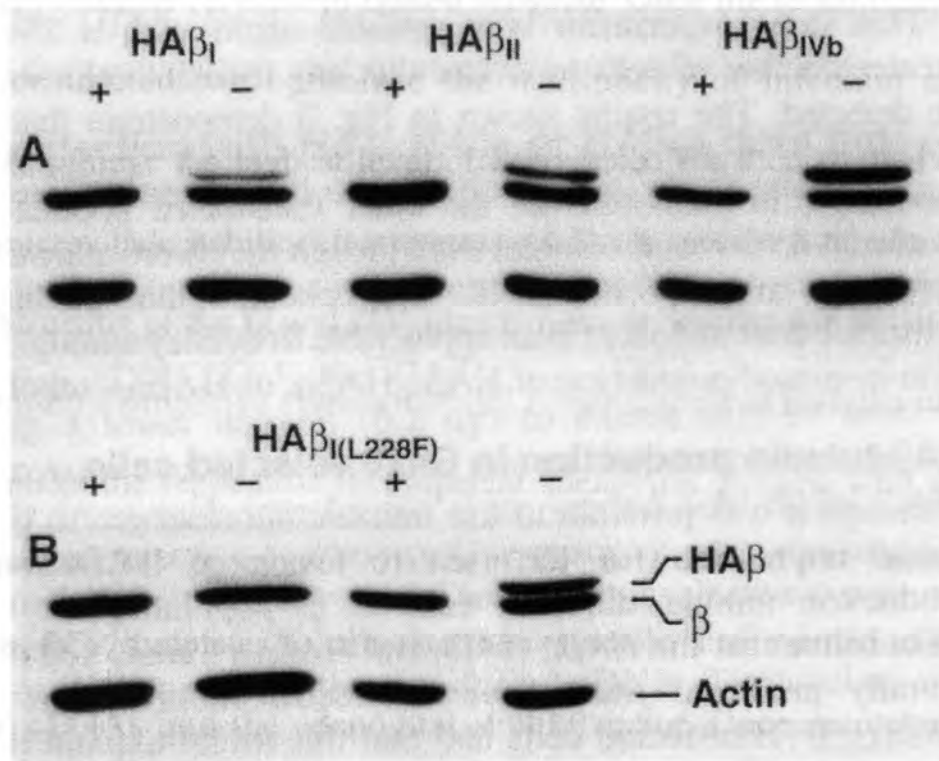


Figure 3-2. Production of HA β -tubulin in transfected cells. Cells transfected with the indicated HA β -tubulin cDNAs and selected in G418 were run on SDS polyacrylamide gels, electroblotted onto nitrocellulose, and probed with antibodies to β -tubulin and actin. Lanes marked with a '+' represent cells grown continuously in 1 μ g/ml tetracycline and lanes marked with a '-' represent cells induced overnight (20 hours) without tetracycline. The relative positions of transfected HA β -tubulin (HA β), endogenous β -tubulin (β), and actin are indicated in B. Also in B, the left 2 lanes represent cells transfected with HA $\beta_{I(L228F)}$ and selected in G418 while the right 2 lanes represent the same transfected cells selected in 0.2 μ g/ml paclitaxel. The left 2 lanes were exposed longer to reveal the minor production of the transfected HA $\beta_{I(L228F)}$ -tubulin in the G418 selected cell population. Note that the transfected tubulin is dramatically increased in the cells selected in paclitaxel.

We next directly tested the hypothesis that overexpression of the β I tubulin isotype can lead to increased microtubule stability in the terminally differentiated adult cardiocyte. For this, we constructed recombinant adenoviruses that allow for the infection of cardiocytes cultured on laminin-coated substrate. Once the recombinant adenoviruses had been constructed, we optimized the multiplicity of infection and kinetics of expression to achieve the highest level of expression. We then studied cardiocytes for changes in microtubule stability after overexpression of specific β -tubulin isotypes.

Construction of the β I and β IV adenoviruses is described in detail in the methods section. We used a simplified system for viral construction that includes recombination in bacteria to make the replication-incompetent adenoviral genome with a cloned cDNA downstream of a CMV promoter (90). The pTOPneoHA β I and pTOPneoHA β IV vectors were used as PCR templates to generate the restriction sites needed to clone the HA β I and HA β IV cDNAs into the adenoviral shuttle vector. Once recombination with the engineered shuttle vector was done, we propagated the virus in the human kidney cell line HEK 293, which provides the missing E1 region of the adenoviral genome in trans (94). Single plaques were selected and amplified for the large-scale isolation of the adenoviruses.

To determine if expression of the β I isotype could confer increased microtubule stability, the goal was to infect cardiocytes with high enough titers of adenovirus for long enough time to achieve replacement of the endogenous β -tubulin with the exogenous β -tubulin. The first step was to determine the optimum multiplicity of infection (MOI) for each viral construct. Cells were plated on laminin-coated culture dishes and treated with increasing numbers of plaque-forming units (PFU). Cells were exposed to virus for 18 hours and were lysed 4-5 days post-infection. Total protein was run on a SDS-PAGE and Western blots were performed with the polyclonal anti-HA antibody. Figure 3-3 shows

MOI: 0 200 400 2000 20000

HA β I



HA β IV



Figure 3-3. Multiplicity of infection for HA β -tubulin adenoviruses. Plated cardiocytes were treated for 18 hours with no virus or one of the HA β -tubulin viruses at increasing multiplicity of infection (MOI). Total protein was isolated 4 days after the start of infection and Western blots were performed with the HA tag antibody. The amount of exogenous tubulin produced peaks at about an MOI of 2000 for both viral constructs.

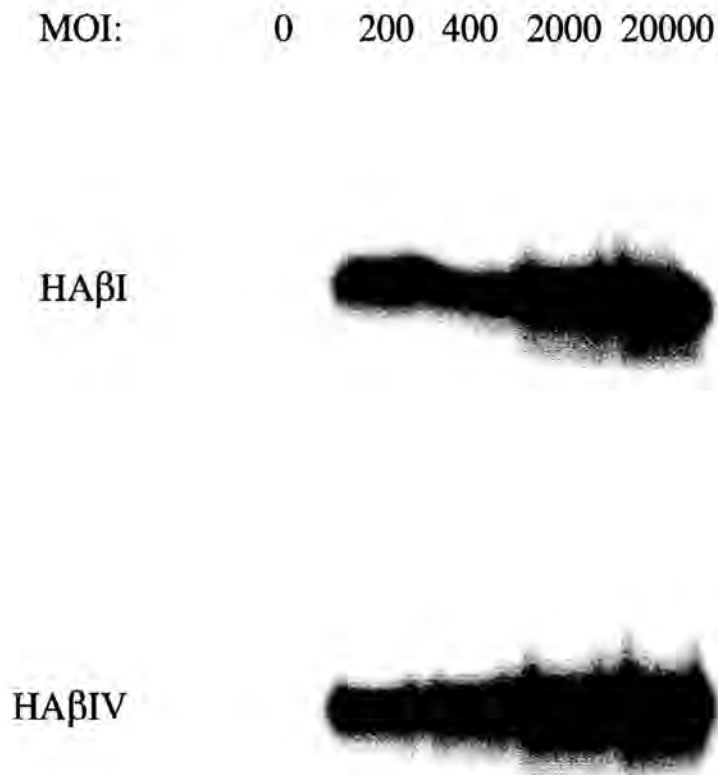


Figure 3-3. Multiplicity of infection for HAβ-tubulin adenoviruses. Plated cardiocytes were treated for 18 hours with no virus or one of the HAβ-tubulin viruses at increasing multiplicity of infection (MOI). Total protein was isolated 4 days after the start of infection and Western blots were performed with the HA tag antibody. The amount of exogenous tubulin produced peaks at about an MOI of 2000 for both viral constructs.

that the ideal MOI for each of the β -tubulin adenoviral constructs is about 2000 PFU/cell. The amount of expressed HA-tagged tubulin levels off at this MOI, and after this point there seems to be an increase in the level of higher and lower molecular weight bands that are detected by the HA antibody (data not shown). It is possible that as the level of expression increases more of the β -tubulin protein is being degraded or collecting into large complexes that are assembly-incompetent. For most of the remaining studies, an MOI of at least 1000 was used.

The next step was to determine at what point post-infection exogenous protein levels were highest. Again, cells were plated on laminin-coated dishes and treated with adenovirus for about 18 hours. Cells were scraped at day 1 through day 5 post-infection and equal amounts of total protein were run on SDS-PAGE. Western blots were done with both the anti-HA antibody as well as the antibody for common β -tubulin. Figure 3-4 shows the results of Western blots of cellular extracts from HA β I and HA β IV infected cardiocytes. The level of expressed protein peaks at about 3-4 days post-infection. Note that the HA-tagged tubulin proteins have a slightly slower electrophoretic mobility, allowing us to see that the level of endogenous β -tubulin at this MOI has been greatly reduced, if not completely replaced by the exogenously expressed protein.

Immunofluorescence confocal microscopy was used to confirm that the expressed β -tubulin proteins were being incorporated into the microtubules of the cardiocytes. Cells were plated on laminin-coated glass coverslips and infected for 18 hours with a control RSV promoter virus that contained no insert, HA β I expressing adenovirus, or HA β IV expressing adenovirus at MOIs of about 5000. After 2-3 days, the cells were fixed and stained with a mouse monoclonal anti-HA antibody and a rat monoclonal anti- α -tubulin antibody. The time course was shortened from the ideal 4-5 days because cells at this time point were better able to survive the extraction and fixation procedure. Cells were

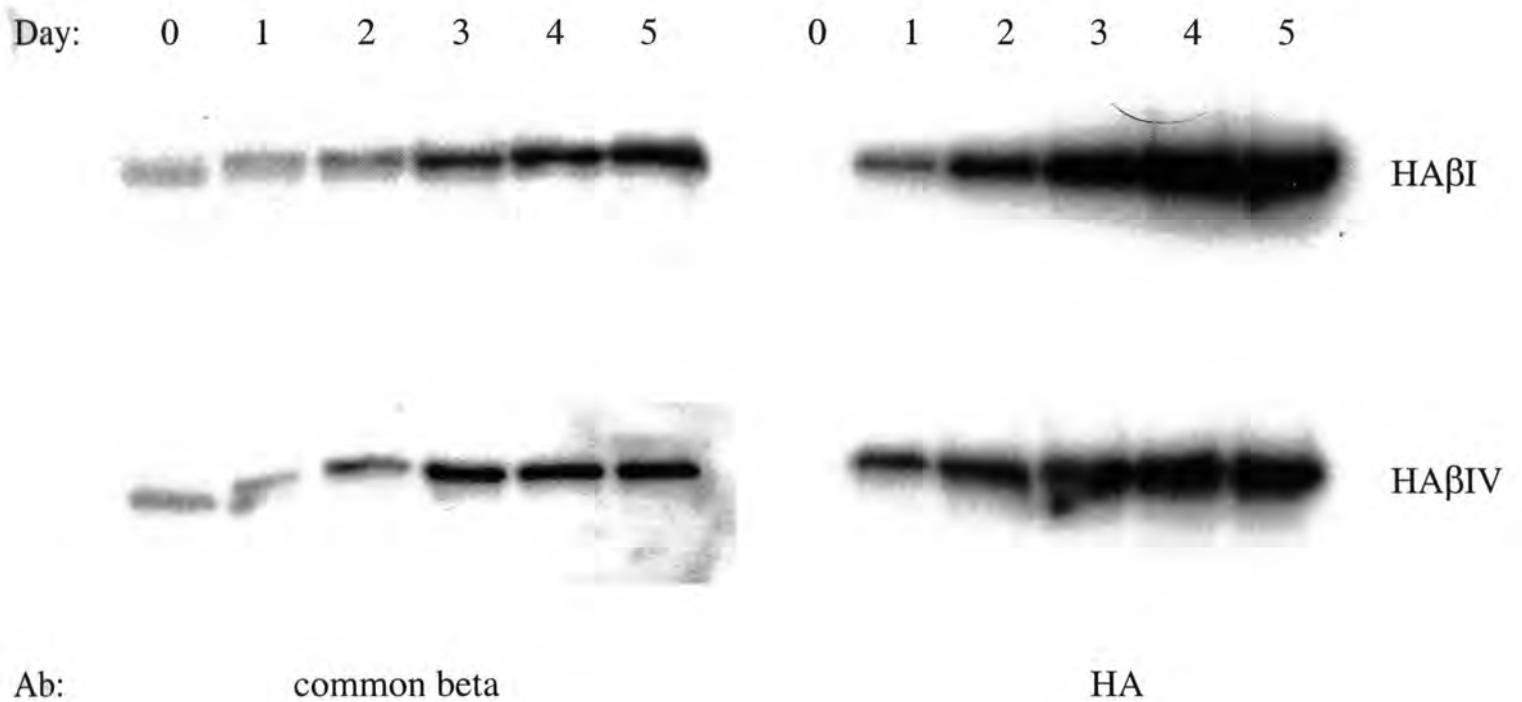


Figure 3-4. Time course for HA β -tubulin adenoviral infection. Plated cardiocytes were treated for 18 hours with one of the HA β -tubulin viruses at an MOI of 2000. Total protein was isolated at the time of infection and every day for 5 days post-infection, and Western blots were performed with a monoclonal β -tubulin antibody and a polyclonal HA tag antibody. For both adenoviral constructs, expression peaked around 4-5 days.

then stained with Cy3-conjugated anti-mouse and FITC-conjugated anti-rat secondary antibodies and observed by confocal microscopy. Figure 3-5 shows that both HA-tagged proteins are homogeneously incorporated into essentially all of the microtubules of the cells. About 70-80% of the cells was infected with the HA β -tubulins.

Once we had established that both adenoviral constructs were expressing high levels of protein in adult cardiocytes, we were able to start qualitatively measuring changes in microtubule stability in cells overexpressing specific β -tubulin isotypes. For a preliminary experiment, we used Western blots to check levels of post-translationally modified α -tubulins in infected versus non-infected cardiocytes. There are three different forms of α -tubulin that are known to indicate microtubule age: the tyr form, or the non-modified α -tubulin that has a carboxy-terminal tyrosine residue; the glu form, which has been modified by the removal of the terminal tyrosine, leaving a carboxy-terminal glutamate residue (95-99); and the $\Delta 2$ form, which has been modified by the further removal of the terminal glutamate (100-102). The presence of the last two forms indicates older, and therefore more stable, microtubules. Extracts from cells infected with HA β I and HA β IV for 3 days in the aforementioned time course experiments were compared with extracts from uninfected cells scraped on the same day from the same cell preparation. Equal amounts of protein were loaded on SDS-PAGE, and Western blots were performed with polyclonal antibodies to unmodified α -tubulin (Tyr-tubulin), de-tyrosinated α -tubulin (Glu-tubulin), and de-tyrosinated/de-glutamylated α -tubulin ($\Delta 2$ -tubulin) (10). Figure 3-6 shows that, while the Western blot with the β -tubulin antibody clearly indicates an almost total replacement of the endogenous β -tubulin with either the HA β I- or HA β IV- tubulin, there are no great changes in the levels of post-translationally modified α -tubulin proteins. This gives preliminary indication that the overexpression of

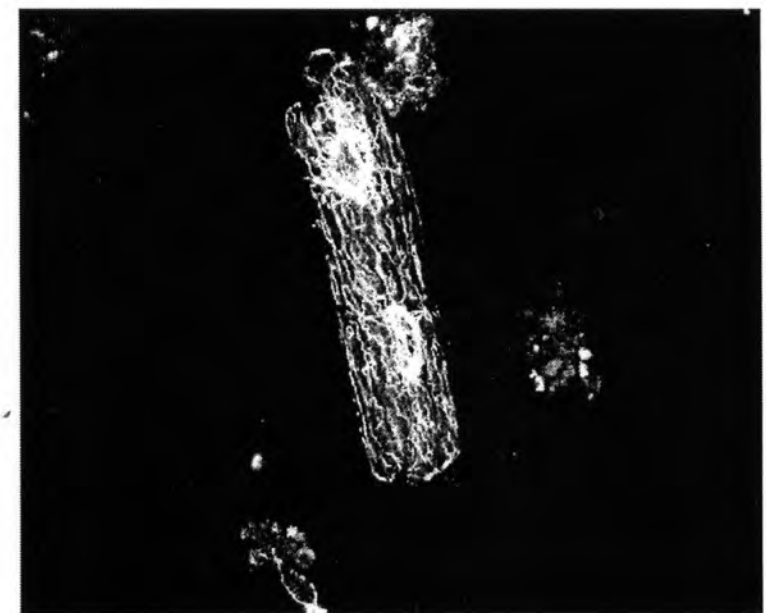
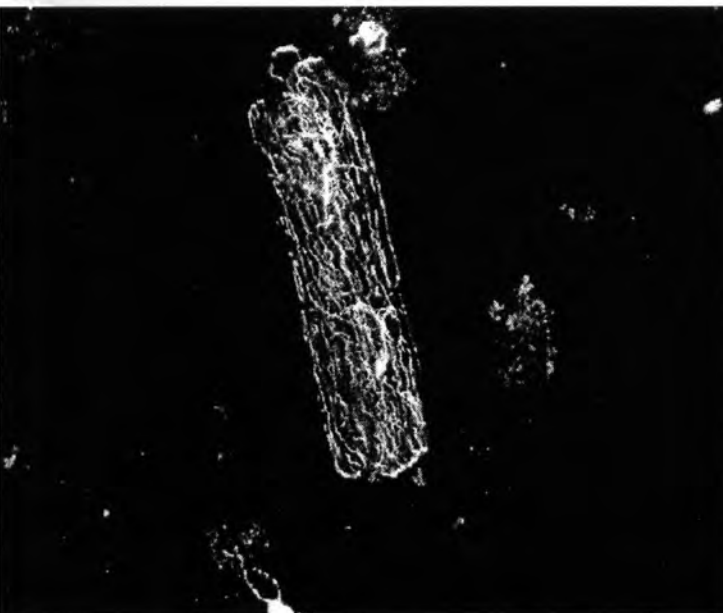
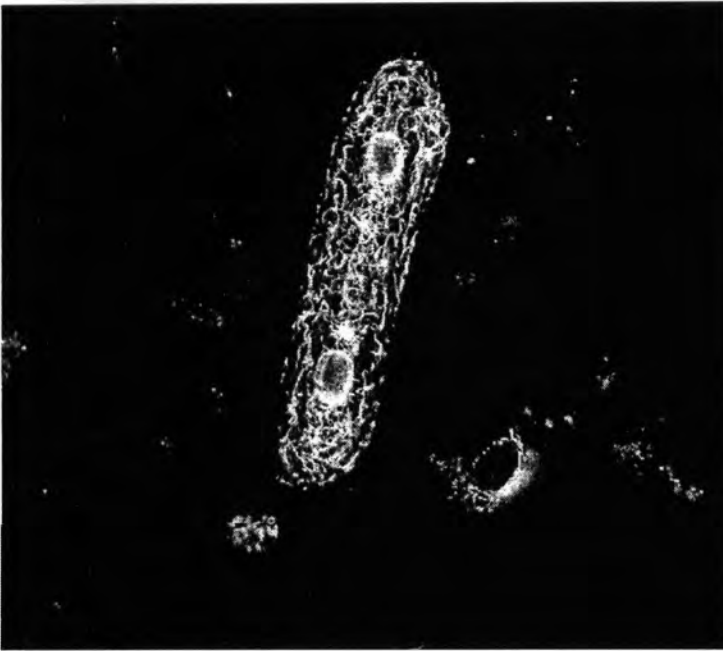
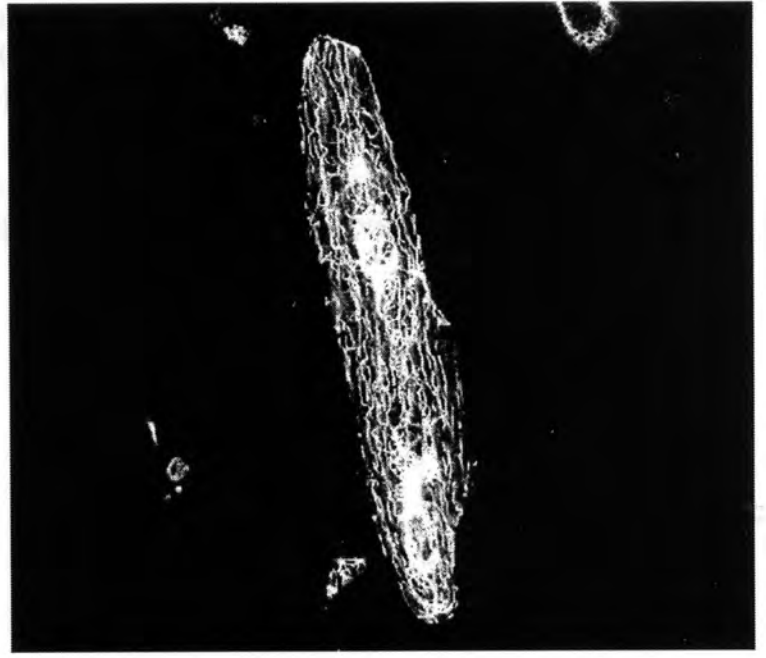
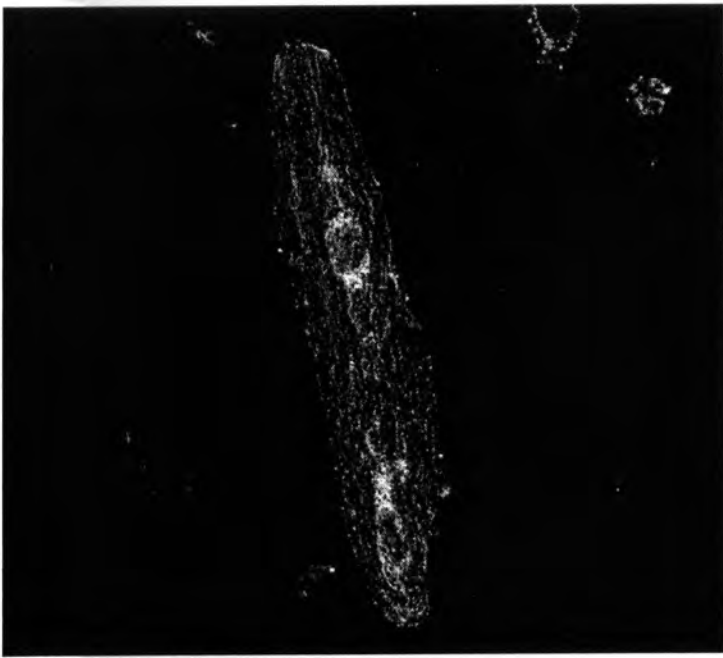
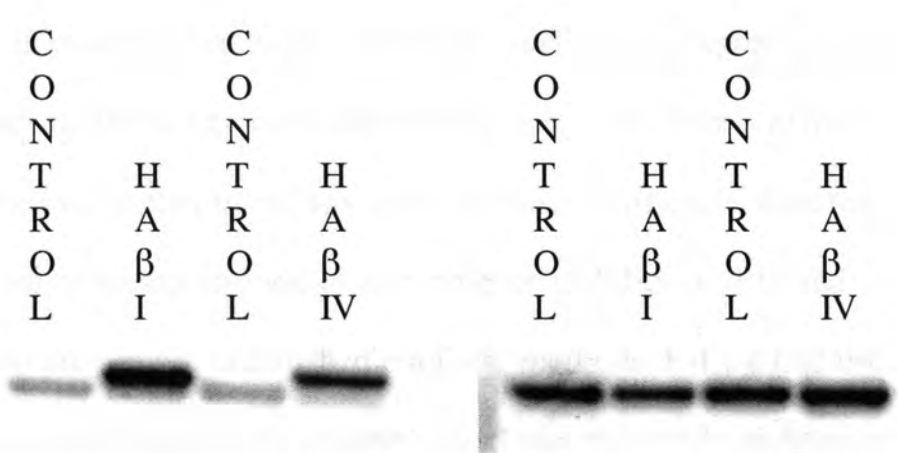
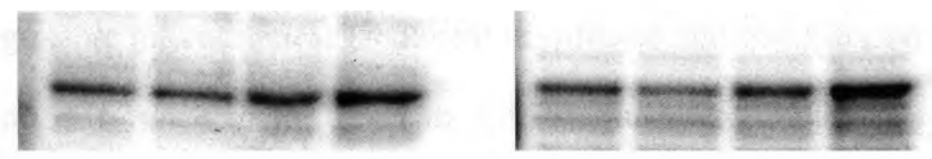


Figure 3-5. The HA β -tubulin proteins are incorporated into the microtubules of the adult cardiocyte. Cardiocytes were plated on laminin-coated coverslips and infected for 18 hours with either control adenoviruses containing an RSV promoter with no insert (top 2 panels) or the HA β I (middle 2 panels) or HA β IV (bottom 2 panels) adenoviruses at an MOI of about 5000. After 3 days the cells were fixed and stained for immunofluorescence with antibodies to the HA tag (panels on left) and α -tubulin (panels on right). The HA β -tubulin constructs appear to be homogeneously incorporated into most of the cells' microtubules.



Ab: common beta anti-tyr



Ab. anti-glu anti-Δ2

Figure 3-6. Post-translationally modified alpha-tubulins in HAβ-tubulin infected cardiocytes. Plated cardiocytes were treated for 18 hours with one of the HAβ-tubulin adenoviruses at an MOI of 2000. Total protein was isolated 3 days after infection and Western blots were performed with a monoclonal β-tubulin antibody and the three alpha tubulin antibodies described in the text. Cells that had not been infected with adenovirus were used as a control.

the BI isotype in adult cardiocytes *in vitro* does not have an effect on microtubule stability.

Since it is possible that 3 days of exogenous tubulin expression does not give the cell enough time to show an observable difference in the levels of post-translationally modified α -tubulins, or that there was some technical difficulty with the antibodies, we wanted to use other means to look at microtubule stability in infected cardiocytes. For this we used two previously established confocal methods that we had used to prove that microtubules are stabilized during pressure overload-induced hypertrophy (10). The first is treatment of cells with cold temperatures (from 4°C to 8°C) to see if there are changes in the levels of cold-stable microtubules. The second is the treatment of cardiocytes with nocodazole, a drug that depolymerizes microtubules, to see if there are changes in the levels of drug-stable microtubules. Treatment of infected and non-infected cardiocytes at 6°C shows no difference in the level of cold-stable microtubules in HA β I-infected cardiocytes (Figure 3-7). In addition, cells were treated at 4°C and at 8°C for 30 minutes to 2 hours and again showed no difference in the level of cold-stable microtubules (data not shown). A total of about 50 cells from 3 different cell preps were examined for each isotype and showed no qualitative difference from control cells in the appearance of the microtubules when treated with cold temperature. Cells were also infected with control virus or one of the HA β -tubulin viruses, treated with varying amounts of nocodazole for as long as 2 hours, fixed, and stained for HA and α -tubulin. Nocodazole caused a depolymerization of microtubules in all of the cardiocytes and infection with HA β I adenovirus did not seem to change the number of drug-stable microtubules (data not shown). All of these studies indicate that, at least *in vitro*, a high level expression of the BI tubulin isotype does not seem to alone cause changes in microtubule stability.

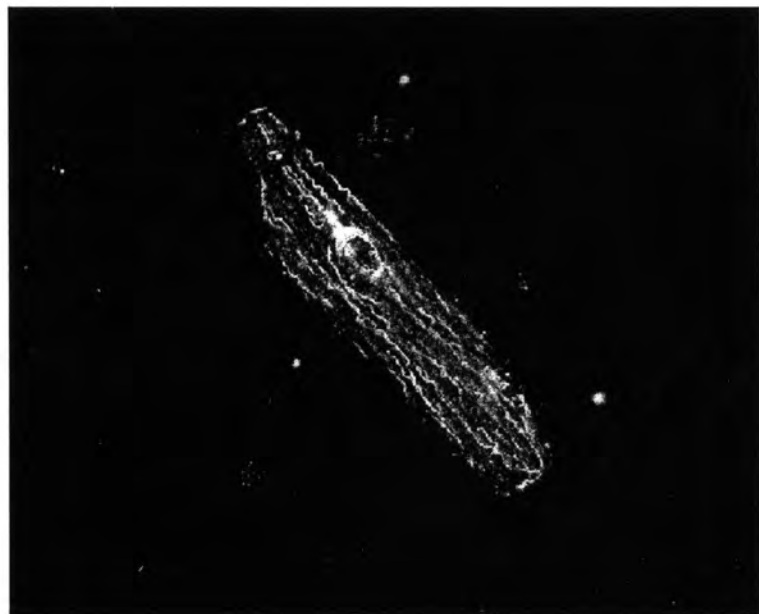
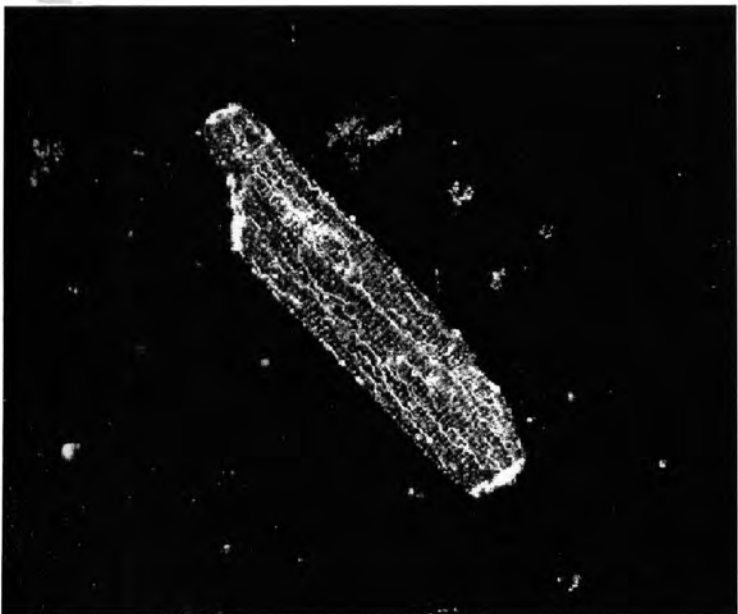
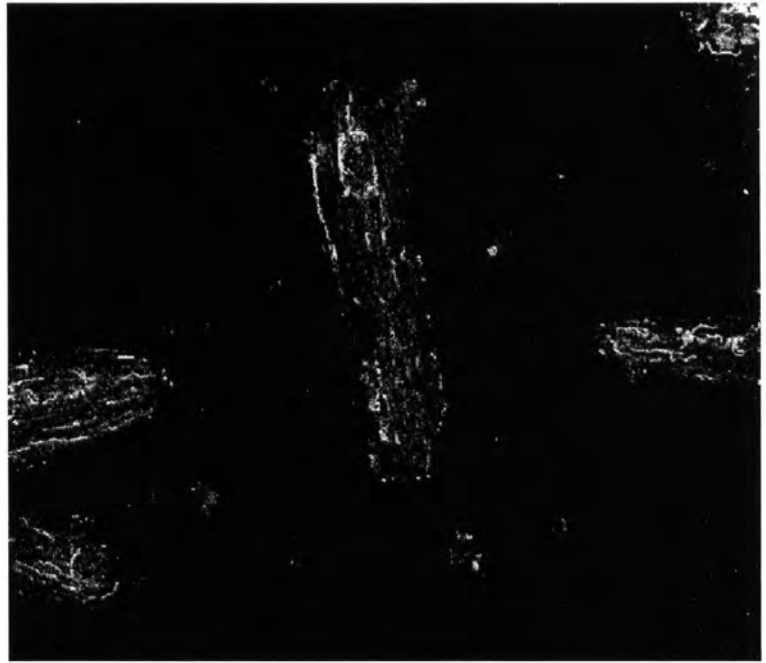
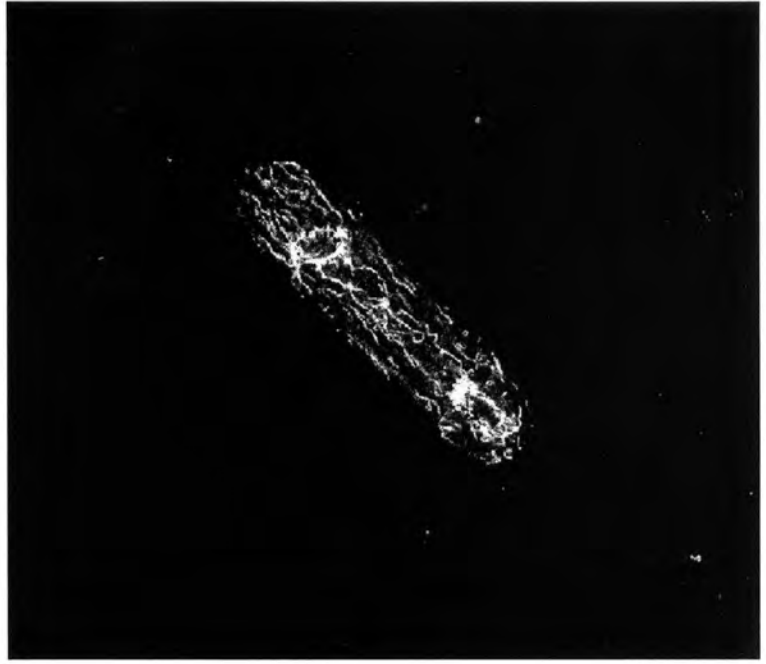
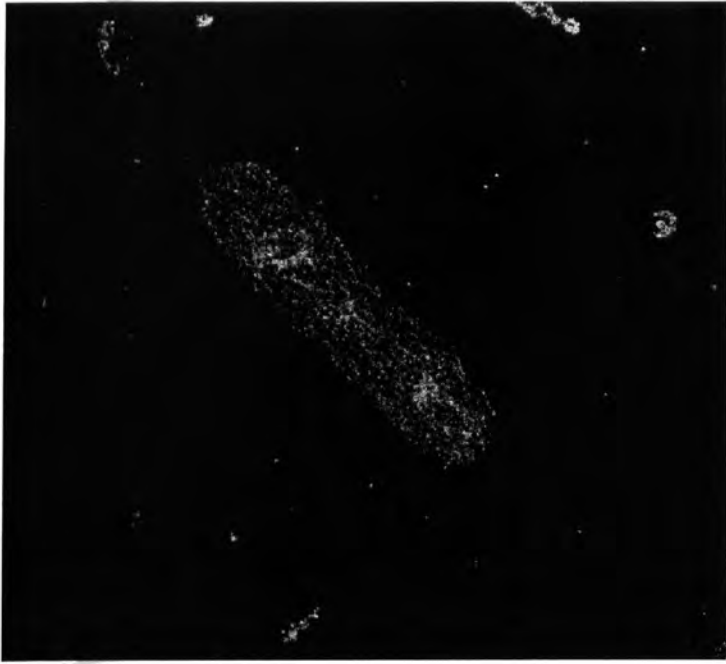


Figure 3-7. Cold stability of microtubules in adenovirally infected adult cardiocytes. Cardiocytes were plated on laminin-coated coverslips and infected for 18 hours with either no adenovirus (top 2 panels), the HA β I adenovirus (middle 2 panels), or the HA β IV adenovirus (bottom 2 panels). After 3 days, the cells were treated to 6°C for 1 hour in HEPES-buffered M199, fixed, and stained for immunofluorescence with antibodies to the HA tag (left panels) and α -tubulin (right panels). Compare to Figure 3-5, which shows the non-treated cardiocyte controls from the same experiment. There is a reduction in the number of microtubules for all of the infected as well as control cardiocytes.

Previous studies in this lab have shown that, along with an increase in the amount of β I tubulin during pressure overload-induced hypertrophy, there is an increase in the level of the predominant fibrous microtubule associated protein in the heart, MAP 4 (10). For this reason, an adenoviral construct expressing a myc-tagged MAP 4 gene from the CMV promoter was also made in this laboratory. When cardiocytes are infected with this virus, they show dramatic changes in their microtubule structure (see Figure 3-8). Specifically, the microtubules seem to be much straighter and more brightly stained, possibly indicating microtubule bundling. This bundling morphology is similar to what has been seen in myocytes treated with Taxol in this lab and others (10) and (103). In addition, as shown in Figure 3-8, when cardiocytes are infected with MAP 4 overexpressing adenovirus, their microtubules are more stable to treatment with nocodazole. To see if co-expression with the β I-tubulin isotype affected these changes, we infected cardiocytes with the HA β I and the MAP 4 adenovirus. We then stained with antibodies to the HA and the myc tags to see if both proteins incorporate into the same microtubules. Figure 3-9 shows that we can easily achieve expression of the HA β I-tubulin protein as well as the MAP 4 protein and that both proteins are then incorporated into the same microtubules. Additionally, the expression of HA β I does not affect the microtubule morphology unless it is in the presence of MAP4 overexpression. Studies that look at the cold-stability and nocodazole-stability of the microtubules in HA β I/MAP 4 co-infected cells have not yet been done. Taken together, the results show that, by these microscopic techniques, we see no appreciable difference in microtubule stability in the cells that overexpress β I-tubulin. However, the overexpression of MAP4 clearly causes increased microtubule stability in the adult cardiocyte.

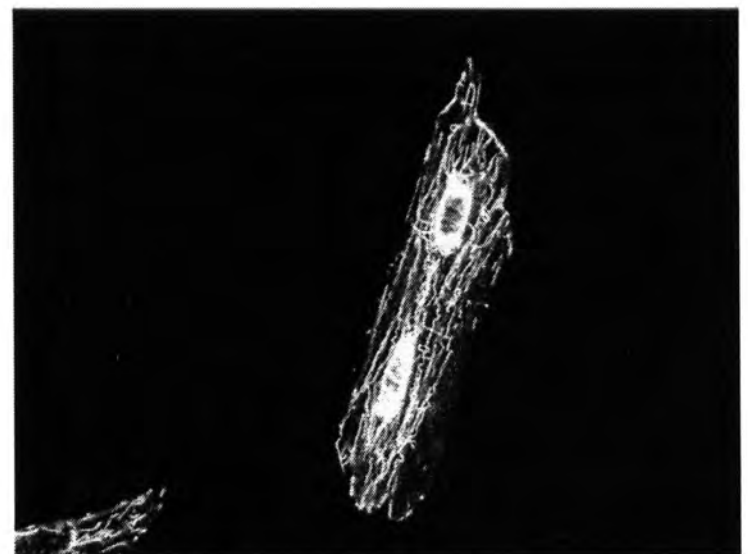
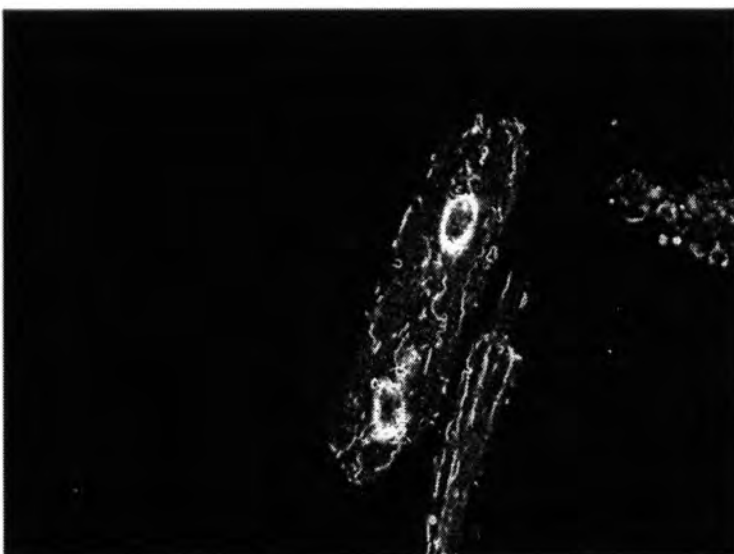
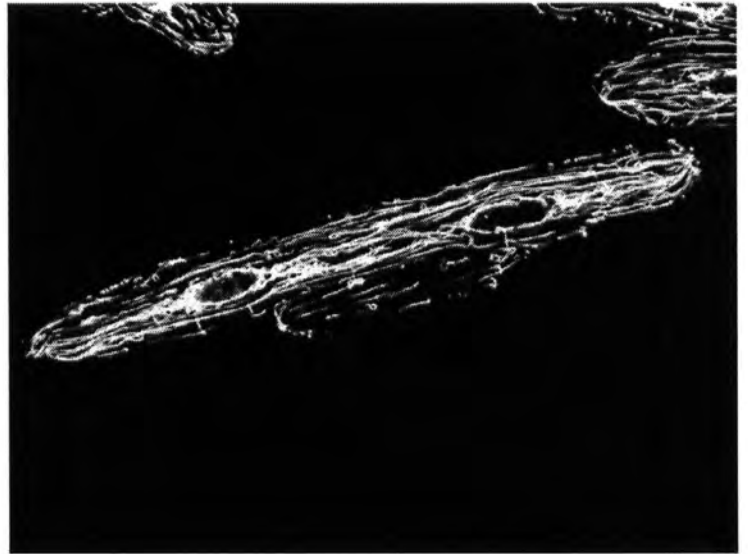
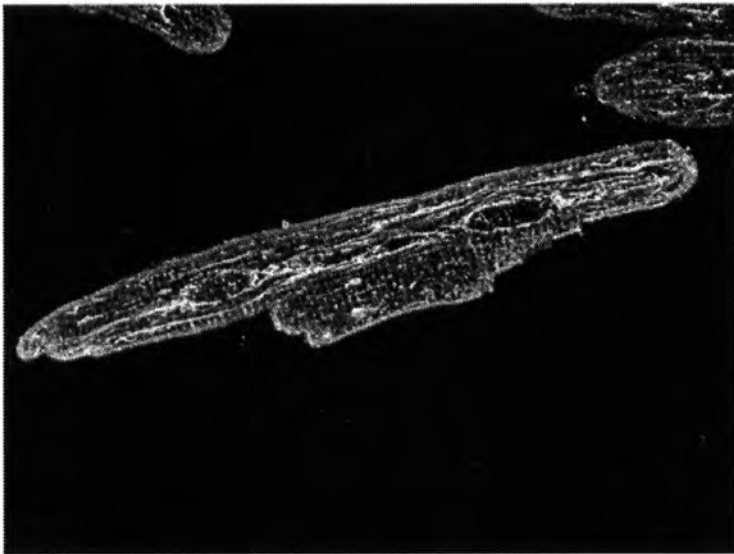
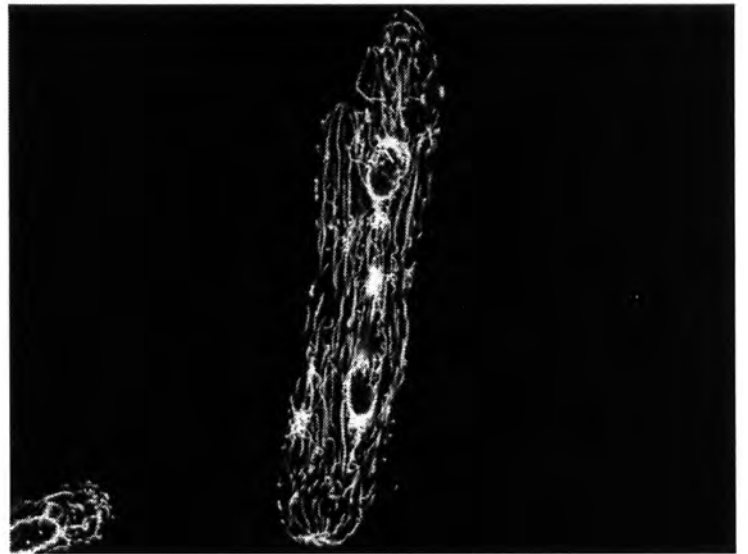


Figure 3-8. Overexpression of MAP 4 in adult cardiocytes. Cells were plated on laminin-coated coverslips and infected overnight with either the control β -gal virus or the myc-tagged MAP 4 expressing adenovirus. The upper panels show a cell that was infected with the control virus, fixed, and co-stained with an antibody to the myc tag (left) and an antibody to α -tubulin (right panel). The middle panels show a cell that was infected with the MAP 4 adenovirus, fixed, and co-stained with the myc tag (left) and α -tubulin antibody (right). The microtubules in this cell appear straighter and more tightly bundled than those in the cell treated with the β -gal virus (compare the upper and middle right panels). The bottom panels show two cells that were infected with either the control virus (left) or MAP 4 virus (right), then treated with nocodazole, fixed, and stained with an antibody to α -tubulin. The MAP 4 overexpressing cell clearly has microtubules that are more resistant to the nocodazole than the control cell.

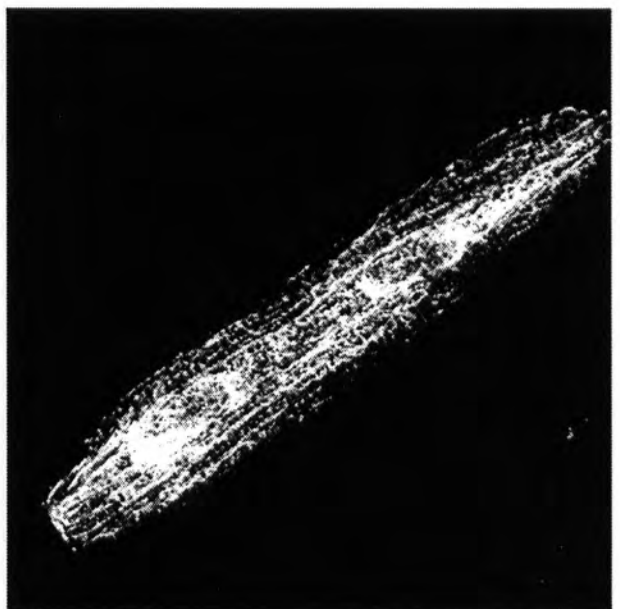
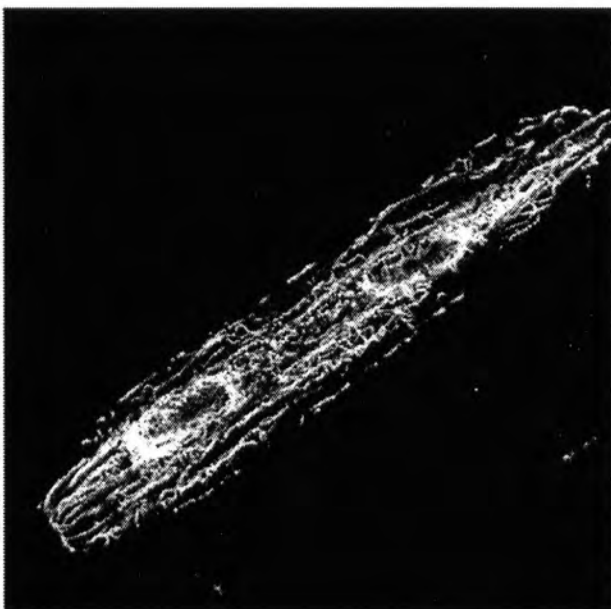
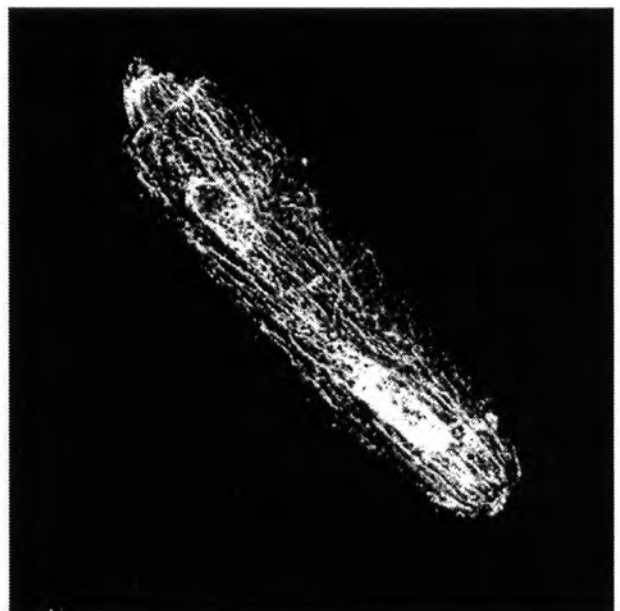


Figure 3-9. Co-expression of the MAP4 and HA β I proteins in adult cardiocytes. Cardiocytes were plated on laminin-coated coverslips and infected for 18 hours with the HA β I-tubulin adenovirus (top 2 panels), the myc-tagged MAP4 adenovirus (middle 2 panels), or both (bottom 2 panels) at a total MOI of 5000. After 3 days, the cells were fixed and stained for immunofluorescence with antibodies to the HA and the myc tags. The microtubule density for both the MAP4-infected and the HA β I and MAP4 co-infected cardiocytes is greater than that of the HA β I-infected cardiocytes. Additionally, the HA β I and mycMAP4 proteins both seem to be incorporated into the same microtubules.

Since some of this work was done, a post-doctoral fellow in our lab, Yuji Ishibashi, has done more experiments that further characterize the effects of MAP 4, β I, and β IV overexpression in adult cardiocytes. His work showed that with several repeat experiments, MAP 4 overexpression was alone able to confer resistance to nocodazole treatment in feline cardiocytes. He showed that treatment with 0.2 μ M, 2 μ M, and even 20 μ M of nocodazole left behind stable, myc-staining microtubules in only those cells infected with MAP 4 adenovirus. In addition, he performed experiments in which he isolated the microtubule and soluble fractions (10) from cells infected with MAP 4 adenovirus and found that, compared with control cells, there was an increased amount of polymerized microtubules in the MAP 4 expressing cells and a decreased amount of soluble tubulin. This difference was not seen in cells infected with either HABI or HABIV alone, and was seen in cells co-infected with HABI and MAP 4 or HABIV and MAP 4. These experiments are being repeated because, in cells that are already separated from the tissue, it is more difficult to shear the cells such that the soluble fraction is not contaminated with polymerized microtubules. However, there was a clear difference between the MAP 4 overexpressing cells and all other cells. Additionally, he infected cells with the HABI and HABIV adenoviruses and treated with nocodazole or cold temperatures, and found that there was no increased microtubule stability in the infected cells as indicated by Western blot with the post-translationally modified α -tubulin antibodies. All of these studies are further support for the data that only MAP 4 overexpression, and not β I-tubulin overexpression, is needed for increased microtubule stability in the adult cardiocyte.

DISCUSSION

We have demonstrated in previous experiments that there is a dramatic change in the pattern of β -tubulin isotype expression during pressure overload-induced hypertrophy (24). As discussed in previous sections of this work, we have confirmed that this change is likely due to the transcriptional upregulation of only certain β -tubulin genes, an expression pattern that recapitulates the developmental pattern seen in the heart (24). Re-expression of embryonic isoforms of structural genes is common during cardiac hypertrophy. However, whether or not these changes have functional significance for the development of hypertrophy or heart failure is not well established. We wanted to know if the upregulation of the β I isotype from around 4% of the total β -tubulin protein to about 20% of the β -tubulin protein (24) during hypertrophy has any functional significance for the stability of the microtubules.

Most of the data concerning the effect of β -tubulin isotype expression on microtubule stability has come from studies on mitotically active cells in relation to chemotherapy drug resistance. In these studies, most of the major isotypes of β -tubulin have been implicated as the cause of microtubule affecting drug-resistance in cell lines or tumors. This runs counter to the notion that specific isotypes would cause specific effects, making it difficult to know whether hypertrophic induction of β I tubulin contributes to increased microtubule stability. Importantly, the isotypes differ mainly in their carboxy-terminal MAP-binding region, and the different isotypes are absolutely conserved in this region among species. Therefore, we hypothesized that because MAP 4 and β I-tubulin were upregulated coordinately, as MAPs and β -tubulin isotypes are in other cell types (31), that the two proteins might have an increased affinity for one another, leading to a synergistic effect on microtubule stability.

For our studies, in collaboration with F. Cabral, we first addressed the conflicting data concerning the supposed ability of β I-tubulin to confer a hypostable phenotype in the presence of Taxol resistance. We asked the simple question of whether or not β I-tubulin overexpression, or indeed any β -tubulin overexpression, could confer resistance to the microtubule stabilizing drug Taxol. These studies also allowed us to look, in an alternate cell system, at the effects of overexpression of normally non-expressed isoforms. Because β II is not normally present in CHO cells and β IVb is present in lesser amounts than β I, these studies confirmed that more rare isoforms can be expressed at high levels and be incorporated freely into the microtubules. This was an important consideration, because there was some question as to whether we would need dual expression of an α -tubulin to enable incorporation of the exogenously expressed β -tubulin. These studies show that overexpression of the β I, β II, and β IVb isoforms cannot confer Taxol resistance, although a mutated β -tubulin protein easily can.

Although our data in CHO cells clearly showed that overexpression of wild-type β I tubulin protein did not confer changes in microtubule stability as seen by differences in drug resistance, these experiments were limited by the fact that CHO cells already express a high level of β I (92), leaving open the possibility that further increase in β I expression does not affect microtubule stability. The adult cardiocyte has the advantage that it expresses relatively low amounts of β I, so that changes in microtubule stability caused by dramatic increases in β I levels should be detectable. Indeed our data show that with overexpression by adenoviral infection, almost 100% replacement of the endogenous β -tubulin with H β I-tubulin can be achieved.

The results clearly show that overexpression of β I alone does not seem to confer any greater microtubule stability than overexpression of β IV. Both, however, seem to cause greater microtubule stability when they are co-expressed with MAP 4. These

results seem to indicate that the principal cause of increased microtubule stability during pressure overload-induced hypertrophy is upregulation of MAP 4. Interestingly, the morphology of the more stable microtubules in MAP 4 overexpressing cells is similar to the bundled morphology of cells that are treated with Taxol, as mentioned in the Results section. The overexpression of MAP4 in these experiments is likely greater than that seen during hypertrophy, and seems to result in a more severe phenotype. The functional significance of these differences is unclear.

There still exists, of course, the possibility that no differences were observed in microtubule stability during these experiments because of the presence of the HA tags at the carboxy termini of the expressed proteins. The carboxy-terminus of the tubulin proteins project out from the microtubule, as shown by the crystal structure of the polymer (104); this region of the molecule is the binding region for fibrous MAPs. Because the tubulin isotypes differ significantly in this area, it has long been hypothesized that different isotypes might have different MAP binding affinities and therefore subtly alter microtubule stability. An increased ability to bind MAPs would be the most likely way that increased expression of β I-tubulin could alter microtubule stability. Therefore, an HA tag that interfered in any way with MAP binding could mask the effects of β I-tubulin expression. Several lines of evidence indicate, however, that this is not so. The HA-tagged proteins freely incorporate into microtubules, seemingly without interference to normal morphology of the microtubules. Additionally, when the HA-tagged proteins are co-expressed with MAP 4, antibodies to both proteins freely co-decorate the same microtubules, as seen in Figure 3-9. Since the HA-tagged tubulins nearly replace the entire endogenous β -tubulin pool, it seems unlikely that MAP 4 would be able to bind the microtubules in these cells if the HA tag did indeed interfere with MAP 4 binding. This is especially pertinent considering the fact that overexpression of

the HA-tagged tubulins in no way affected the ability of MAP 4 to stabilize the microtubules. Finally, while it is unclear that changes in microtubule function would be apparent in quiescent cardiocytes overexpressing HA-tagged tubulins, our work in CHO cells shows that the functionality of the microtubule network is unchanged by HA-tagged proteins (69). This would seem highly unlikely if the proteins were unable to bind endogenous MAPs to a degree that would mask any real effects that overexpression of the isotypes might confer. However, to completely rule out the possibility that the HA-tag is somehow masking a phenotype, future studies in this lab include looking at microtubule stability in cardiocytes infected with adenoviruses encoding the non-tagged forms of the β I- and β IV- tubulin proteins.

While these immunofluorescence studies are all qualitative measures of changes in microtubule stability and cannot completely rule out the possibility of subtle changes in microtubule stability from β I-tubulin overexpression, they are good indicators that MAP 4 is the key player causing changes in microtubule stability during hypertrophy. Former studies in this lab have shown that the kind of increased microtubule stability that is seen during pressure overload-induced hypertrophy is easily detected qualitatively with immunofluorescence microscopy in cells that are given microtubule depolymerizing treatments. Technical difficulties have thus far precluded a thorough quantitative assessment of microtubule stability, but ongoing studies include improved isolation of microtubule and soluble tubulin fractions from cells infected with adenovirus and the comparison of microtubule/soluble tubulin ratios in normal cells versus cells infected with either HABI, HABIV, or MAP 4 constructs. The finding that overexpression of β I does not cause marked increase in microtubule stability, at least not to as great of degree as MAP 4 overexpression, brings forth the question of why does β I-tubulin overexpression occur. It is possible, as others have proposed in the past, that the

expression of certain isotypes is simply part of a tissue-specific developmental plan (25, 105), and that the different isotypes have developed to widen an organism's adaptive ability (22). The possibility that the β I-tubulin gene is an innocent bystander in the heart cell's recapitulation of development during hypertrophy will be discussed more fully later in this work.

CHAPTER 4: OVEREXPRESSION OF THE BETA TUBULIN MUTANTS

INTRODUCTION

This chapter focuses on the work that was done to explore the effects of mutagenesis of the β -tubulin protein on microtubule stability. It had its genesis in the desire of this laboratory to produce models of decreased or increased microtubule stability in the heart of an animal that can be subjected to surgical manipulation. The work was done in collaboration with Fernando Cabral who has previously described CHO cell lines resistant to the microtubule poisons Taxol and colchicine (79). In these cells, the free/ polymerized tubulin ratio is decreased if the cell is resistant to colchicine and increased if the cell is resistant to Taxol (79). In other words, colchicine-resistant cells have hyperstable microtubules and Taxol-resistant cells have hypostable microtubules. These cells have mutations in their α - and β -tubulin genes that obviously interfere with the proteins' ability to assemble like wild-type proteins (78). These tubulin mutants can prove to be valuable tools not only for the study of the regions of the α - and β -tubulin molecules important for microtubule assembly and stability but also for the study of the effects of changes in microtubule stability on different cell systems.

Recently, the structure of the $\alpha\beta$ tubulin heterodimer was determined by electron crystallography of zinc-induced tubulin sheets (104). The authors then docked this structure into a model of the 3D map of a microtubule using data from previous studies (106). The data show that the α - and β -tubulin molecules are almost identical in structure and have 3 domains: an N-terminal GTP binding domain, a smaller second domain, and a predominantly helical C-terminal domain (104). The exchangeable GTP in the β -tubulin

molecule is oriented towards the plus end, or growing end, of the microtubule, and the non-exchangeable GTP bound to the α -tubulin molecule is oriented towards the minus end, or fixed end (106). On the outside surface of the microtubule, there are deep grooves in between the protofilaments, and the C-terminal helices of the tubulin proteins define a shallow zigzag path on the crest of each protofilament (106). The inside surface of the microtubule contains several long loops, some of which form the Taxol-binding pocket (104, 106). The models of the $\alpha\beta$ -tubulin heterodimer and the microtubule itself show that the longitudinal interactions between the two molecules that make up the heterodimer are stronger than the longitudinal interactions between the heterodimers, especially towards the microtubule luminal surface (106). The γ -phosphate on the exchangeable GTP bound to the β -tubulin molecule participates in the interaction between heterodimers, so when it is lost (loss of the GTP cap that is normally found at the end of the microtubule by GTP hydrolysis) the protofilaments curl outward and literally peel away from the structure, causing microtubule disassembly (107). Hydrolysis of the exchangeable GTP could also probably lead to destabilization of the interaction at the lateral interface between protofilaments by changing the conformation of the loop involved in binding between protofilaments (106).

Now that the structure of the $\alpha\beta$ -tubulin heterodimer and microtubule have been so well characterized, the use of mutational analysis of the tubulin proteins is attractive for the resolution at a fine level of the residues involved in the important functions of the microtubule as well as in the determination of the microtubule structure and dynamic instability. The finding of natural mutations of the tubulin proteins that seem to alter assembly dynamics is an important find in the context of resolving the structure-function relationships of the tubulin molecules. Work in F. Cabral's lab has revealed that there is a cluster of mutations in the β -tubulin molecule that causes decreased stability of the

microtubules in the Taxol-resistant cells which express the mutant proteins. Remarkably, sequence analysis of these mutations has revealed that they are found in three leucine residues that are clustered together near the Taxol binding site of the β -tubulin protein and the point of both longitudinal interactions with the α -tubulin protein and lateral interactions between protofilaments (93). The finding of these mutations provides important clues about residues that modulate microtubule dynamics. To further characterize the ability of these mutants to directly alter microtubule stability, we collaborated with Dr. Cabral and made constructs that expressed the mutant proteins for overexpression in CHO cells. In addition, we used these mutants as tools for the exploration of microtubule stability and its affect on cardiocyte function. Our specific aims were as follows: to determine if overexpression of these β -tubulin mutants could directly cause decreased microtubule stability as measured by Taxol resistance, and, if so, to genetically alter mice to overexpress these mutants specifically in the heart. We can ultimately use this model to determine if changes in microtubule stability can ameliorate the effects of pressure overload-induced hypertrophy at the whole heart level.

METHODS

Construction of Plasmids. The pTOPneoHAB1 vector (see chapter 3 methods) and its mutant derivatives were used for all transfections. Site-directed mutagenesis was carried out using the Quickchange Site-Directed Mutagenesis kit (Stratagene) according to manufacturer's protocol.

Transfection. Plasmid DNA was isolated using the QIAfilter Plasmid Maxi Kit (Qiagen, Valencia, CA) and transfected into CHO cell line tTA_{puro} 6.6, obtained by transfecting wild-type CHO cells with pTOP_{puro}-tTA (see chapter 3 methods). Transfections were carried out using Lipofectamine (Gibco BRL) and 1 μ g of plasmid DNA according to the manufacturer's instructions except that 1 μ g/ml tetracycline (Sigma) was included at each step to inhibit expression of the cDNA until the time of analysis. Stable transfectants were isolated and maintained in medium containing 2 mg/ml G418 (Gibco BRL) plus 1 μ g/ml tetracycline, or 0.2 μ g/ml Taxol with no tetracycline.

Western blotting of CHO cell extracts. This was described in the methods section of chapter 3.

Immunofluorescence of CHO cells. Immunofluorescence with the HA tag antibody was described in the methods section of chapter 3. For double label experiments, mouse monoclonal 6-11B-1 (Sigma), specific for acetylated α -tubulin, was added together with rabbit antibody HA11 (Berkeley Antibody Co., Richmond, CA), specific for the HA tag. This was followed with a mixture of goat affinity purified and cross absorbed antibodies consisting of Oregon Green conjugated antirabbit IgG and Rhodamine Red-X-conjugated antimouse IgG (both from Molecular Probes).

Drug resistance. The ability of β -tubulin mutations to confer Taxol resistance was evaluated in 2 ways. In the first, stably transfected cell lines expressing mutant HAB1-tubulin were seeded at approximately 100 cells/well in replicate wells of a 24-well dish

containing increasing concentrations of Taxol. The assay was carried out in duplicate with only one set containing 1 $\mu\text{g/ml}$ tetracycline. After 6-7 d, the medium was removed and the resistant colonies were stained with a solution of 0.1% methylene blue as previously described (88). In a second assay, aliquots ($\sim 7 \times 10^4$ cells for selective and ~ 100 cells for non-selective conditions) from total transfected cell populations were seeded into duplicate 6-well dishes containing normal medium (non-selective), 2 mg/ml G418, or 0.2 $\mu\text{g/ml}$ Taxol, each with or without 1 $\mu\text{g/ml}$ tetracycline. After the appearance of visible colonies (6-7 d), one duplicate dish was stained with methylene blue and colonies were counted. Cells in the second dish were trypsinized and replated onto glass coverslips for immunofluorescence observation.

Measurement of tubulin polymerization. The distribution of tubulin between the soluble and polymerized pools was measured using a previously published procedure (79). Briefly, cells were incubated for 2 generations (24 h) in [^3H]methionine to label the proteins to steady state, the cells were lysed with a microtubule stabilizing buffer, microtubules were separated from soluble tubulin by centrifugation, a constant amount of [^{35}S]methionine labeled CHO cell extract was added to each fraction, the proteins in each fraction were separated by 2D gel electrophoresis, and the $^3\text{H}/^{35}\text{S}$ ratio for β -tubulin was determined by liquid scintillation counting of spots excised from the gels. This method gives very accurate and reproducible measurements of the fraction of tubulin in the assembled state (79).

Making of transgenic mice. We received as a gift from Fernando Cabral a vector containing the wild-type cDNA for hamster βI tubulin with a C-terminal HA tag (pBlskHABI) (86). We used PCR-based site-directed mutagenesis to make the appropriate point mutations in the wildtype βI for two of these Taxol-resistant mutants. The mutations made were a leucine to histidine at position 215 and leucine to arginine at

position 217, corresponding to the Tax 4-9 and Tax 6-9 mutants in (79), respectively. We then used site-directed mutagenesis to remove the Not I site just 3' to the HA tag, and another round of site-directed mutagenesis to introduce a 3' Sal I site. After sequencing to ensure no unwanted mutations were introduced into the coding sequence, we subcloned the HA-tagged mutants into the Sal I site of a α -MHC promoter vector (kindly provided by Michael Kern, Medical University of South Carolina, Charleston, SC). This vector contains the full α -MHC upstream region, as well as part of the α -MHC promoter and the entire intergenic region between the two (108). It also has, just downstream of the multicloning region, the 3' UTR and polyadenylation site of the human growth hormone cDNA. These two α -MHC/tubulin mutant constructs were linearized with Not I to remove all prokaryotic vector sequence, and the resulting 7.5 kb fragments were isolated from a 0.7% agarose gel using the JETsorb gel isolation kit (Genomed, Research Triangle Park, NC). The DNA was then microinjected into eggs that were implanted into pseudopregnant female FVB mice at the Medical University of South Carolina transgenic mouse facility or the University of Cincinnati transgenic mouse facility. To screen for transgenic offspring, DNA was isolated from tail biopsies using the QIAamp tissue kit (Qiagen). PCR was then performed with two sets of primers: one that specifically amplified a 450 bp fragment of the human growth hormone 3' UTR (present only in the transgene) and one that specifically amplified a 300 bp fragment of the endogenous mouse thyroid stimulating hormone gene (109) (to confirm the PCR reaction). Positive mice were confirmed with Southern blot analysis using a probe specific for the 3' UTR of the growth hormone gene.

Western blotting of transgenic mouse tissue. Protein was isolated from tissue as described in chapter 2. Westerns were performed with the HA tag antibody as described in chapter 3.

RESULTS

Previous studies have yielded Taxol-resistant CHO cells that have diminished microtubule assembly (110-112). Several of these clones were analyzed by 2D gel migration and it was determined that 6 of them had alterations in the migration pattern of β -tubulin (93). The β I tubulin gene was cloned from these 6 clones, as well as 7 others that showed no alteration in the β -tubulin 2D electrophoretic pattern. The genes were sequenced and all of the 6 and 3 of the 7 showed mutations in their β I tubulin gene (93). Table 4-1 summarizes the alterations that were found as well as the determination of the level of polymerized tubulin protein in each cell line. In addition, Table 4-1 notes whether each clone is simply Taxol-resistant or Taxol dependent (110, 111, 113). This latter phenotype is easily recognized by a failure of the cells to divide when Taxol is omitted from the growth medium, and is characterized by a change in morphology to large multinucleated cells (114). Particularly noteworthy is the observation that Taxol dependent mutants have a lower extent of microtubule assembly than wild-type or resistant cell lines, suggesting that Taxol dependent cells are not fundamentally different from resistant cells. Rather, they simply have tubulin mutations that are more disruptive to microtubule assembly. Thus Taxol resistance mutations produce a spectrum of alterations in microtubule assembly from minimally disruptive (resistant cells) to highly disruptive (dependent cells). As shown in Table 4-1, the mutated β -tubulin genes from the Taxol-resistant clones showed a concentration of mutations in a small region. All the mutations were found in 3 leucine residues, L215, L217, and L228.

To prove that the β -tubulin mutations discovered could directly cause alterations in microtubule stability, we recreated the L215H, L217R, and L228F mutant cDNAs in wild-type β I tubulin cDNA containing a HA tag and transfected into CHO cells. We circumvented the possibility that overexpression of these mutant genes might be toxic to

Table 4-1. Summary of β -tubulin mutations in Taxol-resistant CHO cells

Cell line	Sequence ^a	β -tubulin alteration	% tubulin in polymer ^b	Resistant or Dependent ^c
Wild-type	-ACTCTCAAGCTCACC-	None	38%	
Tax 1-4	-ACTCACAAGCTCACC-	L215H	22%	R
Tax 2-4 ^d	-ACTCACAAGCTCACC-	L215H	15%	D
Tax 4-9	-ACTCACAAGCTCACC-	L215H	22%	R
Tax 1-19	-ACTCGCAAGCTCACC-	L215R	29%	R
Tax 18	-ACTTTTAAGCTCACC-	L215F	15%	D
Tax 6-21	-ACTTTCAAGCTCACC-	L215F	15%	D
Tax 6-9	-ACTCTCAAGCGCACC-	L217R	31%	R
Wild-type	-AACCACCTCGTCTCG-	None	38%	
Tax 11-3	-AACCACTTCGTCTCG-	L228F	17%	D
Tax 2-5	-AACCACCACGTCTCG-	L228H	19%	D

^aFor the upper series of mutants, codons 215 and 217 are underlined. For the lower series, codon 228 is underlined. Mutations are indicated in bold letters.

^bThe fraction of total tubulin assembled into microtubules was determined as described in (79).

^cR, cells are resistant to Taxol and grow without the drug. D, cells are resistant to Taxol but also require the continuous presence of the drug for cell division.

^dAlthough this cell line has the same mutation as Tax 1-4 and Tax 4-9, its properties, including Taxol dependence, differ significantly from the other mutants. We suspect that

this cell line may have a second mutation in another gene because of its extremely low reversion frequency (110).

transfected cells by inserting the altered tubulin cDNAs into a pTOPneo vector that places the gene to be expressed under the control of a minimum CMV promoter whose activity requires the binding of a tetracycline regulated transactivator to an upstream bacterial *tetO* sequence (87). Each of the mutant cDNAs, as well as an unmodified HA β -tubulin, was transfected into a CHO strain (tTA/puro 6.6) that produces the tetracycline-regulated transactivator in the absence, but not the presence, of tetracycline.

Stable G418-resistant cell lines from each of the transfections were isolated and screened for production of HA tagged β -tubulin by immunofluorescence. Approximately half of the cell lines for each transfection proved to be positive (data not shown) and for each clone, >95% of the cells in the population stained positive for HA β -tubulin production (data not shown). To obtain a more quantitative estimate for the fraction of total β -tubulin represented by the HA β -tubulin in each cell line, Western blot analysis with an antibody that recognizes both forms of β -tubulin was carried out (Figure 4-1). The HA β transfectant exhibited a very high level of HA β -tubulin production, resulting in a cell line in which the majority of the endogenous β -tubulin is replaced by the epitope tagged tubulin at steady state. The HA β _{L217R} and HA β _{L228F} transfectants also had high production of HA β -tubulin, but the endogenous β -tubulin remained a significant component. The lowest level of HA β -tubulin was found in the HA β _{L215H} transfectant, where it accounted for only a small fraction of the total β -tubulin in the cell. In all 4 cases, production of HA tagged tubulin was undetectable by immunofluorescence or Western blot analysis when the cells were grown in tetracycline (data not shown).

Although all transfectants producing wild-type HA β -tubulin grew well in the absence of tetracycline, transfectants producing moderate to high levels of mutant HA β -tubulin grew poorly. These latter cells frequently exhibited extensive multinucleation during interphase, and there was a clear increase in the number of mitotic cells indicating

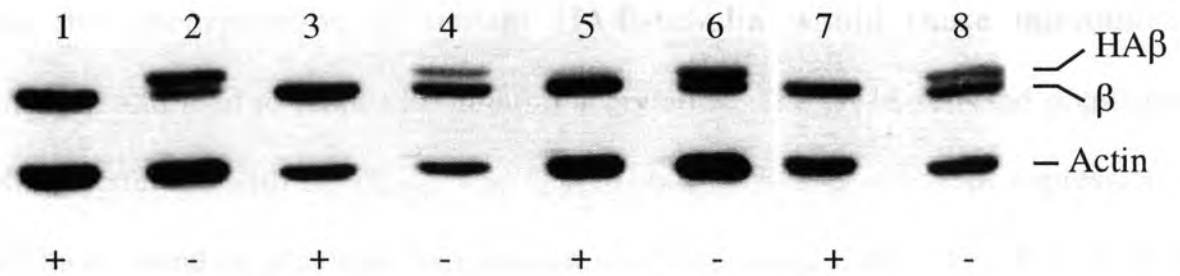


Figure 4-1. Production of wild-type and mutant HAβI-tubulin in transfected cell lines. The stably transfected cell lines were maintained in tetracycline (“+” lanes) or were incubated 24 h in medium without tetracycline (“-” lanes) and cellular proteins were then resolved by SDS gel electrophoresis, transferred onto nitrocellulose, and probed with antibodies specific for β-tubulin and actin. Shown in the figure are cells transfected with HAβI (lanes 1 and 2), HAβI_{L215H} (lanes 3 and 4), HAβI_{L217R} (lanes 5 and 6), and HAβI_{L228F} (lanes 7 and 8). Note that the HA tag causes HAβI-tubulin (HAβ) to migrate more slowly than endogenous β-tubulin (β). An antibody to actin was included to indicate relative protein loading.

a block in mitosis. These observations are consistent with the reduced tubulin assembly measured in the mutants listed in Table 4-1. To further demonstrate that incorporation of mutant HA β I-tubulin destabilizes cellular microtubules, an HA β I_{L215H} transfected cell population was selected in G418 and double stained with antibodies to the HA tag and to acetylated α -tubulin. Work in other laboratories has demonstrated that acetylated tubulin is found in the most stable and least dynamic microtubules in the cell (115, 116). We predicted that incorporation of mutant HA β I-tubulin would cause microtubule destabilization and lead to reduced α -tubulin acetylation. The G418-selected population from cells transfected with HA β I_{L215H} was approximately 50% positive for expression, a value we have noted in previous transfection experiments (29, 86, 117). Figure 4-2A shows two adjacent cells in this population, one of which was positive (small arrow), and the other of which was negative (large arrow), for mutant HA β I-tubulin production. When the same cells were viewed for acetylated α -tubulin staining (Figure 4-2B), a reciprocal relationship was evident. The cell that expressed mutant HA β I-tubulin had little acetylation of α -tubulin, but the cell that did not express mutant tubulin had abundant α -tubulin acetylation. This result supports the notion that incorporation of mutant HA β I-tubulin produces less stable microtubules.

Measurement of drug resistance using a standard cloning efficiency assay was complicated by the observation that clones producing moderate to high levels of mutant HA β I grew poorly and produced many multinucleated cells. This problem was circumvented in 2 different ways. The first came from an observation that, among the multinucleated cells, there were some cells that still looked normal. This suggested that some of the cells in the population might be expressing lower amounts of the mutant tubulin and might be able to survive when cultured without tetracycline. To select these cells, clones transfected with mutant HA β I-tubulin were incubated in tetracycline-free

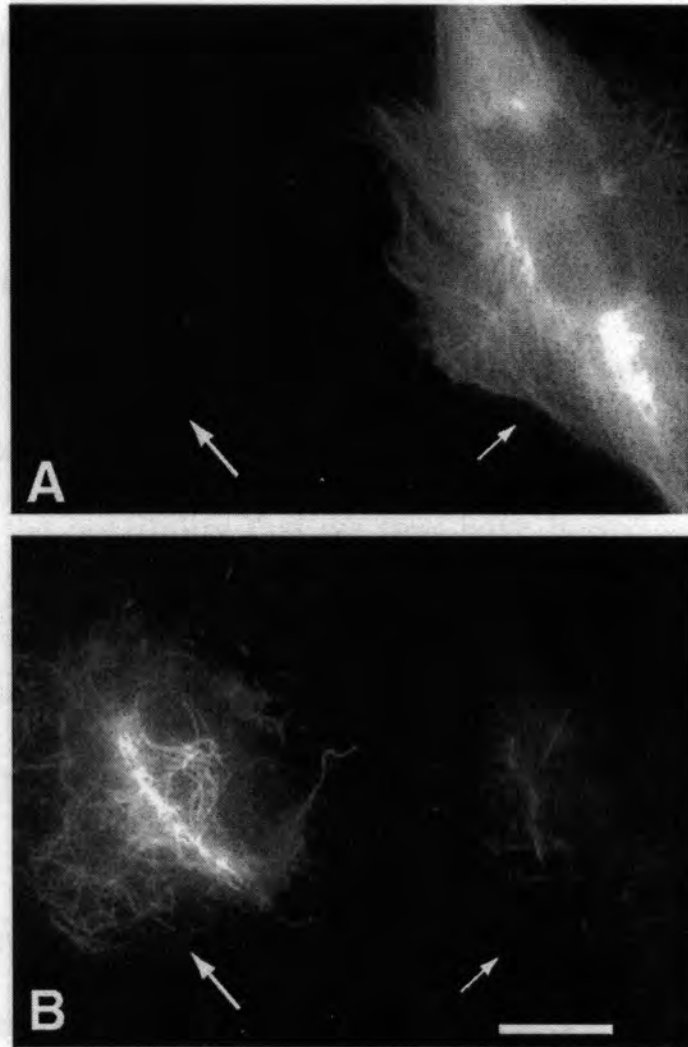


Figure 4-2. Cells expressing HA β I_{L215H} have reduced α -tubulin acetylation. A G418 selected population of cells transfected with HA β I_{L215H} cDNA was grown 24 h without tetracycline and stained for immunofluorescence with antibodies to the HA tag (A) and to acetylated α -tubulin (B). Small arrows indicate a cell that expressed the mutant HA β I-tubulin. Large arrows indicate a neighboring cell that failed to express the mutant HA β I-tubulin. Note that acetylation was greatly reduced in the cell that expressed the mutant β I-tubulin.

medium containing a concentration of Taxol (0.2 $\mu\text{g/ml}$) that is lethal to wild-type cells. Multiple individual colonies were selected and tested for their dose response to Taxol. HABI, HABI_{L215H}, HABI_{L217R}, and HABI_{L228F} expressing cells were all tested for Taxol sensitivity in the presence or absence of tetracycline. It was found that the HABI transfected cells had the same sensitivity to Taxol regardless of whether the HABI tubulin is expressed (no tetracycline) or not expressed (with tetracycline) (data not shown). The cells transfected with mutant HABI-tubulin also had wild-type Taxol sensitivity when grown with tetracycline, but exhibited clear resistance to the drug when mutant tubulin production was induced by growing the cells without tetracycline (data not shown).

To rule out the possibility that we may have biased the results by examining specific clones of mutant HABI-tubulin expressing cells, we also tested the relative abilities of G418 and Taxol to select mutant HABI-tubulin positive cells from the total transfected cell populations. We reasoned that Taxol should be a powerful agent for selection of mutant HABI-tubulin expressing cells if, and only if, the mutant tubulin is capable of conferring resistance to the drug. To test this prediction, aliquots from an HABI_{L215H} transfected cell population were grown under 6 different conditions: normal medium, medium containing 2 mg/ml G418, and medium containing 0.2 $\mu\text{g/ml}$ Taxol, each in the presence or absence of 1 $\mu\text{g/ml}$ tetracycline. Using the number of colonies obtained under nonselective conditions (normal medium containing tetracycline) as a control, the relative cloning efficiencies under the various selective conditions are summarized in Table 4-2. The highest cloning efficiency under selective conditions was obtained with G418 in the presence of tetracycline. This was expected because, under these conditions, HABI_{L215H} cDNA is not expressed and, therefore, transfected cells should be capable of expressing the neomycin resistance gene without suffering negative consequences of HABI_{L215H}-tubulin production. The efficiency using G418 under inducing

Table 4-2. Cloning efficiencies of HAβ1_{L215H} transfected cells under various selective conditions.

	+Tetracycline	-Tetracycline
αMEM	1	0.98
G418	1.3 X 10 ⁻³ (100)	7.9 X 10 ⁻⁴ (60)
Taxol	1.4 X 10 ⁻⁵ (1)	2.3 X 10 ⁻⁴ (18)

CHO cell line tTA_{puro} 6.6 was transfected with HAβ1_{L215H} cDNA. At 24 h post-transfection, the cells were trypsinized and replated in normal medium (αMEM), medium containing 2 mg/ml G418, or medium containing 0.2 μg/ml Taxol, all either in the presence or absence of 1 μg/ml tetracycline. After 6-10 d (when visible colonies were seen) the cells were stained with methylene blue and the surviving colonies were counted. The cloning efficiency was calculated as the number of colonies obtained under selective conditions (G418 or Taxol) divided by the number of colonies obtained under nonselective conditions (αMEM + tetracycline). Numbers in parentheses are the number of colonies obtained relative to G418 + tetracycline which was arbitrarily set at 100.

conditions (no tetracycline) was about 40% lower, consistent with the expectation that high expression of HABI_{L215H} is deleterious to cell growth. To demonstrate that this is the correct explanation, cells selected under both conditions were compared by immunofluorescence using antibodies to the HA tag. The population selected in G418 under non-inducing conditions but assayed following induction contained approximately 50% HA-positive cells (Figure 4-3A). In stark contrast, cells selected in G418 under inducing conditions were fewer than 10% HA-positive and exhibited weaker fluorescence, indicating that only the cells with lower levels of expression were able to survive (Figure 4-3B).

Selection in Taxol under inducing conditions was 5 times less efficient than in G418 with tetracycline (Table 4-2). This can be explained by the loss of cells that produce too little HABI_{L215H}-tubulin to confer resistance or produce too much HABI_{L215H}-tubulin to survive. In contrast to the G418 selected cells, virtually all the cells selected in Taxol expressed HABI_{L215H}-tubulin (Figure 4-3D). Thus, Taxol more consistently selected HABI-tubulin expressing cells, or transfected cells, than did G418; this strongly argues that HABI_{L215H} tubulin confers resistance to the drug. Consistent with this interpretation, cells selected with Taxol under non-inducing conditions formed 18-fold fewer colonies. Cells selected under these conditions grew very poorly and needed to be cultured an additional week in order to obtain enough cells for analysis. The resultant cells (Figure 4-3C) were <5% positive for HABI_{L215H}-tubulin expression and exhibited weaker fluorescence than the cells selected under inducing conditions. Unlike the cells selected for Taxol resistance under inducing conditions, which repressed HABI_{L215H} tubulin expression upon tetracycline addition, the HA-positive cells selected under noninducing conditions remained positive regardless of whether tetracycline was present or absent (data not shown). These results indicated that the few cells selected with Taxol in the

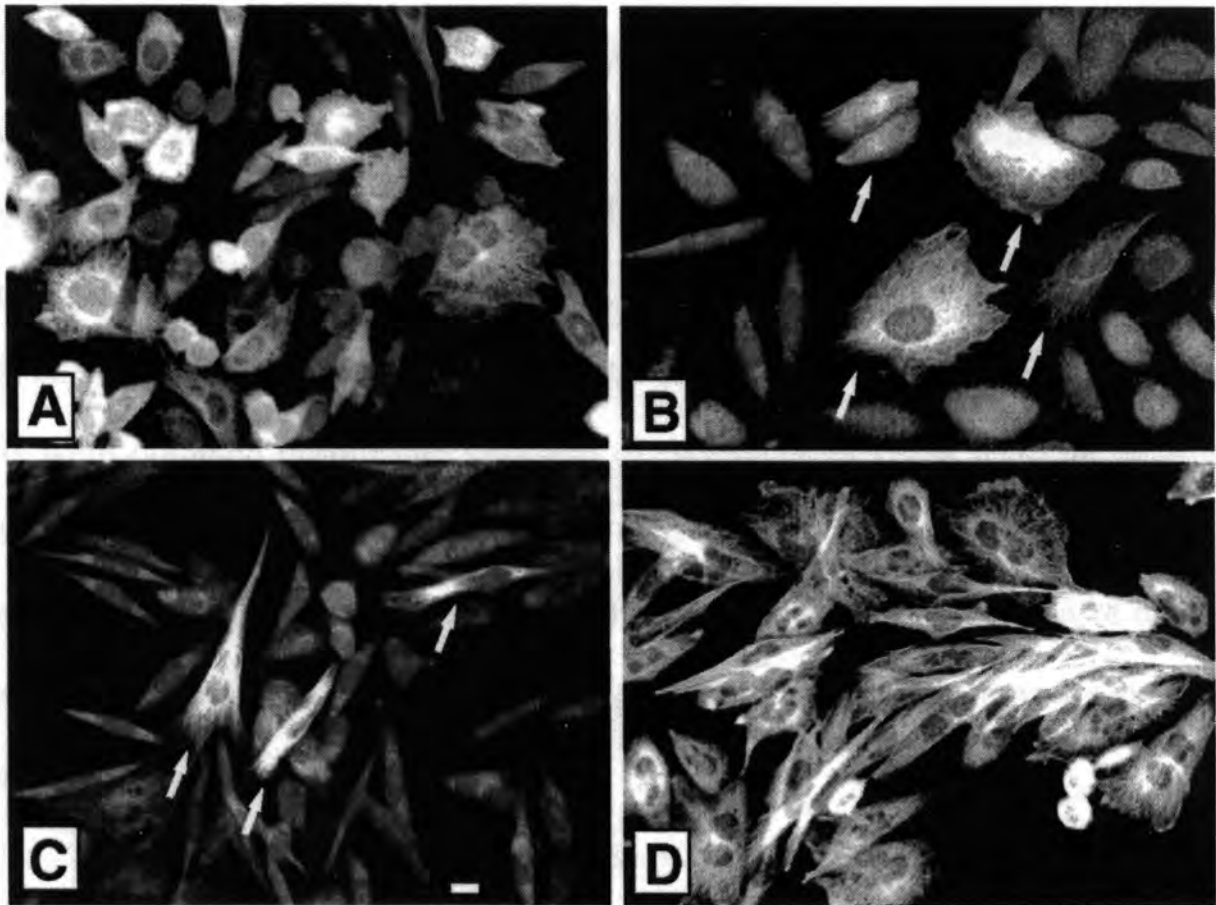


Figure 4-3. Taxol selects for transfected cells that express mutant HA β I-tubulin. Cells transfected with HA β I_{L215H} cDNA were selected for resistance to G418 (A, B) or Taxol (C, D) either in the presence (A, C) or absence (B, D) of 1 μ g/ ml tetracycline. The total resistant cell population was then trypsinized and replated for 24 h in medium without tetracycline or Taxol before processing for immunofluorescence with an antibody specific for the HA tag. Arrows in B and C indicate cells that were positive for HA β I_{L215H}-tubulin expression. Approximately 50% of the cells in panel A, and 100% of the cells in panel D were positive for expression. Bar = 10 μ m.

presence of tetracycline consisted of non-transfected cells with borderline Taxol resistance (and severe growth problems) and transfected cells with low, unregulated HABI_{L215H}-tubulin production.

The preceding data gave us confidence that direct selection of Taxol-resistant transfected cells, followed by analysis of transfected gene expression in the selected population, can serve as a rapid and reliable method for testing the ability of various mutations to confer drug resistance. Indeed, when the procedure was repeated three times with HABI, or with HABI_{G38E} (a random mutation in Tax 11-3) cDNAs, no Taxol-resistant cells were obtained despite the selection of thousands of G418 resistant colonies. In contrast, HABI_{L217R} and HABI_{L228F} cDNAs behaved like the HABI_{L215H} cDNA and gave many Taxol-resistant colonies, all of which were positive for expression of the mutant gene. We conclude that HABI_{L215H}, HABI_{L217R}, and HABI_{L228F} mutations are sufficient to confer Taxol resistance in CHO cells.

The data generated by overexpression of the β -tubulin mutants in CHO cells gave us confidence that the mutant proteins could be used as tools to confer Taxol resistance to cells that expressed them at high enough levels. Because the original cells from which these mutant proteins were isolated had less stable microtubules (79), we were confident that the proteins could act as dominant negative regulators of microtubule stability. This afforded us the opportunity to alter microtubule stability in the context of *in vivo* pressure overload-induced hypertrophy to see what kinds of effects decreased microtubule stability could have on the development of heart failure *in vivo*. The mouse model of transverse aortic constriction would allow us to study pressure overload-induced hypertrophy in an animal that can be easily genetically manipulated (118). Many other labs have used the α -myosin heavy chain promoter (α MHC) to achieve relatively high

levels of expression of transgenes in the adult left ventricle of the mouse (reviewed in (119)).

We constructed plasmids that expressed two of the mutants isolated from Taxol-resistant CHO cells from the α -MHC promoter. As detailed in the methods section, we used PCR-based site-directed mutagenesis to make the appropriate point mutations in the wildtype β I. The mutations made were a leucine to histidine at position 215 and leucine to arginine at position 217, corresponding to the Tax 4-9 and Tax 6-9 mutants in (79), respectively. The mutants were then subcloned into an α -MHC promoter vector (kindly provided by Michael Kern). This vector ensures expression of the cloned genes primarily in adult cardiac ventricular tissue (108).

The mutant constructs were injected into FVB mouse oocytes that were implanted in pseudopregnant females. The L215H mutant yielded 39 possible founder mice, and the L217R mutant yielded 13 possible founders. When the mice were weaned, they were ear-clipped for identification, tail biopsies were obtained, and genomic DNA was isolated. The DNA was analyzed by PCR for presence of the transgene (data not shown). Using Southern analysis with a probe specific for the human growth hormone 3' UTR, we confirmed that 4 of 39 and 1 of 13 possible founders for L215H and L217R, respectively, had taken up the transgene (Figure 4-4).

The founder mice were then bred with wild-type FVB mice. These F₀ offspring were also tested for transgene incorporation by PCR. Table 4-3 summarizes the transgenic status of the offspring. The numbers show that close to the expected 50% of offspring for the L215H lines #1 and #2 are positive for the transgene, whereas only about 1% of the offspring for the L217R line #1 is positive. This means that the L217R founder is probably a mosaic. One of the offspring for this line was bred with a wild-type

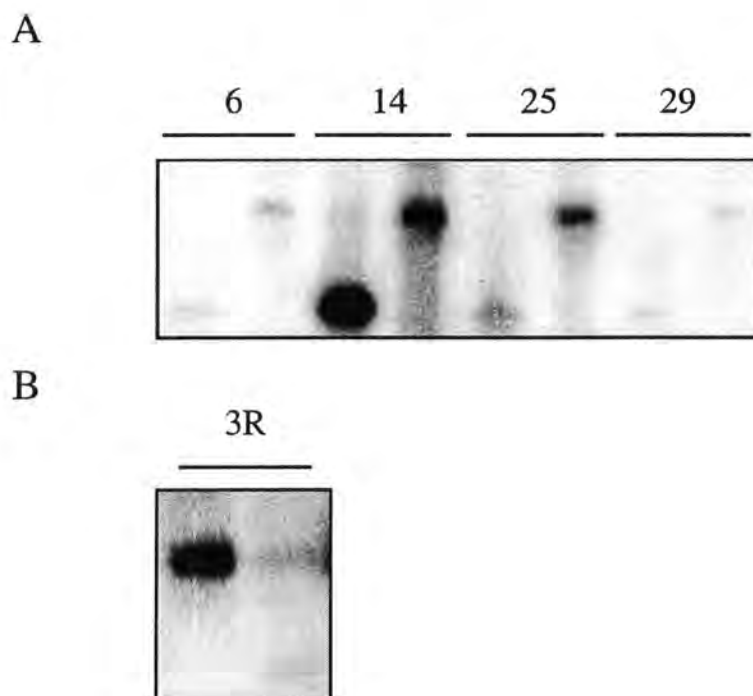


Figure 4-4. Southern analysis of transgenic mice. Panel A shows genomic DNA digested with Bam HI in the first lane and Eco RI in the second lane for each mouse found positive for the transgene α -MHC/HA β I_{L215H}. Panel B shows DNA digested with Eco RI in the first lane and Bam HI in the second lane for the mouse found positive for α -MHC/HA β I_{L215R}. For each, a 600 b.p. band was expected for the Bam HI digestion and a 900 b.p. band was expected for the Eco RI digestion when a probe specific for the 3' UTR was used. The founder number is given above each pair of lanes. Mouse number 25 and mouse number 29 both died at about 3 weeks of age, but it is not known if this was because of expression of the transgene. Mouse number 14 founded the L215H #1 line, mouse number 6 founded the L215H #2 line, and mouse number 3R founded the L217R #1 line.

Table 4-3. F₀ offspring of transgenic founders.

Line	No. of Offspring	No. Positive	Percent Positive
L215H #3	34	19	56%
L215H #4	7	6	86%
L217R #1	63	3	0.5%

FVB mouse, and the F₁ offspring were screened for the transgene with PCR. From this mating, 23 of 42 offspring born were positive for the transgene.

One of the transgenic offspring from the L215H #1 line was sacrificed and total protein was isolated from several tissues, including the left ventricle of the heart. Figure 4-5 shows the results of Western blots performed with total protein from this mouse using the anti-HA antibody. Normal FVB mouse tissues were used as a control. The figure shows that the highest level of expression occurs in the left ventricle. Once these mice are bred to higher numbers, they will hopefully serve as a model for lower microtubule stability in the left ventricle of the heart.

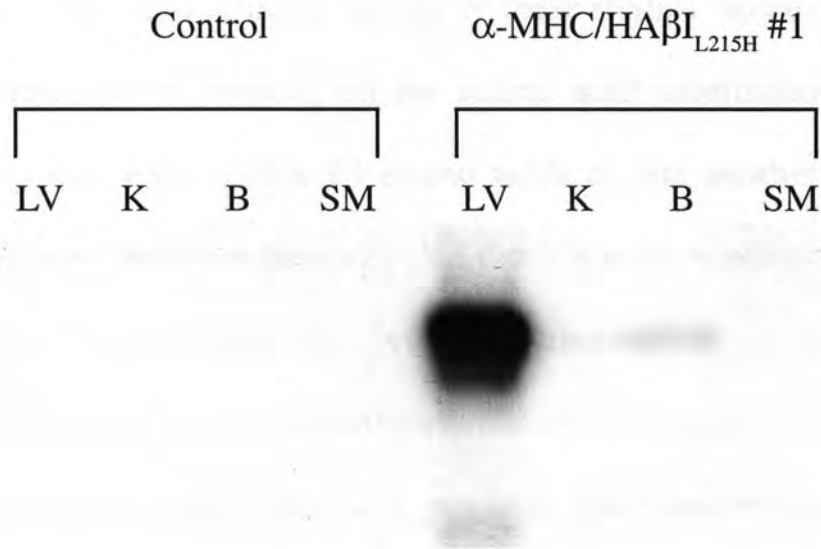


Figure 4-5. HA β -tubulin levels in tissue from a transgenic mouse. Total protein was isolated from various tissues from a non-transgenic control mouse and an L215H mutant-expressing mouse. The transgenic mouse was an adult male from line #1, which had the highest copy number according to Southern blot analysis. The proteins were subjected to Western blotting with the HA tag antibody. The tissues were as follows: LV=left ventricle, K=kidney, B=brain, and SM=skeletal muscle. There is a low amount of expression in the brain as well as the LV.

DISCUSSION

Previous studies have clearly shown that there are β -tubulin mutants present in Taxol-resistant cells that have hypostable microtubules (79). However, these studies are the first direct proof that expression of the mutant tubulin proteins can directly confer Taxol resistance. The most striking finding of these studies, however, is that of 9 mutant β -tubulins cloned and sequenced, all the amino acid substitutions changed one of 3 leucine residues that were within 14 amino acids of one another. An alignment of β -tubulin sequences in GenBank indicates that the 3 leucine residues are invariant with the exception of an isoleucine for leucine substitution at amino acid 217 in *Schizosaccharomyces pombe*. Furthermore, the conservation of leucines at 215 and 228 extends to α - and γ -tubulin (120). It is possible that these residues are important for interactions between different tubulin proteins.

The recent publication of the crystal structure of the tubulin molecule (104) indicates that mutations in codons 215 and 217 are in a loop connecting helices H6 and H7, while the 228 mutation falls within the H7 helix itself (see Figure 4-6 for placement of the mutated residues within the β -tubulin molecule). While this is in the region of the β -tubulin protein reported to bind the Taxol molecule, it is distinct from the residue L275 that forms the main interaction with the taxane ring (104). Mutations isolated from Taxol-resistant CHO cells have occurred with equal frequency in both α - and β -tubulin, whereas only the β -tubulin protein binds Taxol. In addition, many of the resistant clones isolated in the past have been Taxol-dependent, meaning that they must still be able to bind Taxol. For these reasons, we believe that the mutations conferring Taxol resistance do not cause decreased ability of the Taxol to bind, but rather a weakening of the binding between the tubulin molecules themselves. The fact that these mutants destabilize microtubule assembly in the absence of the drug implies a direct effect on subunit-

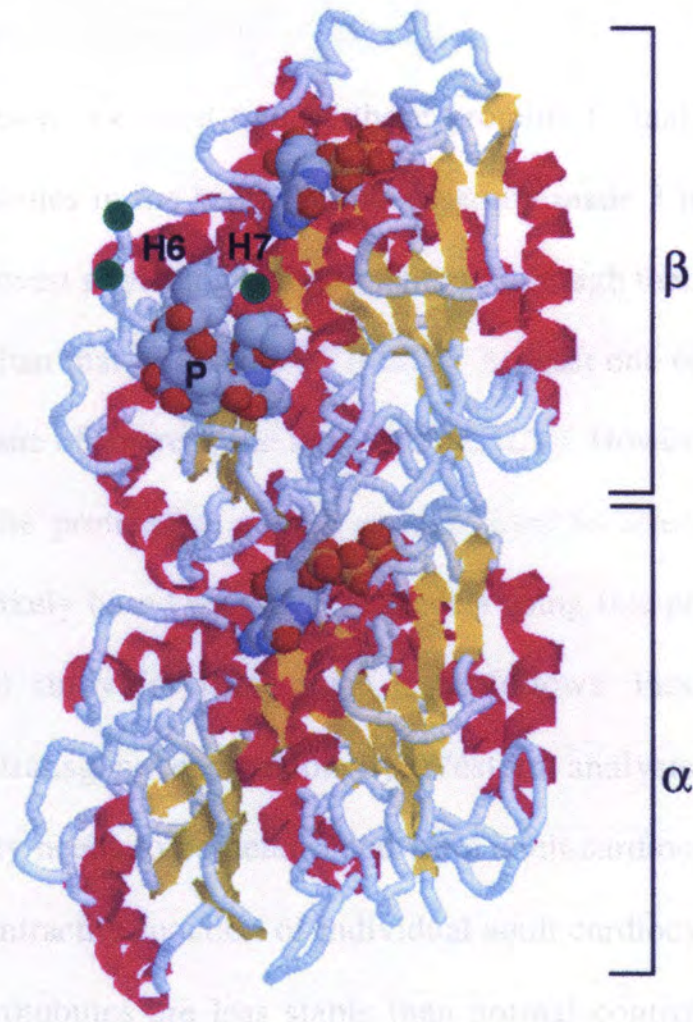


Figure 4-6. Location of mutated residues in the crystal structure of tubulin. The approximate location of the mutated residues is indicated by the green circles in this representation of the tubulin heterodimer (93). H6 and H7 are helical regions of β -tubulin near the mutations. P, paclitaxel.

subunit interactions. For this reason, these mutant proteins are wonderful tools for studying the effects of decreased microtubule stability in different cell systems, including the adult cardiocyte.

For this reason, we used two of these proteins to make a mouse model with hypostable microtubules in the heart. We successfully made 3 mouse lines. These mice do not display any overt physiologic abnormalities, although their spontaneous death rate is possibly higher than that of normal FVB mice. At least one of the lines expresses the transgene in the tissue of interest, the left ventricle (LV). However, it is still unknown if the mice express the proteins at a high enough level to affect microtubule stability, although it seems likely based on previous models using this promoter construct (119). The future plan of study for these mice is as follows. First, all lines need to be characterized for transgene expression by Western analysis. Second, the state of microtubule stability needs to be determined from adult cardiocytes isolated from these mice. Third, the contractile function of individual adult cardiocytes needs to be studied. Fourth, if the microtubules are less stable than normal controls, the mice need to be studied for ability to show hypertrophy and/ or decreased contractility at the whole organ and cardiocyte level after transverse aortic banding (118). If our model of hyperstable microtubules causing decreased contractility during pressure overload-induced hypertrophy is correct, the transgenic mice should show lesser contractile dysfunction after banding than normal controls. Additionally, these mice could be bred with transgenic mice that display other forms of cardiac disease (119) to see if there is any therapeutic value of decreased microtubule stability in the setting of cardiac pathology.

CHAPTER 5: GENERAL DISCUSSION

The results of these studies answered several questions about the regulation of β -tubulin proteins during pressure overload-induced cardiac hypertrophy as well as questions concerning what factors can affect microtubule stability in both terminally differentiated cardiocytes as well as mitotically active cells. Although these studies originated with the specific task of discovering what might cause increased microtubule stability during hypertrophy, they also were fruitful in answering general questions about the kinetics of an extremely important polymer in all cell types.

Specifically, chapter 2 addresses the hypotheses that, during pressure overload-induced hypertrophy, certain β -tubulin genes are upregulated transcriptionally and that the autoregulation of β -tubulin message by free β -tubulin heterodimers does not occur. The results of chapter 2 show that the β -tubulin genes are regulated transcriptionally during pressure overload-induced hypertrophy, and that only the normally embryonically expressed isotypes, β I and β II, are upregulated. In addition, the autoregulation of β -tubulin message stability by β -tubulin protein is possible in a terminally differentiated cell. More importantly, the results suggest that this regulatory mechanism is only invoked by a rapid increase in free tubulin heterodimer levels and/ or a change in the free heterodimer/ incorporated heterodimer ratio.

Chapter 3 addresses the hypotheses that overexpression of specific β -tubulin isotypes in CHO cells cannot directly cause Taxol resistance, but that overexpression of β I-tubulin in adult cardiocytes can cause an increase in microtubule stability. The results show that the overexpression of specific β -tubulin isotypes, including β I, do not directly

cause changes in microtubule stability, as measured by induction of Taxol resistance, in CHO cells. The results also show that overexpression of β I-tubulin in the adult cardiocyte, which normally has low levels of this protein, does not cause increased microtubule stability. Therefore, the results suggest that the primary mechanism of increased microtubule stability during pressure overload-induced hypertrophy is probably not the overexpression of the β I tubulin molecule, but rather the increased expression of the predominant cardiocyte microtubule associated protein, MAP 4.

Finally, chapter 4 reveals an area of the β -tubulin molecule that is critical for the maintenance of microtubule stability. The results confirm that mutations in specific leucine residues in this H6/ H7 loop area can confer on the β -tubulin protein the ability to cause decreased stability of microtubules as measured by Taxol resistance in CHO cells. These mutations led to the development of a useful model for the generation of less stable microtubules in the adult heart, allowing for a direct test of the therapeutic value of microtubule destabilization for heart failure *in vivo*.

While all of these results are important clues about how the β -tubulin protein might regulate microtubule stability, they leave several questions unanswered. The most obvious question that arises out of the results of chapters 2 and 3 is, if the upregulation of β I- and β II-tubulin is not important for the increased microtubule stability seen during hypertrophy, then why does it occur. A more general but related question is why do embryonic genes get upregulated during hypertrophy. Transcriptional regulation has been studied in detail for many heart-specific genes during hypertrophy. Unfortunately, most of these studies have been carried out in α -adrenergic agonist, growth factor, or mechanically stimulated neonatal rat cardiocytes. This system has many advantages, which include the induction of genes known to be upregulated during cardiac hypertrophy *in vivo*, and an increase in cellular protein content and cell mass; however, it

has many disadvantages that limit its use. In particular, neonatal cardiocytes are not fully differentiated; therefore, the factors and signaling pathways mediating growth may be very different from those in the terminally differentiated adult cardiocyte. However, these studies have led to a host of information about how cardiac-specific genes are regulated in response to certain stimuli that might imitate hypertrophic stimuli. Several transcription factors that upregulate different genes during hypertrophy are known. One is TEF-1 (121), which binds to the M-CAT factor that is important for heart and skeletal muscle expression of some genes. Another is serum response factor (SRF) (121), which binds to CArG elements, sequences that have high homology to the serum response element known to mediate regulation of some immediate early genes during hypertrophy. Still another is GATA-4 (122), which binds to the GATA element and is one of a family of transcriptional factors known to regulate cardiac-specific expression of some genes. While all of these factors have been implicated in cardiac specific expression of many different genes, no systematic studies have been done to show whether or not they regulate cardiac genes at specific points during development. In short, no studies to date that have studied transcriptional regulation of genes during hypertrophy have fully explained why cells that are exposed to a hypertrophic stimulus might respond by a recapitulation of embryonic gene expression. In addition, as discussed in chapter 2, it is unclear that the recapitulation of embryonic genes is a universal phenomenon during hypertrophy. Importantly, some reports have even demonstrated that the upregulation of some genes during hypertrophy is by a mechanism that is independent of those genes' regulation in perinatal development (123).

The developmental regulation of the β -tubulin genes has been studied primarily in neuronal cells, where the genes are regulated coordinately with both the α -tubulin and MAP genes. The BI- and BII-tubulin isotypes are both expressed primarily in the early

developmental stages of both the central and peripheral nervous systems, and, in the peripheral nervous system, axotomy results in the upregulation of the β II-tubulin isotype (22). No studies to date have shown what promoter elements might be involved in the upregulation of the β -tubulin genes in any tissue. It seems safe to assume that the elements are not cardiac-specific, like many of the ones mentioned above for regulation of other genes during hypertrophy. However, many studies have implicated mitogenic signaling pathways, such as the Ras/Raf/MEK/ERK pathway, in the stimulation of genes during cardiac hypertrophy that are normally expressed embryonically. It seems reasonable to presume that these mitogenic signals might affect such basic cellular components as tubulin proteins, especially in light of the fact that these genes are functionally important during the cell cycle. In essence, the upregulation of these genes might be part of a general mitogenic plan that leads not to mitosis in the terminally differentiated cell, but rather cell growth.

Neurons rely heavily on their microtubule network for transport of cellular components down their axons and dendrites as well as for the growth of these structures. Neurons, like cardiocytes, are large, terminally differentiated cells and, therefore, need intracellular transport for growth. Microtubule stability is increased during neuronal differentiation (124-126); this is accompanied by a sorting of β II-tubulin into colchicine stable microtubules (76). Additionally, this increased use of β II-tubulin in stable microtubule populations coincides with the upregulation of MAP 1B, MAP2C, and tau in developing neurons (76). It is reasonable to speculate, then, that the different tubulin isotypes are important in a functional sense for modulation of microtubule structure for the purpose of cell growth. This is why our original hypothesis of increased β I-tubulin causing increased microtubule stability seemed so attractive. We speculate that the change in microtubule stability during cardiac hypertrophy is an attempt by the cell to

modulate microtubule dynamics to allow for increased transport of the proteins and/ or mRNA molecules needed to manufacture new sarcomeres. Previous studies in skeletal muscle cells showed the importance of MAP 4 for the maintenance of microtubule structure needed for sarcomerogenesis (30). We presumed that the increase in β I-tubulin, along with the increased MAP 4, might help stabilize the microtubules needed for transport, similar to the way that β II-tubulin and the neuronal MAPs seem to affect the microtubules needed for transport in the developing neuron. It is possible, however, that MAP 4 expression alone is enough to stabilize the microtubules and that the expression of the β I- and β II-tubulin genes is simply part of the developmental program of gene expression invoked by growth signals, with their overexpression having no real functional significance. In essence, our results show that overexpression of tubulin proteins of any isotypic persuasion, coupled with increased MAP4 expression, gives the cell the tools it needs to stabilize its microtubules. This is further supported by data that showed that during muscle cell development *in vitro*, β IV-tubulin was found in colchicine stable microtubules (76).

More experiments are necessary to confirm the data. One experiment that is underway was discussed in chapter 3: the overexpression of the untagged β I- and β IV-tubulin isotypes. It is possible that the HA tag interferes in some way with MAP binding to mask the synergistic effect of β I-tubulin and MAP 4 overexpression. However, the ability to coexpress HA β -tubulin and MAP 4 in the same cells without affecting MAP 4's ability to stabilize the microtubules makes this unlikely. We have shown that high overexpression of MAP 4 can lead to microtubule stabilization, but we have yet to prove that overexpression at a more physiologic level can increase microtubule stability. Also, the data from overexpression studies in this work were all generated in cell culture systems. To definitively prove that overexpression of MAP 4 can cause increased

microtubule stability *in vivo*, transgenic mice need to be generated that have discrete levels of MAP 4 overexpression specifically in the heart. These studies are also currently underway. Finally, in order to explore the promoter elements involved in the transcriptional upregulation of the β -tubulin as well as MAP 4 genes, a cell culture system needs to be found that can mimic the changes seen *in vivo*. This work failed to find such a system because stimulated neonatal cardiocytes do not exactly mimic pressure overload-induced hypertrophy and we failed to homogeneously differentiate serum-starved muscle cell lines. However, new cardiac cell lines that are transfectable are continually being isolated in other labs, and some of these may undergo dramatic changes in β -tubulin isotype expression needed to study transcriptional regulation of these promoters.

The data concerning the autoregulation of β -tubulin message generated in chapter 2 bring about another question not answered by this study: what is the mechanism by which this regulation occurs and how does it distinguish between a rate and amount increase in the free heterodimer concentration? Careful studies done primarily in Don Cleveland's laboratory showed that, for both α - and β -tubulin messages, increased amounts of free tubulin heterodimers led to decreased message stability. This was true even with the direct injection of a small amount of free tubulin heterodimers (35). Our data support the hypothesis that this is not true in the adult cardiocyte, because we see at least a two-fold increase in the steady-state levels of free tubulin heterodimers with a large increase of message level. However, rapid depolymerization of microtubules in the terminally differentiated cardiocyte resulted in decreased message stability, proving this hypothesis to be false. We believe this gives an important clue to the mechanism of autoregulation of tubulin message stability by free tubulin heterodimers. The two main differences between the depolymerization of microtubules in one experiment versus the increased expression of tubulin in the other experiment is rate of increase in free tubulin

heterodimers and ratio to polymerized tubulin protein. This implies that the factor that mediates this autoregulatory mechanism can somehow sense either the rate of protein increase or the comparison to polymerized protein levels. While I have no specific candidates in mind for what this factor may be, one useful study might be the rate-controlled injection of free tubulin heterodimers in individual cultured cells and subsequent analysis of changes in mRNA levels to at least address the hypothesis of a rate sensitive mechanism. Then, careful analysis of proteins that are known to bind to free tubulin might be a next step. It would seem likely that any protein that modulates this control mechanism would also need to bind to mRNA or some part of the ribosomal/mRNA complex, since the autoregulation only occurs on actively translated tubulin messages.

The data generated in chapter 4 begin to address the question of how the structure of the β -tubulin molecule might affect the function of the microtubule. They show that mutation of leucine residues in the H6/ H7 loop region of the β -tubulin molecule dramatically affects the stability of the microtubule polymer. However, the data don't answer the question of how the leucine residues that can be mutated to give Taxol-resistance are related to the structure of the polymer. In this context, it is important to establish exactly what residues can be placed at these positions and in the surrounding areas. Both hydrophobic and charged residue substitutions at these positions gave Taxol-resistance (93), suggesting that the charge of the amino acid is less important than the size. Further studies of β -tubulin molecules mutated at position 215 have shown that any substitution other than leucine is detrimental to microtubule stability (K. Blade, G. Bell, D. Menick, F. Cabral, unpublished results). This makes it likely that there is an absolute need for the leucine cluster in this region to ensure proper polymerization of the microtubule.

The presence of this cluster of leucines makes it likely that the H6/ H7 loop in which it occurs is important for the stability of the microtubule. For this reason, studies are now being done to determine what interacts with this region of the β -tubulin molecule. The H6/ H7 loop appears to be situated in a region where it could potentially interact longitudinally with α -tubulin in the next heterodimer along the protofilament, or laterally with a neighboring β -tubulin in the next adjacent protofilament (Fernando Cabral, personal communication). To determine if this is true, a method called second site suppressor analysis will be used. This will take advantage of the fact that a structural change in one subunit can often be compensated by a complimentary change in an interacting subunit, leading to restoration of function or assembly. Specifically, randomly generated mutants of α - and β -tubulin can be transfected into a Taxol-dependent cell line. Any recovery of Taxol sensitivity will then indicate that a compensating mutation is present, possibly indicating a structure-function relationship. These studies, as well as other mutation studies, are being done in F. Cabral's laboratory to further define the regions and interactions that are critical to microtubule assembly and stability.

The primary impetus for the work in our laboratory is to discover why the normally compensatory mechanism of hypertrophy fails to work after continuous pathologic stimulation of the heart. One of the more exciting models that may help us to answer this question is the canine aortic banding model that self-segregates into the hypertrophy and failure groups. These animals only have increased microtubule stability when they are unable to compensate and have a small amount of hypertrophy. This leads us to propose that not only is microtubule densification detrimental to contractile function through a viscous dampening of sarcomere motion, but that it is also detrimental for the development of compensatory hypertrophy. It is possible that the heart, in its attempt to modulate microtubule dynamics by overexpressing MAP 4 to facilitate growth, is

hampering growth, possibly through the interference of transport by binding of the MAP 4 molecules themselves. Current studies in this lab are focused on studying, hopefully in skeletal muscle cells, the effect of overexpression of MAP 4 on mRNA transport to determine if MAP 4 is detrimental to cell growth.

These studies are simply a beginning for determining, at a molecular level, possible mechanisms for the clinical condition of heart failure. The data generated have helped focus studies of microtubule stability in the adult cardiocyte on the effects of MAP 4 overexpression. As such, they have opened the possibility that modulation of MAP 4 in the heart can be a mechanism for the relief of contractile dysfunction and lack of compensation found in many pathologic forms of cardiac hypertrophy. This is a novel approach to therapy of heart failure, a disease that causes an enormous amount of morbidity and mortality in man.

LIST OF REFERENCES

1. Poole-Wilson, P.A. 1997. History, definition, and classification of heart failures. In *Heart Failure: Scientific Principles and Clinical Practice*. P.A. Poole-Wilson, W.S. Colucci, B.M. Massie, K. Chatterjee, and A.J. Coats, editors. New York: Churchill-Livingstone. 269-277.
2. Kannel, W.B. 1997. Epidemiology of heart failure in the United States. In *Heart Failure: Scientific Principles and Clinical Practice*. P.A. Poole-Wilson, W.S. Colucci, B.M. Massie, K. Chatterjee, and A.J. Coats, editors. New York: Churchill-Livingstone. 279-288.
3. Schwartzkopff, B., and Strauer, B.E. 1997. Hypertension and cardiac hypertrophy. In *Heart Failure: Scientific Principles and Clinical Practice*. P.A. Poole-Wilson, W.S. Colucci, B.M. Massie, K. Chatterjee, and A.J. Coats, editors. New York: Churchill-Livingstone. 321-337.
4. Cooper, G. 1997. Basic determinants of myocardial hypertrophy: a review of molecular mechanisms. *Annu Rev Med* 48:13-23.
5. Sadoshima, J., and Izumo, S. 1997. The cellular and molecular response of cardiac myocytes to mechanical stress. *Annu Rev Physiol* 59:551-571.
6. Chien, K.R., Grace, A.A., and Hunter, J.J. 1999. Molecular and cellular biology of cardiac hypertrophy and failure. In *Molecular Basis of Cardiovascular Disease : a Companion to Braunwald's Heart Disease*. K.R. Chien, editor. Philadelphia: Saunders. 211-250.
7. Beinlich, C.J., Rissinger, C.J., and Morgan, H.E. 1995. Mechanisms of rapid growth in the neonatal pig heart. *J Mol Cell Cardiol* 27:273-281.

8. Cooper, G., Puga, F.J., Zujko, K.J., Harrison, C.E., and Coleman, H.N. 1973. Normal myocardial function and energetics in volume-overload hypertrophy in the cat. *Circ Res* 32:140-148.
9. Cooper, G., Satava, R.M., Jr., Harrison, C.E., and Coleman, H.N. 1973. Mechanisms for the abnormal energetics of pressure-induced hypertrophy of cat myocardium. *Circ Res* 33:213-223.
10. Sato, H., Nagai, T., Kuppuswamy, D., Narishige, T., Koide, M., Menick, D.R., and Cooper, G. 1997. Microtubule stabilization in pressure overload cardiac hypertrophy. *J Cell Biol* 139:963-973.
11. Mann, D.L., Urabe, Y., Kent, R.L., Vinciguerra, S., and Cooper, G. 1991. Cellular versus myocardial basis for the contractile dysfunction of hypertrophied myocardium. *Circ Res* 68:402-415.
12. Koide, M., Nagatsu, M., Zile, M.R., Hamawaki, M., Swindle, M.M., Keech, G., DeFreyte, G., Tagawa, H., Cooper, G., and Carabello, B.A. 1997. Premorbid determinants of left ventricular dysfunction in a novel model of gradually induced pressure overload in the adult canine. *Circulation* 95:1601-1610.
13. Tagawa, H., Koide, M., Sato, H., Zile, M.R., Carabello, B.A., and Cooper, G. 1998. Cytoskeletal role in the transition from compensated to decompensated hypertrophy during adult canine left ventricular pressure overloading. *Circ Res* 82:751-761.
14. Tsutsui, H., Ishihara, K., and Cooper, G. 1993. Cytoskeletal role in the contractile dysfunction of hypertrophied myocardium. *Science* 260:682-687.
15. Marino, T.A., Kent, R.L., Uboh, C.E., Fernandez, E., Thompson, E.W., and Cooper, G. 1985. Structural analysis of pressure versus volume overload hypertrophy of cat right ventricle. *Am J Physiol* 249:H371-379.

16. Tagawa, H., Wang, N., Narishige, T., Ingber, D.E., Zile, M.R., and Cooper, G. 1997. Cytoskeletal mechanics in pressure-overload cardiac hypertrophy. *Circ Res* 80:281-289.
17. Burns, R.G. 1991. Alpha-, beta-, and gamma-tubulins: sequence comparisons and structural constraints. *Cell Motil Cytoskeleton* 20:181-189.
18. Mitchison, T., and Kirschner, M. 1984. Dynamic instability of microtubule growth. *Nature* 312:237-242.
19. Desai, A., and Mitchison, T.J. 1997. Microtubule polymerization dynamics. *Annu Rev Cell Dev Biol* 13:83-117.
20. Shirasu, M., Yonetani, A., and Walczak, C.E. 1999. Microtubule dynamics in *Xenopus* egg extracts. *Microsc Res Tech* 44:435-445.
21. Wordeman, L., and Mitchison, T.J. 1994. Dynamics of microtubule assembly *in vivo*. In *Microtubules*. J.S. Hyams, and C.W. Lloyd, editors. New York: Wiley-Liss. 287-301.
22. Luduena, R.F. 1998. Multiple forms of tubulin: different gene products and covalent modifications. *Int Rev Cytol* 178:207-275.
23. Khan, I.A., and Luduena, R.F. 1996. Phosphorylation of beta III-tubulin. *Biochemistry* 35:3704-3711.
24. Narishige, T., Blade, K.L., Ishibashi, Y., Nagai, T., Hamawaki, M., Menick, D.R., Kuppuswamy, D., and Cooper, G. 1999. Cardiac hypertrophic and developmental regulation of the beta-tubulin multigene family. *J Biol Chem* 274:9692-9697.
25. Cleveland, D. 1987. The multitubulin hypothesis revisited: What have we learned? *J Cell Biol* 104:381-383.

26. Maccioni, R.B., Rivas, C., and Vera, J.C. 1988. Differential interaction of synthetic peptides from the carboxyl-terminal regulatory domain of tubulin with microtubule-associated proteins. *EMBO J* 7:1957-1963.
27. Tsutsui, H., Tagawa, H., Kent, R.L., McCollam, P.L., Ishihara, K., Nagatsu, M., and Cooper, G. 1994. Role of microtubules in contractile dysfunction of hypertrophied cardiocytes. *Circulation* 90:533-555.
28. Tagawa, H., Rozich, J.D., Tsutsui, H., Narishige, T., Kuppuswamy, D., Sato, H., McDermott, P.J., Koide, M., and Cooper, G. 1996. Basis for increased microtubules in pressure-hypertrophied cardiocytes. *Circulation* 93:1230-1243.
29. Barlow, S., Gonzalez-Garay, M.L., West, R.R., Olmsted, J.B., and Cabral, F. 1994. Stable expression of heterologous microtubule-associated proteins (MAPs) in Chinese hamster ovary cells: evidence for differing roles of MAPs in microtubule organization. *J Cell Biol* 126:1017-1029.
30. Mangan, M.E., and Olmsted, J.B. 1996. A muscle-specific variant of microtubule-associated protein 4 (MAP4) is required in myogenesis. *Development* 122:771-781.
31. Oblinger, M.M., and Kost, S.A. 1994. Coordinate regulation of tubulin and microtubule associated protein genes during development of hamster brain. *Brain Res Dev Brain Res* 77:45-54.
32. Cleveland, D. 1988. Autoregulated instability of tubulin mRNAs: A novel eukaryotic regulatory mechanism. *Trends Biochem Sci* 13:339-342.
33. Caron, J.M., Jones, A.L., and Kirschner, M.W. 1985. Autoregulation of tubulin synthesis in hepatocytes and fibroblasts. *J Cell Biol* 101:1763-1772.
34. Ben-Ze'ev, A., Farmer, S.R., and Penman, S. 1979. Mechanisms of regulating tubulin synthesis in cultured mammalian cells. *Cell* 17:319-325.

35. Cleveland, D., Pittenger, M., and Feramisco, J. 1983. Elevation of tubulin levels by microinjection suppresses new tubulin synthesis. *Nature* 305:738-740.
36. Cleveland, D., Lopata, M., Sherline, P., and Kirschner, M. 1981. Unpolymerized tubulin modulates the level of tubulin mRNAs. *Cell* 25:537-546.
37. Pittenger, M.F., and Cleveland, D.W. 1985. Retention of autoregulatory control of tubulin synthesis in cytoplasts: demonstration of a cytoplasmic mechanism that regulates the level of tubulin expression. *J Cell Biol* 101:1941-1952.
38. Pachter, J.S., Yen, T.J., and Cleveland, D.W. 1987. Autoregulation of tubulin expression is achieved through specific degradation of polysomal tubulin mRNAs. *Cell* 51:283-292.
39. Yen, T.J., Gay, D.A., Pachter, J.S., and Cleveland, D.W. 1988. Autoregulated changes in stability of polyribosome-bound beta-tubulin mRNAs are specified by the first 13 translated nucleotides. *Mol Cell Biol* 8:1221-1235.
40. Frohman, M.A., Dush, M.K., and Martin, G.R. 1988. Rapid production of full-length cDNAs from rare transcripts: amplification using a single gene-specific oligonucleotide primer. *Proc Natl Acad Sci U S A* 85:8998-9002.
41. Cooper, G., Mercer, W.E., Hooper, J.K., Gordon, P.R., Kent, R.L., Lauva, I.K., and Marino, T.A. 1986. Load regulation of the properties of adult feline cardiocytes. *Circ Res* 58:692-705.
42. Chomczynski, P., and Sacchi, N. 1987. Single-step method of RNA isolation by acid guanidinium thiocyanate-phenol-chloroform extraction. *Anal Biochem* 162:156-159.
43. Barnes, K.V., Cheng, G., Dawson, M.M., and Menick, D.R. 1997. Cloning of cardiac, kidney, and brain promoters of the feline *ncx1* gene. *J Biol Chem* 272:11510-11517.

44. Foster, K.A., McDermott, P.J., and Robishaw, J.D. 1990. Expression of G proteins in rat cardiac myocytes: Effect of KCl depolarization. *Am J Physiol* 259:H432-H441.
45. Tagawa, H., Koide, M., Sato, H., and Cooper, G. 1996. Cytoskeletal role in the contractile dysfunction of cardiocytes from hypertrophied and failing right ventricular myocardium. *Proc Assoc Am Physicians* 108:218-229.
46. Lewis, S.A., Lee, M.G.S., and Cowan, N.J. 1985. Five mouse tubulin isotypes and their regulated expression during development. *J Cell Biol* 101:852-861.
47. Wang, D., Villasante, A., Lewis, S., and Cowan, N. 1986. The mammalian β -tubulin repertoire: Hematopoietic expression of a novel, heterologous β -tubulin isotype. *J Cell Biol* 103:1903-1910.
48. Lee, M.G.S., Lewis, S.A., Wilde, C.D., and Cowan, N.J. 1983. Evolutionary history of a multigene family: An expressed human β -tubulin gene and three processed pseudogenes. *Cell* 33:477-487.
49. Makhlof, A.A., and McDermott, P.J. 1998. Increased expression of eukaryotic initiation factor 4E during growth of neonatal rat cardiocytes in vitro. *Am J Physiol* 274:H2133-2142.
50. Thelen, M.H., Simonides, W.S., and van Hardeveld, C. 1997. Electrical stimulation of C2C12 myotubes induces contractions and represses thyroid-hormone-dependent transcription of the fast-type sarcoplasmic-reticulum Ca^{2+} -ATPase gene. *Biochem J* 321:845-848.
51. Hannan, R.D., Luyken, J., and Rothblum, L.I. 1996. Regulation of ribosomal DNA transcription during contraction-induced hypertrophy of neonatal cardiomyocytes. *J Biol Chem* 271:3213-3220.

52. Hannan, R.D., Stefanovsky, V., Taylor, L., Moss, T., and Rothblum, L.I. 1996. Overexpression of the transcription factor UBF1 is sufficient to increase ribosomal DNA transcription in neonatal cardiomyocytes: implications for cardiac hypertrophy. *Proc Natl Acad Sci U S A* 93:8750-8755.
53. Nakao, K., Minobe, W., Roden, R., Bristow, M.R., and Leinwand, L.A. 1997. Myosin heavy chain gene expression in human heart failure. *J Clin Invest* 100:2362-2370.
54. Lowes, B.D., Minobe, W., Abraham, W.T., Rizeq, M.N., Bohlmeier, T.J., Quaife, R.A., Roden, R.L., Dutcher, D.L., Robertson, A.D., Voelkel, N.F., Badesch, D.B., Groves, B.M., Gilbert, E.M., and Bristow, M.R. 1997. Changes in gene expression in the intact human heart. Downregulation of alpha-myosin heavy chain in hypertrophied, failing ventricular myocardium. *J Clin Invest* 100:2315-2324.
55. Moskowitz, P.F., and Oblinger, M.M. 1995. Transcriptional and post-transcriptional mechanisms regulating neurofilament and tubulin gene expression during normal development of the rat brain. *Brain Res Mol Brain Res* 30:211-222.
56. Sisodia, S.S., Gay, D.A., and Cleveland, D.W. 1990. *In vivo* discrimination among beta-tubulin isotypes: selective degradation of a type IV beta-tubulin isotype following overexpression in cultured animal cells. *New Biol* 2:66-76.
57. Watson, P.A., Hannan, R., Carl, L.L., and Giger, K.E. 1996. Contractile activity and passive stretch regulate tubulin mRNA and protein content in cardiac myocytes. *Am J Physiol* 271:C684-689.
58. Cleveland, D.W., and Theodorakis, N.G. 1994. Regulation of tubulin synthesis. In *Microtubules*. J.S. Hyams, and C.W. Lloyd, editors. New York: Wiley-Liss. 47-58.
59. Taha, C., and Klip, A. 1999. The insulin signaling pathway. *J. Membrane Biol.* 169:1-12.

60. Tsakiridis, T., Tong, P., Matthews, B., Tsiani, E., Bilan, P.J., Klip, A., and Downey, G.P. 1999. Role of the actin cytoskeleton in insulin action. *Microsc. Res. Tech.* 47:79-92.
61. Haghghat, A., Mader, S., Pause, A., and Sonenberg, N. 1995. Repression of cap-dependent translation by 4E-binding protein 1: competition with p220 for binding to eukaryotic initiation factor-4E. *Embo J* 14:5701-5709.
62. Kido, Y., Nakae, J., and Accili, D. 2001. The insulin receptor and its cellular targets. *J. Clin. Endocrinol. Metab.* 86:972-979.
63. Keith, C.H., Feramisco, J.R., and Shelanski, M. 1981. Direct visualization of fluorescein-labeled microtubules in vitro and in microinjected fibroblasts. *J Cell Biol* 88:234-240.
64. Bond, J.F., Fridovich-Keil, J.L., Pillus, L., Mulligan, R.C., and Solomon, F. 1986. A chicken-yeast chimeric beta-tubulin protein is incorporated into mouse microtubules in vivo. *Cell* 44:461-468.
65. Schatz, P.J., Solomon, F., and Botstein, D. 1986. Genetically essential and nonessential alpha-tubulin genes specify functionally interchangeable proteins. *Cell BiolMol* 6:3722-3733.
66. Solnica-Krezel, L., Diggins-Gilicinski, M., Burland, T.G., and Dove, W.F. 1990. Variable pathways for developmental changes in composition and organization of microtubules in *Physarum polycephalum*. *J Cell Sci* 96:383-393.
67. May, G.S. 1989. The highly divergent beta-tubulins of *Aspergillus nidulans* are functionally interchangeable. *J Cell Biol* 109:2267-2274.
68. Lewis, S.A., Gu, W., and Cowan, N.J. 1987. Free intermingling of mammalian beta-tubulin isotypes among functionally distinct microtubules. *Cell* 49:539-548.

69. Blade, K., Menick, D.R., and Cabral, F. 1999. Overexpression of class I, II, or IVb β -tubulin isotypes in CHO cells is insufficient to confer resistance to paclitaxel. *J Cell Sci* 112:2213-2221.
70. Luduena, R.F. 1993. Are tubulin isotypes functionally significant. *Mol Biol Cell* 4:445-457.
71. Laferriere, N.B., MacRae, T.H., and Brown, D.L. 1997. Tubulin synthesis and assembly in differentiating neurons. *Biochem Cell Biol* 75:103-117.
72. Hoyle, H.D., and Raff, E.C. 1990. Two Drosophila beta tubulin isoforms are not functionally equivalent. *J Cell Biol* 111:1009-1026.
73. Banerjee, A., Roach, M.C., Trcka, P., and Luduena, R.F. 1992. Preparation of a monoclonal antibody specific for the class IV isotype of beta-tubulin. Purification and assembly of alpha beta II, alpha beta III, and alpha beta IV tubulin dimers from bovine brain. *J Biol Chem* 267:5625-5630.
74. Lu, Q., and Luduena, R.F. 1994. *In vitro* analysis of microtubule assembly of isotypically pure tubulin dimers. Intrinsic differences in the assembly properties of alpha beta II, alpha beta III, and alpha beta IV tubulin dimers in the absence of microtubule-associated proteins. *J Biol Chem* 269:2041-2047.
75. Panda, D., Miller, H.P., Banerjee, A., Luduena, R.F., and Wilson, L. 1994. Microtubule dynamics *in vitro* are regulated by the tubulin isotype composition. *Proc Natl Acad Sci USA* 91:11358-11362.
76. Falconer, M.M., Echeverri, C.J., and Brown, D.L. 1992. Differential sorting of beta tubulin isotypes into colchicine-stable microtubules during neuronal and muscle differentiation of embryonal carcinoma cells. *Cell Motil Cytoskeleton* 21:313-325.
77. Cabral, F., and Barlow, S.B. 1989. Mechanisms by which mammalian cells acquire resistance to drugs that affect microtubule assembly. *Faseb J* 3:1593-1599.

78. Cabral, F., Brady, R.C., and Schibler, M.J. 1986. A mechanism of cellular resistance to drugs that interfere with microtubule assembly. *Ann N Y Acad Sci* 466:745-756.
79. Minotti, A.M., Barlow, S.B., and Cabral, F. 1991. Resistance to antimitotic drugs in Chinese hamster ovary cells correlates with changes in the level of polymerized tubulin. *J Biol Chem* 266:3987-3994.
80. Haber, M., Burkhart, C.A., Regl, D.L., Madafiglio, J., Norris, M.D., and Horwitz, S.B. 1995. Altered expression of M beta 2, the class II beta-tubulin isotype, in a murine J774.2 cell line with a high level of taxol resistance. *J Biol Chem* 270:31269-31275.
81. Kavallaris, M., Kuo, D.Y.S., Burkhart, C.A., Regl, D.L., Norris, M.D., Haber, M., and Horwitz, S.B. 1997. Taxol-resistant epithelial ovarian tumors are associated with altered expression of specific beta-tubulin isotypes. *J Clin Invest* 100:1282-1293.
82. Jaffrezou, J.P., Dumontet, C., Derry, W.B., Duran, G., Chen, G., Tsuchiya, E., Wilson, L., Jordan, M.A., and Sikic, B.I. 1995. Novel mechanism of resistance to paclitaxel (Taxol) in human K562 leukemia cells by combined selection with PSC 833. *Oncol Res* 7:517-527.
83. Ranganathan, S., Dexter, D.W., Benetatos, C.A., and Hudes, G.R. 1998. Cloning and sequencing of human betaIII-tubulin cDNA: induction of betaIII isotype in human prostate carcinoma cells by acute exposure to antimicrotubule agents. *Biochim Biophys Acta* 1395:237-245.
84. Boggs, B.A., Gonzalez-Garay, M.L., and Cabral, F. 1996. Significant divergence in nucleotide sequences for beta-tubulin from different laboratory strains of Chinese hamster ovary cells. *DNA Seq* 6:171-174.

85. Boggs, B., and Cabral, F. 1987. Mutations affecting assembly and stability of tubulin: evidence for a nonessential beta-tubulin in CHO cells. *Mol Cell Biol* 7:2700-2707.
86. Gonzalez-Garay, M.L., and Cabral, F. 1995. Overexpression of an epitope-tagged beta-tubulin in Chinese hamster ovary cells causes an increase in endogenous alpha-tubulin synthesis. *Cell Motil Cytoskeleton* 31:259-272.
87. Gossen, M., and Bujard, H. 1992. Tight control of gene expression in mammalian cells by tetracycline- responsive promoters. *Proc Natl Acad Sci U S A* 89:5547-5551.
88. Cabral, F., Sobel, M.E., and Gottesman, M.M. 1980. CHO mutants resistant to colchicine, colcemid or griseofulvin have an altered beta-tubulin. *Cell* 20:29-36.
89. Laemmli, U.K. 1970. Cleavage of structural proteins during the assembly of the head of bacteriophage T4. *Nature* 227:680-685.
90. Chartier, C., Degryse, E., Gantzer, M., Dieterle, A., Pavirani, A., and Mehtali, M. 1996. Efficient generation of recombinant adenovirus vectors by homologous recombination in *Escherichia coli*. *J Virol* 70:4805-4810.
91. Shockett, P., Difilippantonio, M., Hellman, N., and Schatz, D.G. 1995. A modified tetracycline-regulated system provides autoregulatory, inducible gene expression in cultured cells and transgenic mice. *Proc Natl Acad Sci U S A* 92:6522-6526.
92. Sawada, T., and Cabral, F. 1989. Expression and function of beta-tubulin isotypes in Chinese hamster ovary cells. *J Biol Chem* 264:3013-3020.
93. Gonzalez-Garay, M.L., Chang, L., Blade, K.L., Menick, D.R., and Cabral, F. 1999. A beta-tubulin leucine cluster involved in microtubule assembly and paclitaxel resistance. *J Biol Chem* 274:23875-23882.

94. Westfall, M.V., Rust, E.M., Albayya, F., and Metzger, J.M. 1997. Adenovirus-mediated myofilament gene transfer into adult cardiac myocytes. *Methods Cell Biol* 52:307-322.
95. Raybin, D., and Flavin, M. 1975. An enzyme tyrosylating alpha-tubulin and its role in microtubule assembly. *Biochem Biophys Res Commun* 65:1088-1095.
96. Gundersen, G.G., Kalnoski, M.H., and Bulinski, J.C. 1984. Distinct populations of microtubules: tyrosinated and nontyrosinated alpha tubulin are distributed differently in vivo. *Cell* 38:779-789.
97. Thompson, W.C., Deanin, G.G., and Gordon, M.W. 1979. Intact microtubules are required for rapid turnover of carboxyl-terminal tyrosine of alpha-tubulin in cell cultures. *Proc Natl Acad Sci U S A* 76:1318-1322.
98. Wehland, J., and Weber, K. 1987. Turnover of the carboxy-terminal tyrosine of alpha-tubulin and means of reaching elevated levels of detyrosination in living cells. *J Cell Sci* 88:185-203.
99. Wehland, J., and Weber, K. 1987. Tubulin-tyrosine ligase has a binding site on beta-tubulin: a two-domain structure of the enzyme. *J Cell Biol* 104:1059-1067.
100. Paturle, L., Wehland, J., Margolis, R.L., and Job, D. 1989. Complete separation of tyrosinated, detyrosinated, and nontyrosinatable brain tubulin subpopulations using affinity chromatography. *Biochemistry* 28:2698-2704.
101. Paturle-Lafanechere, L., Manier, M., Trigault, N., Pirollet, F., Mazarguil, H., and Job, D. 1994. Accumulation of delta 2-tubulin, a major tubulin variant that cannot be tyrosinated, in neuronal tissues and in stable microtubule assemblies. *J Cell Sci* 107:1529-1543.

102. Paturle-Lafanechere, L., Edde, B., Denoulet, P., Van Dorsselaer, A., Mazarguil, H., Le Caer, J.P., Wehland, J., and Job, D. 1991. Characterization of a major brain tubulin variant which cannot be tyrosinated. *Biochemistry* 30:10523-10528.
103. Webster, D.R. 1997. Neonatal rat cardiomyocytes possess a large population of stable microtubules that is enriched in post-translationally modified subunits. *J Mol Cell Cardiol* 29:2813-2824.
104. Nogales, E., Wolf, S.G., and Downing, K.H. 1998. Structure of the alpha beta tubulin dimer by electron crystallography. *Nature* 391:199-203.
105. Raff, E.C. 1994. The role of multiple tubulin isoforms in cellular microtubule function. In *Microtubules*. J.S. Hyams, and C.W. Lloyd, editors. New York: Wiley-Liss. 85-109.
106. Nogales, E., Whittaker, M., Milligan, R.A., and Downing, K.H. 1999. High-resolution model of the microtubule. *Cell* 96:79-88.
107. Mandelkow, E.M., Mandelkow, E., and Milligan, R.A. 1991. Microtubule dynamics and microtubule caps: a time-resolved cryo- electron microscopy study. *J Cell Biol* 114:977-991.
108. Subramaniam, A., Jones, W.K., Gulick, J., Wert, S., Neumann, J., and Robbins, J. 1991. Tissue-specific regulation of the alpha-myosin heavy chain gene promoter in transgenic mice. *J Biol Chem* 266:24613-24620.
109. Wassarman, P.M., and DePamphilis, M.L. 1993. *Methods in Enzymology: Guide to Techniques in Mouse Development*. San Diego, CA: Academic Press.
110. Schibler, M.J., and Cabral, F. 1986. Taxol-dependent mutants of Chinese hamster ovary cells with alterations in alpha- and beta-tubulin. *J Cell Biol* 102:1522-1531.
111. Cabral, F.R. 1983. Isolation of Chinese hamster ovary cell mutants requiring the continuous presence of Taxol for cell division. *J Cell Biol* 97:22-29.

112. Cabral, F., Abraham, I., and Gottesman, M.M. 1981. Isolation of a taxol-resistant Chinese hamster ovary cell mutant that has an alteration in alpha-tubulin. *Proc Natl Acad Sci U S A* 78:4388-4391.
113. Cabral, F., Wible, L., Brenner, S., and Brinkley, B.R. 1983. Taxol-requiring mutant of Chinese hamster ovary cells with impaired mitotic spindle assembly. *J Cell Biol* 97:30-39.
114. Cabral, F., and Barlow, S.B. 1991. Resistance to antimitotic agents as genetic probes of microtubule structure and function. *Pharmacol Ther* 52:159-171.
115. Schulze, E., and Kirschner, M. 1987. Dynamic and stable populations of microtubules in cells. *J Cell Biol* 104:277-288.
116. Piperno, G., LeDizet, M., and Chang, X.J. 1987. Microtubules containing acetylated alpha-tubulin in mammalian cells in culture. *J Cell Biol* 104:289-302.
117. Gonzalez-Garay, M.L., and Cabral, F. 1996. alpha-Tubulin limits its own synthesis: evidence for a mechanism involving translational repression. *J Cell Biol* 135:1525-1534.
118. Hamawaki, M., Coffman, T.M., Lashus, A., Koide, M., Zile, M.R., Oliverio, M.I., DeFreyte, G., Cooper, G., and Carabello, B.A. 1998. Pressure-overload hypertrophy is unabated in mice devoid of AT1A receptors. *Am J Physiol* 274:H868-873.
119. James, J., and Robbins, J. 1997. Molecular remodeling of cardiac contractile function. *Am J Physiol* 273:H2105-2118.
120. Erickson, H.P. 1998. Atomic structures of tubulin and FtsZ. *Trends Cell Biol* 8:133-137.
121. Karns, L.R., Kariya, K., and Simpson, P.C. 1995. M-CAT, CArG, and Sp1 elements are required for alpha 1-adrenergic induction of the skeletal alpha-actin promoter during cardiac myocyte hypertrophy. Transcriptional enhancer factor-1 and

- protein kinase C as conserved transducers of the fetal program in cardiac growth. *J Biol Chem* 270:410-417.
122. Hasegawa, K., Lee, S.J., Jobe, S.M., Markham, B.E., and Kitsis, R.N. 1997. cis-Acting sequences that mediate induction of beta-myosin heavy chain gene expression during left ventricular hypertrophy due to aortic constriction. *Circulation* 96:3943-3953.
123. Santalucia, T., Boheler, K.R., Brand, N.J., Sahye, U., Fandos, C., Vinals, F., Ferre, J., Testar, X., Palacin, M., and Zorzano, A. 1999. Factors involved in GLUT-1 glucose transporter gene transcription in cardiac muscle. *J. Biol. Chem.* 274:17626-17634.
124. Lim, S.S., Sammak, P.J., and Borisy, G.G. 1989. Progressive and spatially differentiated stability of microtubules in developing neuronal cells. *J Cell Biol* 109:253-263.
125. Black, M.M., and Greene, L.A. 1982. Changes in the colchicine susceptibility of microtubules associated with neurite outgrowth: studies with nerve growth factor-responsive PC12 pheochromocytoma cells. *J Cell Biol* 95:379-386.
126. Black, M.M., Aletta, J.M., and Greene, L.A. 1986. Regulation of microtubule composition and stability during nerve growth factor-promoted neurite outgrowth. *J Cell Biol* 103:545-557.